EVALUATING NONDESTRUCTIVE TESTING TECHNIQUES TO DETECT VOIDS IN BONDED POST-TENSIONED DUCTS

Final Report

Submitted to

Florida Department of Transportation
(Contract No. BC 354-49)

By

Larry C. Muszynski, Abdol R. Chini, and Elie G. Andary

M.E. Rinker, Sr. School of Building Construction
University of Florida
Gainesville, FL 32611

Technical Report Documentation

1. Report No. DOT HS 809 412	2. Government Accession No.	3. Recipient's Catalog No.	
4. Title and Subtitle Nondestructive Testing Methods To Detect Voids in Bonded Post-Tensioned Ducts		5. Report Date May 30, 2003 6. Performing Organization Code	
7. Author(s) Larry C. Muszynski, Abdol R. Chini, Elie G. Andary		8. Performing Organization Report No.	
9. Performing Organization Name and Address M.E. Rinker, Sr. School of Building Construction University of Florida Gainesville, FL 32611		10. Work Unit No. (TRAIS) 11. Contract or Grant No. BC 354	
12. Sponsoring Agency Name and Address Florida Department of Transportation 605 Suwannee Street Tallahassee, FL 32399-0450		13. Type of Report and Period Covered Final (September 10, 2001 – May 30, 2003) 14. Sponsoring Agency Code	
15. Supplementary Notes Prepared in cooperation with the U.S. Department of Transportation and Federal Highway Administration			

16. Abstract

The use of post-tensioning in bridges provides durability and structural benefits to the system while expediting the construction process. However, there is considerable interest to determine whether a tendon duct is properly filled with grout or not. Implementing non-destructive testing can be vital to the integrity of the structure because loss of post-tensioning can result in catastrophic failure.

Objectives: The purpose of this work was to develop and validate a non-destructive testing and evaluation (NDT&E) method that can be used in the field to detect internal concrete conditions such as voids and cracks in grouted tendon ducts during bonded post-tensioned applications.

Methods: These are three techniques that were evaluated in this research effort: Impact Echo (IE), Spectral Analysis of Surface Waves (SASW), and Ultrasonic Tomography Imaging (UTI).

Results: Based on the results from all three tests, we suggest that the IE scanning test should be used to evaluate the internal condition of the grouted duct. Impactechograms may also be used as a way to present the results since the plot provides more information in IE frequency data. The image results from UTI showed locations of both ducts clearly in all three cases. Unfortunately, the images did not show details inside the ducts.

Conclusion: Scanning Impact Echo, IE, tests showed the most promise for assessing internal grout conditions of the steel duct. For a plastic duct, it was more difficult to identify grout conditions due to partial debonding conditions between the plastic duct and concrete wall.

17. Key Words • NDT, post-tensioning, grouted ducts, impact echo, SASW, velocity tomograms	18. Distribution Statement This report is available from the National Technical Information Service in Springfield, Virginia 22161, (703) 605-6000		
19. Security Classif. (of this report) Unclassified	20. Security Classif. (of this page) Unclassified	21. No. of Pages	22. Price

NONDESTRUCTIVE TESTING METHODS TO DETECT VOIDS IN BONDED POST-TENSIONED DUCTS

This report is prepared in cooperation with the State of Florida Department of Transportation and the U.S. Department of Transportation.

The opinions, findings, and conclusions expressed in this report are those of the authors and not necessarily those of the State of Florida Department of Transportation or the U.S. Department of Transportation.

EXECUTIVE SUMMARY

The use of post-tensioning in bridges can provide durability and structural benefits to the system in the construction field. In bonded post-tensioned construction, Portland cement grout is used to form a sheath around the steel tensioning strand, and act as a solid impermeable barrier to the ingress of chlorides from reaching the steel and initiating corrosion. Too often, voids are formed in the post-tensioning duct from incomplete grouting, trapped air pockets, or from evaporation of bleed water due to poor grout design or poor grouting procedures or both. Due to the large tensile stress that the tendons are subjected to, tendon failure due to corrosion would result in the failure of the concrete member, leading to a severe damage for the whole structure that might lead to a disaster. That's why those types of structures need to be adequately tested to ensure acceptable performance during their service life.

There are three techniques that were evaluated in this research: Scanning Impact Echo (IE), Spectral Analysis of Surface Waves (SASW), and Ultrasonic Tomography Imaging (UTI).

1. Scanning Impact Echo

Scanning Impact Echo, IE, tests showed the most promise for assessing internal grout conditions of the steel duct. For a plastic duct, it was more difficult to identify grout conditions due to partial debonding conditions between the plastic duct and concrete wall. In this investigation, internal conditions of grouted ducts were successfully evaluated using the IE thickness results together with a shift in the IE peak frequency.

2. Spectral Analysis of Surface Waves (SASW)

The Spectral Analysis of Surface Waves, SASW, tests showed good promise for steel ducts only. The surface wave velocity results from the fully grouted steel duct showed the highest velocity while the velocity results from the empty steel duct showed lowest velocity. However, the test results from the plastic duct did not yield similar results.

3. Ultrasonic Tomography Imaging, (UTI)

The image results from the Ultrasonic Tomography Imaging, UTI, tests showed locations of the ducts. Unfortunately, the image results did not show grout condition details inside the ducts. This was because the frequency of the transducers used in this investigation was 54 kHz, which is standard for concrete. This range of frequency yielded a wavelength longer than the diameter of the ducts, therefore higher frequency/shorter wavelength transducers, should be used on 3-inch I.D. ducts.

Based on the results from all three tests, we suggest that scanning Impact Echo should be incorporated as a practical method to evaluate the internal condition of the grout in actual field conditions for bonded post-tensioning systems. Also, based on this investigation, the use of plastic ducts for bonded post-tensioning systems should be discouraged, since scanning IE verification of fully grouted tendons is not reliable for plastic duct systems.

ACKNOWLEDGMENTS

This research reported here was sponsored by the Florida Department of Transportation. Sincere thanks are due to Micchael Bergin, P.E., State Structural Materials Engineer, State Materials Office in Gainesville, Florida for his guidance, support and encouragement.

Special thanks to Larry Olson, President of Olson Engineering, Wheat Ridge, Colorado for his support and contributions to this effort and to Dr. Yajai Promboon, Project Engineer, Olson Engineering, for her efforts in training and analyzing the NDT data.

TABLE OF CONTENTS

LIST OF TABLES

LIST OF FIGURES

CHAPTER 1

INTRODUCTION

The use of post-tensioning in bridges can provide durability and structural benefits to the system while expediting the construction process. However, applying non-destructive testing on those members of the post-tensioning system is vital to the integrity of the structure because loss of post-tensioning can result in catastrophic failure. Chloride induced corrosion of steel in concrete is one of the most costly forms of corrosion each year. Coastal substructure elements are exposed to seawater by immersion or spray, and inland bridges may also be at risk due to the application of deicing salts.

1.1 Background

Portland cement grout is often used in post-tensioned structures to provide bond between the tendon and the surrounding concrete and also as corrosion protection for the tendons. Grout for bonded post-tensioning is a combination of Portland cement and water, along with any admixtures necessary to obtain required properties such as fluidity, thixotropy, and reduced permeability. The grout plays a crucial role in the corrosion protection of the system since it may be the “last line of defense” against chloride attack of the post-tensioning strands; an optimum grout combines desirable fresh properties along with good corrosion protection.

In bonded post-tensioned structures, the Portland cement grout is often the last barrier against ingress of chlorides to the prestressing strand. Grouts with properties such as fluidity, low permeability, and bleed resistance can provide maximum protection when

combined with proper grouting procedures.

Voids can be formed in the post-tensioning duct from incomplete grouting, trapped air pockets, or from the evaporation of bleed water pockets. Top quality grout is of little benefit if poor grouting procedures result in large void formations, which provide no protection to the strand and no transfer of bond. Proper venting of the post-tensioning duct is critical for complete grouting. The void between the tendon and the post-tensioning duct is a very complex space. For instance, a parabolic shaped duct with a tensioned tendon may have a number of small voids of varying shapes and sizes, and a very stiff grout may not fill the interstices.

Bleed lenses can form a result of the separation of water from the cement. This sedimentation process is accentuated by the addition of seven-wire strand, which act as a "water-important mechanism". The spaces within the individual twisted wires that form the strand are large enough to allow easy passage of water but not cement. Ducts with vertical rises will typically cause more bleed due to the increased pressure within the grout section of the duct exposing the tendon. Even in parabolic draped ducts, any bleed water will tend to gather near the highest intermediate points, leaving voids in the duct.

Grouts containing anti-bleed admixture, or thixotropic grouts, can be bleed resistant even when used in ducts with large vertical rises. The grouts are able to retain their water even under high pressures and can eliminate significant void formation when proper grouting procedures are followed.

1.2 Objective

The objective of the research contained in this thesis is to evaluate nondestructive testing (NDT) techniques to detect voids in bonded post-tensioned ducts. NDT techniques have been practically used for testing concrete elements but there is a need to speedup the field test process and improve the analysis procedures of this testing. Moreover, it would be useful to identify the advantages and the disadvantages of each technique and compare the effectiveness and the accuracy of their results and outputs.

1.3 Scope

The scope included FDOT and the University of Florida conducting a joint investigation in order to meet the study objectives. The first step will be to generate a literature review of past studies involving testing post-tensioned concrete elements and ducts. A survey will be generated and distributed to all state departments of transportation to establish a possible idea about the use of post-tensioning, ducts, failures and the availability of testing procedures for post-tensioned concrete members. The results of this survey will be analyzed using a certain statistical analysis. Next, concrete samples including plastic and metal ducts will be produced for experimental purposes of testing them using the various testing techniques. Olson Engineering Inc. will provide the equipment needed to accomplish the testing. Finally, comparisons of the results will be made, and conclusions and recommendations presented.

CHAPTER 2

LITERATURE REVIEW

2.1 Wang, X., Chang C., and Fan L

Introduction

The American Society of Nondestructive Testing (ASNT), NDT defines as the examination of an object or material using technology that does not affect its future usefulness. NDT can be used without destroying or damaging a product or material. The next step is NDE, Nondestructive Evaluation. This is more quantitative in nature, and used, for example, not only to locate a damage or a defect, but also to measure something about that defect such as size, shape, and orientation.

At this point, it is necessary to consider why damage and defects are induced in bridge structures. A bridge is built on the basic premise that it will carry certain loads safely. The meaning of "safely," is rather obscure. It should be based on a chosen load-induced response, i.e., a stress, or on serviceability criteria. In current engineering practice for designing bridges, the following limit states are considered:

Serviceability limit state. This limit state refers to restrictions on stresses, deformations, and crack widths under regular service condition. Its purpose is to ensure acceptable performance of a bridge during its service life.

Strength limit state. This is the strength and stability required of various structural components to safely resist the statistically significant load combinations a bridge is;

likely to experience during its service life. These loading conditions may lead to extensive distress and structural damage, but the overall structural integrity is expected to be maintained.

Extreme-event limit state. Extreme events are unique occurrences whose return period is significantly greater than the design life of the bridge. A major earthquake, a flood, or an ice flow are examples of extreme events. The design should ensure the structural survival of the bridge during these rare occurrences, although damage may be sustained.

2.2 Martin, J., Broughton, K.J., Giannopolous, A., Hardy, M.S.A., and Forde, M.C. (2001)

This study illustrates a theory and an experimental procedure called the Ultrasonic tomography theory and Tomographic survey instrumentations and experimental procedure.

2.2.1 Ultrasonic tomography theory

The mathematical theory was established by Radon in 1917 in which it is shown that the internal characteristics of an object can be exactly reconstructed by a complete set of projections through the object. Energy transmitted through the specimen is measured and the section constructed. This is the simplest form of tomography and can be performed by measuring the times-of-flight of a series of stress pulses along different paths through the specimen. The basic concept is that the stress pulse on each projection travels through the specimen and interacts with its internal construction. Variations in the internal conditions result in different

tunes-of-flight being measured. The tomographic software reconstructs the section by combining the information contained in a series of these projections, obtained at different angles through the section. The greater the number of measurements taken, the more accurate are the results. For the surveys undertaken, the travel time alone was measured and the section reconstructed using the information contained in these times alone.

2.2.2 Tomographic survey instrumentations and experimental procedure.

The travel times for these investigations were measured using an ultrasonic digital tester, PUNDIT. This instrumentation has been widely used to non-destructively test concrete and is robust and therefore suitable for use onsite. A test grid was set up at the section to be investigated using a similar distance between test points on all test surfaces. Each transducer location and corresponding time-of-flight was noted and subsequently input into a model to be analyzed by MIGRATOM software. The internal wave velocities calculated were then presented as a contour plot across the section.

Ultrasonic tomographic investigation involves measuring the time-of-flight of an ultrasonic pulse, along many ray paths through a section of the beam. The data is then processed using tomographic software and the results given as a contour plot of velocity across the section.

2.2.3 Conclusion

1. Field trials have shown that time-of-flight tomography potentially provides a highly successful method of investigating post-tensioned concrete beams.
2. The method is somewhat time consuming and so should be used in conjunction with a simpler testing method, eg. Sonic impact-echo, which identifies areas of interest.
3. The smaller the ducts to be investigated, the smaller the increase in the on-site testing time.
4. Array systems could be developed which would greatly reduce the testing time.

2.3 Chang, Y., Wang C., and Hsieh C. (2001) Reflection seismology

Chang, Wang, and Hsieh, describe the theory of reflection seismology. The multi-sources and multi-receivers are distributed on the surface of a two-layer system to generate and pick up the ultrasonic waves, respectively. Offset is the distance between the source and receiver. The near offset and far offset are the distances from source to first receiver and last receiver in a spread, respectively. When source 1 is trigged, 48 receivers in spread 1 simultaneously record the reflected echoes from the interface of the two-layer system. After the source 1 shot, the source and all receivers move forward a unit distance, then source 2 is triggered and the 48 receivers in spread 2 record the reflected echoes, and so forth. The middle point between source 1 and receiver 1 on the interface of the two-layer model is the common depth point (CDP) CDP1, and the middle point between source 1 and receiver 2 is the CDP2, and so on. The fold number is defined as the number of time

histories having the same CDP and the time histories will be stacked (added) together. In this configuration, the CDP1, and CDP2 have 1-fold and CDP3 has 2-fold. The time histories having different offsets but the same CDP are sorted to a CDP gather which is a side-by-side display of time histories. The normal move out (NMO) is the time difference of the echoes reflected from the CDP between the zero offset measurement (source and receiver located at same point) and some offset measurement. Before stacking (adding) the time histories in a CDP gather, the (NMO) corrections for the time histories are required. After stacking, the new time history can be considered as the echoes recorded directly above CDP using the single-probe pulse-echo method. The section is constructed by side-by-side display of the new time histories and contains information of any cracks presented in the concrete

The advantages of this method are that the signals reflected from the interface will be enhanced and it is not necessary to pick the travel times or the waveform of the reflected echoes for analysis. The necessary data processing can be conducted using a personal computer and the output represents an image of the geometry of the reflecting interface.

2.3.1 Conclusion

The ability of detecting cracks in concrete relies strongly on the capability of the sensing system, techniques, and theories of detection, and signal processing techniques for record data. The ultrasonic system and data processing techniques, that we used in this study, demonstrate that horizontal cracks of length 3 cm, depth 6 cm and of length 5 cm, depth 14 cm and an inclined crack with a 15^0 dip

angle, 6 cm deep can be imaged successfully. Although not all the cracks in concrete can be detected, some of the small cracks in concrete structures can be detected by the reflection seismology method that other ultrasonic nondestructive methods would miss. This paper shows that the more weakness of the echoes reflected (or diffracted) from the crack, the more measurements from different surveying angles (offsets) are required for the stacking process on order to make a correct estimation of the crack. The quality and resolution of the signals can be improved by stacking the measurements after some necessary correction.

2.4 Titman, T.J. (2001)

Infrared thermography

According to Titman, infrared thermography is a well-established tool in the armory of non-destructive testing (NDT) and monitoring techniques. It can be used to investigate a very broad range of situations where variation in surface temperature may indicate a problem in or a particular property of the material(s) below the surface.

In the context of this paper, the successful application of thermography has become possible due to the development of sophisticated portable thermal imagers, specifically designed for NDT and condition monitoring.

In view of its totally non-destructive and non-invasive nature, a thermographic survey may, in general, be very rapidly completed, with minimal access requirements and can therefore be very cost-effective. The 'visual' nature of the output can frequently lead to an immediate interpretation by a skilled practitioner.

One aim of this paper is to increase awareness of the potential range of applications in civil and structural engineering. It is also important to mention limitations; situations where thermal imaging may not be appropriate.

High winds can reduce the effectiveness of outdoor surveys due to surface temperature shear effects. Similarly, rain may lead to surface cooling, thus masking thermal effects from below the surface. Standing water on roofs must be avoided.

2.4.1. General principles

All bodies above absolute zero temperature emit electromagnetic radiation. Whilst visible light occupies a narrow spectral band (0.4-0.7 μm), thermography, as the name implies, utilizes the ability of specialized imagers to detect radiation in the 'thermal' part of the infrared spectrum, typically in the 3-5 or 8-14 μm windows.

There are three types of conditions necessary for thermography to be useful. These are as follows:

Heat (cold) source

An object at depth is hotter (or colder) than the medium in which it is embedded. The corresponding raising (or lowering) in surface temperature directly over this object may enable its location. The temperature of the object (relative to the general surrounding material), together with its depth below the surface, will have a bearing on its detectability or resolution from adjacent similar warm objects.

Thermal gradient

If a stable thermal gradient exists through an element of a structure and there is no significant variation in thermal conductivity of the materials

within the element, (then the surface temperature over the warm face should be constant; and similarly for the cool face. Material omission, or local damage within the element, lead to variations in conductivity which are indicated by surface temperature fluctuations.

Induced heating

In the absence of either of the above, application of a hot (or cold) source to a surface will cause the surface to heat up (or cool down) at varying rates and to differing ultimate surface temperatures depending on the thermal resistance

2.4.2 Conclusion

A wide range of structural situations has been considered where a thermographic survey can be useful. Whether used in isolation or in combination with other techniques, thermal imaging can prove highly cost effective in view of its speed and the general lack of access requirements compared with other methods. The results, in the hands of a skilled practitioner, can be very graphic and immediate to understand.

2.5 Halabe, U., and Franklin, R. (1999) Spectral Analysis or Ultrasonic Signals

Halabe and Franklin describe the use of spectral analysis or ultrasonic signals in identifying areas of distress in different construction materials. Despite the success with time domain analysis for certain applications, several researchers have recognized its limitation and suggested the use of frequency domain analysis to enhance the sensitivity

and reliability of ultrasonic testing. Horne and Duke have shown the need for using normalized power spectrum to analyze ultrasonic signals shat are dispersive using three case studies. Fast Fourier Transforms (FFT) has been used to characterize wave attenuation in wooden members. Some researchers have stressed the need for frequency domain analysis for crack detection. Also, power spectral density (PSD) analysis has been used to detect cracks in metal plates.

Engineers emphasize the use of frequency domain analysis and employs power spectrum analysis in conjunction with time-of-flight measurements to detect flaws in structural materials. The underlying philosophy of the spectral analysis has been discussed along with the necessary measurement conditions. The methodology presented here will greatly help in identifying areas of distress in infrastructures built with various construction materials as in aluminum, wooden, and composite wrapped concrete members.

2.5.1 Conclusion

The advantages of using spectral analysis have been illustrated in this paper using three case studies involving metallic, wooden, and composite structural members. Parameters related to the PSD curve, namely the area, third moment, and central frequency; provide additional information which can be very useful in identifying and characterizing defects. The necessity of using suitable couplant as well as proper clamping forces for consistent and repeatable amplitude measurement and spectral analysis has been emphasized in this paper.

2.6 Yeih, W., and Huang, R. (1998) Ultrasonic Testing

In a study made by Yeih and Huang, the amplitude attenuation method in ultrasonic testing was used to evaluate the corrosion damage of reinforced concrete members. It is found that the amplitude attenuation method has good performance in corrosion detection for reinforced concrete members. There exists a consistent relationship between the average amplitude attenuation and the electrochemical parameters such as open circuit potential values, the instantaneous corrosion rate, and thickness loss.

UT has not been used in concrete detection as commonly as it has been used in metal detection. The reason for the limited applications of UT in concrete structures is that the penetration depth required in concrete members is usually much longer than that in metal members. For full penetration of ultrasonic wave in RC members, a lower excitation frequency (e.g., 500 KHz) should be used. However, a lower excitation frequency induces longer wave length, so that a loss of resolution may occur. The UT method (direct pitch and catch method) employs an excited transducer, usually Piezometric Transducer (PZT), to excite a mechanical wave and the mechanical wave propagates inside the object to be detected. A receiver (PZT) is mounted on the other side of the object to receive the signals of this mechanical wave. According to the wave signals, two important parameters, pulse velocity and amplitude, are frequently used to analyze the integrity of the object. The pulse velocity is calculated from dividing the total wave path length by the total flying time it required. When a flaw (for example, a major crack) is along the wave path, the total flying time of the wave is longer due to the diffraction of

wave. The amplitude attenuation is mainly due to the dispersion and dissipation of wave. In a corroded RC structure, the scattering phenomenon of wave by cracks, the dissipating oscillation due to cracks, and reduction of transmitted wave due to the change of acoustic impedance either from cracks inside the concrete or rust on the concrete-rebar interface result in additional amplitude attenuation compared to an undamaged body. According to the UT method (10), the wave signals reflect information along the wave path. When only a spot is examined, this is called an A-scan. When spots are connected into a line, this is called a B-scan. When the lines of B-scan are combined, information on the examined surface can construct the C-scan. For a 3-D view, the D-scan can be constructed by combining information on all surfaces of the object.

Although application of the UT method in concrete detection has been limited, there have been several successful attempts. Concrete strength was reported to have an empirical relation with UT pulse velocity and the pulse velocity method was used to evaluate cracks in concrete.

2.6.1 Conclusion

The average UT amplitude attenuation percentages have been found to have interesting relationships with electromechanical parameters in accelerated corrosion experiments. The average UT amplitude attenuation in the higher strength concrete was easier to detect because of the brittle microstructure. Due to the rebar size effect, specimens with smaller size rebars had more significant UT amplitude attenuation than those with larger size rebars in the beginning stage of corrosion process.

This paper can provide another possible method for evaluating corrosion damage. Although the proposed approach is not as mature as traditional electrochemical methods, it appears that this method is a fruitful area for further research.

2.7 Popovics, J. S., Achenbach, J. D., and Song, W. (1999) New Ultrasound and Sound Generation Methods.

According to Popovics et al. transient stress waves offer a powerful approach for non-destructive condition evaluation of concrete structures. However, currently used stress-wave-generating techniques are limited by poor controllability and/or penetrating ability. Stress wave generation must therefore be improved so that the application of existing and new ultrasonic and sonic non-destructive testing techniques to concrete structures will be more effective.

In this paper, electromagnetic and piezoelectric based stress wave sources are investigated for potential applicability with existing concrete non-destructive evaluation (NDE) techniques. A suitable stress wave source must be flexible in terms of input signal control, in order to be used with the various non-destructive stress wave techniques. The final signal source must also be effectively applicable to rough surfaces of unprepared concrete structures. In particular, the following characteristics should be considered for each potential stress wave source:

(a) Frequency-content control (a frequency range of 1-50 kHz is desired)

(b) Control of the magnitude of the .loading force (the source must be able to propagate signals through attenuating material with large path lengths and unprepared surfaces)

(c) Wave mode generation (the ability to generate longitudinal-type and/or surface-type waves is desired).

2.7.1 Current methods for stress wave generation in concrete.

At present, two methods are commonly used for the generation of transient stress waves for testing concrete: traditionally excited piezoelectric sources and impact events.

1. Traditional piezoelectric excitation

Transient ultrasonic waves generated by traditional piezoelectric excitation are a result of the resonance vibration of a piezoelectric crystal, housed within a transducer unit, in direct contact with the inspected concrete structure. The crystal is driven by an electrical signal supplied by an attached pulser-receiver unit; the driving signal typically has the form of a voltage spike and the amplitude can range from 300 to 1000 V. The control of frequency content and pulse length is therefore achieved by changing the piezoelectric transducer, as each transducer has a characteristic resonant frequency and bandwidth, while the electrical driving signal remains the same. This source type is designed primarily for the inspection of engineering materials other than concrete, and transducers with a relatively high frequency range of 0-25 to 10 MHz are typically utilized. The principal drawback of using traditionally excited piezoelectric transducers as stress wave sources for concrete is the

inability to generate controllable and usable signals in the desired frequency range of 150 kHz which may be applied in existing NDE techniques.

2. Impact

The use of mechanical impact, such as a single ball drop or hammer strike, as a source of transient stress waves for specific non-destructive tests of concrete has been widely reported in the literature.'" The technique is popular because relatively large stress wave energies may be easily generated. Since the character of the generated stress wave is primarily a function of the vibration properties of the impactor, the pulse shaping ability (centre frequency and frequency content control) is limited to controlling the impact duration and intensity. Theoretically, the frequency content of the wave action generated by a ball drop on an elastic half-space can be controlled by varying the ball size and drop height, as defined by the Hertz solution for impact; the size of the impacting ball is the most significant factor in controlling the input frequency content. The frequency distribution of impact-generated wave pulses is generally broad, and the frequencies are relatively low-generally below 30 kHz. Control of the generated stress wave field in the material is limited: impact sources generate all wave modes (longitudinal, transverse and surface) with non-planar wave fronts. The principal drawbacks of Using impact sources for stress wave generation in conjunction with concrete-testing techniques

are poor signal consistency. Poor signal controllability in terms of frequency content and poor stress wave field directivity control.

2.7.2 New methods for stress wave generation in concrete.

1. Frequency-modulated chirp driving signal.

The use of piezoelectric-based stress wave sources which are driven with a frequency-modulated (FM) chirp electrical signal in place of a voltage spike has recently been reported for use in concrete testing. In contrast to traditionally excited piezoelectric sources, the characteristics of the electrical driving signal, rather than the resonance of the piezoelectric crystal, primarily determine the character of the resulting stress wave. The advantages of such excitation are improved control of the character of the stress wave in terms of centre frequency and frequency content and increased signal penetrating ability within the frequency region of interest, assuming that the driven source is suitably well behaved in a given frequency region. A drawback of FM chirp signals is the need for an advanced random signal synthesizer to generate the signal. An application of these stress wave sources for existing, practical concrete-testing techniques could not be found in the literature.

2. Amplitude-modulated driving signal.

Electrical signals in the shape of amplitude-modulated (AM) sine bursts may also be used to drive the stress wave generators. AM burst-driven sources have the same advantages as those driven by

FM chirps. However, sophisticated signal synthesizers are not required to generate AM burst signals. AM burst signals are obtained from two basic waveform generators connected together: one generator, designated as the carrier signal generator, generates a sine burst (tone burst) of a given frequency and cycle length; the other generator, designated as the modulating signal generator, amplitude-modulates the burst with a sine or ramp function of lower modulating frequency. The only requirements for the signal generators are that the carrier signal generator must have tone burst generation and eternal AM input capabilities and that the modulating signal generator must have an external trigger input capability.

2.7.3 Conclusions

The following conclusions are drawn on the basis of the data presented in t this study.

a) Basic, readily obtainable signal generators and laboratory equipment may be assembled to generate AM-Burst driving signal.
b) Piezoelectric ultrasonic transducers and electromagnetic modal shakers which are driven by AM bursts provide controlled and usable stress wave pulses in the frequency range needed for concrete testing: an appropriate electromagnetic modal shaker provides the lower-frequency signals (below 10KHz), while an

appropriate piezoelectric transducer provides the higher range (15=50KHz).

c) Piezoelectric ultrasonic transducers and electromagnetic modal shakers which are driven by amplified AM bursts provide stress waves with sufficient energy to test full sized concrete structures.

d) The versatility of AM-burst driven sources makes them eminently suitable for application to concrete testing techniques such as the impact echo and spectral-analysis-of-surface-waves tests.

e) AM-burst-driven stress wave sources offer excellent frequency-content control and significant noise reduction capability not found in the stress wave sources currently used with concrete test.

2.8 Wang, X., Chang C., and Fan L. (2001)

2.8.1 Direct measurement NDT&E techniques

Direct measurement techniques can be used to measure the properties of materials and the corrosion state in bridge damage detection directly. These techniques could be based on various physical parameters. However, a technique is sometimes not suitable for in situ application. In a slightly destructive manner, however, samples could be taken from a bridge by using DS. HCPM can be used for detecting the rate of the corrosion of the steel bars in reinforced concrete. MFL can be used for locating the fracture of steel rebar in reinforced concrete and for detecting the corroded and broken cables for bridge cables.

2.8.2 Inquiring agency ND T&E techniques.

Inquiring agency techniques use an inquiring agent as a probe and which can be active or passive. The agent usually is a wave packet. In active techniques, the wave packet is generated by the testing instrument and transmitted into the materials to be tested. The examples are UT and GPR. The probe agent, the wave packet, interacts with the material and the foreign objects if it exists. Then it gives out some signals, which are carrying the information about the specimen. In passive techniques, the wave packet stems from the tested specimen itself and carries the information about the process the specimen is undergoing. An example is AE.

Mechanical Wave Techniques (MWT)

The MWT take mechanical waves as the working agency. The principle of these techniques is the generation, propagation and reception of mechanical waves. The wave packet transmitted into the materials to be tested interacts with the material and changes its own parameters, which carries the information about the properties of the tested object. MWT can meet most of requirements for NDT&E in bridge engineering. They are accurate in determining shape, size and depth of the defective areas, with high sensitivity, deep penetration, low cost, easy and fast operation, and convenient for in-situ use. Working in the ultrasonic band, as an active method, UT can locate and identify defects, fractures, voids and inhomogeneous regions can measure thickness and size of defects, can estimate strength of steel and concrete in bridges. AE is one of the most

important passive NDT&E techniques. Due to its passive measurement nature, AE can be applied to measure the object when the loads are actively added on a specimen and to monitor the dynamic behavior of structures such as bridges and buildings. It has been used to measure stress, identify rebar corrosion, locate corrosion position, estimate corrosion rate and monitor the cracking behavior of concrete. It is an extremely powerful technique for evaluating properties of the fracture and corrosion process. Working in the acoustic and low ultrasonic frequency band, as an active method, IE can be used to detect and locate flaws, fractures, voids, and delaminations in bridge deck and girder. It can also measure the depth of the flaws.

Electromagnetic Microwave Techniques (EMT)

The EMT uses the special band of electromagnetic wave as the inquiring agency. As an active method, it is based on the physical laws on microwave generation, propagation and reception. By determining the wave velocity, reflection coefficient, and the attenuation and the velocity of the microwave packet to be tested, reliable and reproducible results can be obtained, which also depend on electromagnetic parameters of the material and the geometrical parameters of the object. By measuring the time of flight of microwaves, or the attenuation during passing through the testing object, or the reflection/transmission coefficients, one can deduce the parameters of the tested object, hence, to deduce some information

about the structure and the mechanical properties of the tested object. As most of the non-metal materials are transparent to electromagnetic waves, EMT possesses many advantages over other techniques. It can penetrate more deeply than ultrasound and is very sensitive in detecting the foreign metal objects inside the non-metal matrix, such as steel bars in concrete. It can detect a flat defect, which is difficult to detect by X-ray techniques. It is not sensitive to aggregate size and type. It can precisely locate the objects and has a wide range of measurement from microns of thickness of paint coating to meters of concrete articles. GPR is one of the most successful techniques using in bridge damage detection. It has been used for detecting bridge pier scour and deck delamination.

Optical Techniques (OT)

The OT uses light waves as the inquiring agency. It is an active method and is based on interferometry and energy transportation. Representative of OT techniques applied in bridge damage detection is Infrared Detection (IRD). IRD uses the infrared light as the inquiring agency. It does not rely on the wave properties as do other wave based techniques. The thereto-properties of materials provide the basis for the measurements. It is also a non-contact, remote, and real time technique.

The temperature resolution can reach 0.01 ^{o}C. Different kinds of Infrared Thermometer (IRT) systems are used in the implementation of IRD. IRT maps the isotherms over the surface of a component using a heat-sensitive

device. By being loaded with heat energy, for example the sun's radiation, the object to be tested is pre-heated. There is a temperature distribution formed and the defects beneath the surface will affect the surface temperature and cause differences in the surrounding area, which can then be recognized from the map. IRT systems have been used for detecting delamination of reinforcement concrete bridges.

Yanev (1995), Zachar et al (1992), and Maser et al (1990) have presented the principles and application of IRT for detecting deterioration of bridge decks. TFHRC (1997) has reported two ongoing projects applying IRT: 1) to detect and quantify the fatigue cracks in steel highway bridges; 2) to develop a dual-band IRT imaging system for bridge deck inspection.

Other Techniques

There are also many other NDT&E techniques applied in bridge damage detection. These techniques could be an innovation and/or an integration of the techniques mentioned above. One example is the embedded corrosion microsensor (ECMS). The ECMS is developed to quantitatively measure the corrosion activity inside concrete. It is small and inexpensive which will allow hundreds or thousands of them to be embedded in concrete structures. The integrated circuit provides electrochemical measurements of corrosion rate with polarization resistance, and measures chemical parameters such as pH, chloride ion concentration, and

temperature in an embeddable package. It is powered and it telemeters sensor data via wireless communication.

2.8.3 Conclusion

There are thousands of research papers which have contributed to vibration-based damage detection methods. These methods have been successful to a certain extent, especially when the overall damage is significant. However, their application in bridge structures is often challenged since significant local damage might not cause observable difference in the observed quantities and because the number of measurements which can be made is limited. Much of this is related to systematic errors between the model and the structure and the non-stationary of the structure, and the modal data of concrete structure is particularly different to interpret, due to the non-uniformity of the material. Robust identification techniques that are able to locate damage based on realistic measure data sets still seem a long way from reality. Certainly however, if the horizons are reduced and significant prior knowledge of the structure is included and sufficient measurements are taken, some progress can be made in some applications.

One scenario is that damage detection using low frequency vibration is undertaken to identify those areas where more detailed local inspection should be concentrated. The most promising methods seem to be based on modal data and rely on the forward type identification methods. Even so, relying on low frequency vibration data will always be able to locate damage with a limited accuracy because of the global nature of the methods.

Special instruments have shown great advantages in doing some specialized things better and more effectively than the general one. More commercial instruments for different specific purposes need to be developed. To select the proper NDT&E techniques is important. In bridge damage detection a problem usually requires different NDT&E techniques. Two or more independent techniques are needed for confidence in the results. However, information from different NDT systems can be conflicting, incomplete or vague if studied as discrete data. The new data fusion techniques seem to light the way to correct answers.

2.9 Karagouz, M., Bilgutay, N., Akgul, T., and Popovics, S. (1998) Split Spectrum Processing

SSP was initially introduced to enhance the signal-to-noise ratio for nondestructive testing of materials. This technique was shown to be effective in flaw enhancement, particularly in the detection of targets with similar spectral characteristics, yielding the hidden target information. The SSP method has been successfully used for noise suppression in non destructive testing of stainless steel and has the potential to improve detection of discontinuities in concrete as well. However, application of SSP to concrete is difficult because the internal structure of concrete varies within much wider limits than that of polymer composites or material, and the scatterers in concrete vary in size to a much greater extend than in metals. There are several different scatterers in concrete, such as aggregate particles, voids, cracks, delaminations, etc. This is a more complex

microstructure than in metals; the aggregate type and quantity can vary within can vary within wide limits in concrete. However, the preliminary tests have produced encouraging results with SSP, which appears to be a promising new technique for concrete inspection.

In SSP, the backscattered wideband signal from concrete passed through a Gaussian filter bank to obtain signals at different normalized individually, giving zero-mean outputs. This introduces weighing to the frequency bands, which should have the effect of flattening the original spectrum, thus broadening the effective bandwidth and improving the system resolution. Subsequently these signals are combined nonlinearly to obtain the processed signal where the interference noise caused by backscattering is suppressed.

2.9.1 Conclusion

Split spectrum processing makes it possible to use ultrasound of MHz frequencies for testing. Despite the presence of significant scatterer noise, both the minimization and polarity shareholding algorithms reduce the noise level and help identify the ultrasonic signals reflected from the back surface and targets of interests.

The experimental results demonstrate the potential of SSP for signal-to-noise enhancement of high-frequency ultrasound signals in concrete. This improvement can be related to the decorrelation of grain echoes resulting from frequency shifts between the transmitted signals. These results not only illustrate the capability of

SSP in detecting multiple targets simultaneously, but also the ability of detecting discontinuities that are not readily visible in the unprocessed data.

The results presented in this study indicate that SSP is effective for detection of discontinuities and thickness measurement in concrete. The methods can be easily extended to two dimensional ultrasonic imaging of concrete, which is planned in future work.

2.10 Rens, K., Transue, D., and Schuller, P. (2000) Acoustic Tomographic Imaging of Concrete Infrastructure

According to Rens et al, Schuller et al. (1994) used the tomography technique to monitor the effectiveness of grouting repairs to masonry structures. Tomograms taken before and after grout injection were compared. The postrepair tomograms showed areas of increased velocity, indicating sound material. Rhazi et al. (1996) report success using a similar method.

Several successful efforts have been made to image concrete sections with X-ray and gamma-ray tomographic systems. Morgan et al. (1980) used X-ray scanners to create tomograms of concrete cylinders. Narrow cracks of <1 mm in width were clearly identifiable. Martz et al. (1993) produced images of reinforced concrete specimens with a spatial resolution of 1 mm in the laboratory using a gamma-ray scanner. Where Martz scanned from all angles, Heiskanen et al. (1991) used a gamma-ray tomographic system to image reinforced concrete specimens from a limited number of angles.

Olson and Sack (1995) developed an acoustic imaging system for quality assurance testing of drilled pier foundations. Adapting the geophysical technique of cross borehole tomography, boreholes are cast in the foundations and sending and receiving probes are sent down the water-filled holes. Tomographic images are created from this data to check the integrity of the material between the boreholes. The writers have successfully located defects in the field with this system.

Jalinoos and Olson (1995) developed a high-speed ultrasonic tomography system to detect flaws in concrete structures with two-sided access. such as bridge members, columns, and walls. This research effort focused on the development of a rapid data acquisition method in order to make the technique practical for general use. A rolling ultrasonic transducer was used to send signals at regular spatial intervals to an array of fixed receivers on the opposite side of a test wall. This system proved capable of locating flaws that had been cast into the test wall.

Schuller and Atkinson (1995) and Woodham et al. (1996) developed an acoustic tomography system for structural concrete and masonry. This system can locate large steel inclusions, voids, cracks, and zones of low density. This system provided useful results for an evaluation of a masonry structure, where tomographic images were used to identify cracks and deteriorated material in a masonry wall.

2.10.1 Conclusion

The radiographic methods mentioned in the literature review produce excellent tomographic images but require expensive equipment that is not field portable at this time. The images produced using acoustic tomography have less resolution than those of the radiographic methods (-5-20 cm as opposed to 1 mm), but the equipment is more economical and does not require extensive training and safety precautions. The cost of the X-ray and gamma-ray systems is about 10 times that of an acoustic system. The data collection for acoustic tomographic analysis is performed using the same equipment that is commonly used for ultrasonic testing, with the exception of the multiplexing system.

The results of a survey of the state DOTs indicate that such applications are attractive to the practicing NDE community. The lack of standards for the technique is a drawback for routine use, but the procedure is relatively straightforward and could lend itself well to standardization. Colorado, working group sessions were held to help brainstorm standardization techniques for several different construction materials and NDE techniques. In the official working group report that followed these sessions (Schuller and Woodham 1996), recommendations toward the standardization of tomography were proposed. Copies of the working group report were forwarded to the American Society for Testing Materials. Leiphart et al. (1999) developed a statistical process called a gauge potential study, which improves the reliability of acoustic tomography. This gauge study also holds possibilities for incorporation into a standard.

The responses of the questionnaire also indicated concerns about interpretation and speed of the actual results. As indicated in Case Study 2 and 3, the use of the array halved the time required collecting a data set. Concerns about result interpretation continue to be a problem associated with all non destructive techniques. Unfortunately most NDT results are still user dependent and interpretation can take some degree of ingenuity.

2.11 Koehler, B., Hentges, G., Mueller W. (2001) A Novel Technique For Advanced Ultrasonic Testing Of Concrete By Using Signal Conditioning Methods And A Scanning Laser Vibrometer

The pulse echo technique is carried out by sending frequency modulated chirp signals and performing a cross correlation between the received and the transmitted signal. In combination with the application of recently available ultrasonic concrete probes as transmitter, this leads to an improvement of the signal to noise ratio. A laser doppler interferometer, equipped with a random speckle modulator, is used as detector of the ultrasound. Finally, the data sets can be processed with various methods, involving the time signals of several space points. Examples are the space averaging and the synthetic aperture focusing technique (SAFT). The advantage of the suggested technique is demonstrated by practical measurements. The improvement compared to standard laser interferometric measurements will increase the feasibility of laser interferometric detection for non-destructive testing in civil engineering.

The difficulties of non destructive testing of concrete by ultrasonic methods result from the strong signal attenuation, caused mainly by scattering at the in homogeneities of concrete. Besides decreasing the transmitted ultrasonic signal, it leads to strong coherent noise. This noise can mask even large back wall echoes totally. Scattering diminishes for decreasing frequencies. Therefore, rather low frequencies in the range of about 100 kHz must de used. There has been some progress in resent time. Highly efficient transducers have been developed and are available now. Pulse-compression is known to improve the signal to noise ratio in situations with a high insertion loss. It has been applied to ultrasonic testing of concrete successfully. It is well known from ultrasonic testing in other fields, that space averaging techniques suppress the coherent back-scattering noise effectively). For applying such methods, signals from a large number of measurement points are necessary. They can be obtained in a convenient way by using laser interferometric detection. In the interferometric detection is performed in a 2D scanning aperture and the measured data are reconstructed by the 3D-SAFT algorithm involving itself spatial averaging. Till now the main problem of laser interferometry has been the insufficient sensitivity, resulting in a low signal to noise (S/N) ratio. This is a special problem in an automatic scanning mode, because no fine focusing can be performed, resulting in large incoherent (electronic) noise of the interferometer. Thus, improvement of the signal to noise ratio is crucial for application of laser interferometric detection and space averaging techniques. We improve the S/N ratio by several methods. On the one hand we increase the signal by applying the very efficient probes mentioned above as transmitter and including the pulse compression technique in our system and on the other hand we reduce the laser vibrometer noise by implementation a random speckle

modulation technique C). By this method we get signals of tolerable incoherent noise appropriate for signal processing to suppress the additional coherent scattering noise.

2.11.1 Conclusion

The first results demonstrate the efficiency of ultrasonic testing with laser interferometric detection. In co-operation with pulse compression and random speckle modulation the signal to noise ratio can be reduced so that laser interferometric detection becomes practicable. The technique has to be developed to increase the processing speed. The described technique may help to improve the acceptance for ultrasonic methods in civil engineering. The 3D-SAFT reconstruction is able to increase the signal to noise ratio further and leads to a 3D-image of reflector distributions inside the specimen. Furthermore, the presented technique can be used as an advanced tool for experimental verification of modeling results concerning the propagation of ultrasonic waves in concrete. This is subject of current investigations.

2.12 Watanabe, T., Ohtsu, M., and Tomoda, Y. (1999) Impact-Echo Technique for Grouting Performance in Post-Tensioning Duct.

Impact-echo technique is a method for nondestructive evaluation, detecting elastic waves due to a mechanical impact. Although the impact-echo is reported to be promising for quantitative estimation, applicability to evaluation of post-tensioning tendon ducts is not confirmed yet. To this end, the basic theory of the impact-echo should be clarified. In this paper, a specimen containing ungrouted duct is tested. Theoretically, frequency responses of the specimen depend on the size, orientation of the void, and P-wave

velocity, while wave motions in concrete structures are characterized by material properties, incident waves, and size of members. Thus, the frequency response is studied from the relationship between the wave length and the depth of duct. Experimentally, impact tests are conducted by dropping steel balls and shooting aluminum bullets. The analysis is carried by the boundary element method (BEM). As a result, the detection of resonance frequency due to the presence of void is clarified, relating with impact frequencies and the depth of duct.

2.13 NDTnet (1996)
Comparison of Pulse-Echo-Methods for Testing Concrete

One of the principal objectives of the development of NDT-CE techniques is a reliable assessment of the integrity or detection of defects of concrete members even when they are accessible only from a single surface. Especially on reinforced concrete structures such inspections could in the past only be solved by means of radiography (for concrete thickness less than 0.6 m) or by using more or less destructive methods. Some of the current research aims are outlined below:

- location of tendons
- detection of voids in tendon ducts
- detection of compression faults or honeycombing
- information on geometrical dimensions

The used methods are briefly described below.

2.13.1 Radar

The radar investigation has been performed with the nominal 900 MHz antenna (center frequency: 1 GHz). First the transmission velocity of the electromagnetic waves was determined at different positions of both specimens. From these velocities, average dielectric constants of (8.7 +/- 0.2) and (9.4 +/- 0.3) were determined for specimens 1 and 2, respectively.

For locating the metallic duct and for thickness determination, the antenna has been moved in parallel tracks over the surface of the specimen. The amplitudes illustrate the strength of the reflections. From the dielectric constant and the transmission time, a concrete thickness of (508 +/- 10) mm is calculated. The concrete cover on the duct is (340 +/- 10) mm. The lateral position of the duct can be determined with an accuracy of +/- 10 mm.

The measurement results of both types of specimens with different Aggregate size do not differ significantly. Because of electromagnetic shielding the Radar measurements are not suitable to detect voids in the metallic ducts.

2.13.2 Impact-Echo

The impact-echo testing was performed using an impactor with a spring driven mass and piezo-electric displacement transducer, the frequency analysis was affected using a laptop. The multiple reflections of the longitudinal waves are analyzed to locate the duct and to measure the thickness. This gives clear peaks when only back wall reflections are apparent. When the duct position is measured

from the near surface, the maximum corresponding to the position of voids in the duct (17.3 kHz) is clearly detectable together with the back wall echo at 3.9 kHz. The impact response from the filled duct. The frequency of the reflections from the duct is characterized by multiple peaks with lower amplitude (interface section) and differs from the signals from an unfilled duct. The result shows that it is feasible to use the impact-echo method to detect the ducts, but has to be improved by field studies.

2.13.3 Ultrasonic Pulse Echo, A-scan

In order to overcome the specific problems of concrete, a specially developed low frequency flaw detector for construction site testing of strongly attenuating (sound scattering) materials was applied in combination with low frequency probes especially optimized for this field of application. Its A-scan display enables, even with concrete, the evaluation of the signal amplitudes and times of flight as with common ultrasonic material testing. Most of the test tasks set here could be solved for the specimen 1 (8 mm maximum Aggregate size) with satisfactory results.

2.13.4 Ultrasonic Pulse Array

The tests were performed with an array consisting of seven transducers. The fast setting mortar used as coupling agent is well matched to the acoustic properties of concrete. Another advantage is that the transducer array is held in the desired position without any additional device. The equipment used is described in detail in these proceedings. Measurements were made at all transmitter/receiver-

combination of adjacent transducers. This means a total of 24 single shots which cover an area of approximately 150 mm in diameter. The signals are processed by spatial averaging to suppress the effects of scattering at Aggregate particles. Signal processing was done by matched filtering and calculation of the envelope by utilizing the complex analytic signal. An explanation for the slight deviation of the depth measurement is the fact that the array covers an area so that the geometrical situations are not exactly the same for all single measurements.

2.13.5 Ultrasonic Pulse Echo, B-scan

By manually moving the US-IE transducer along the concrete surface (specimen 1, surface A) B-scans were generated on-line. This permits a lateral localization of the duct within ñ 5mm. This was repeated along 16 axes of the surface, so that the localization of the duct could be measured precisely. The position in the depth was interpreted from the simultaneous measured A-scans in the range from 102 to 78 mm depending on the site. The measurements were also possible from the reinforced half of the specimen, but yet no difference between void and filled duct could be detected. Further details are described.

2.13.6 Ultrasonic Pulse Echo, B-scan, LSAFT

Ultrasonic data is recorded in single transducer pulse echo technique along a linear aperture at regular spacing. A SAFT-imaging algorithm is employed to reconstruct a 2-dimensional section of the material below the aperture. The

resulting images, usually B-scans and demodulated SAFT-images, are plotted by means of the analysis software.

Aggregate size, sound path, and transducers contact to surface are most important to influence the quality of the images. The accuracy of the localization of an object depends on the knowledge of the exact pulse velocity which in turn depends on the length of the transit path due to dispersion.

2.13.7 Ultrasonic Pulse Echo: 2D-Synthetic Aperture and 3D-SAFT

When the two dimensional synthetic aperture technique is utilized with separate transmitter and receiver probes, the echoes from different directions will overlay. The negative influence of statistical materials in homogeneities can better be minimized than with a linear aperture. Additionally the measurement accuracy will be improved when shading appears. When the method of phase corrected superposition is applied (algorithm for thickness measurement on the basis of 100 A-scans), the thickness of a specimen without and with mesh reinforcement can be very accurately determined.

A large number of data is required for applying the 3D-SAFT algorithms. They are produced in our investigations by using a scanning laser Doppler vibrometer as an ultrasonic detector (typical number of dots 1000, screen width 10 mm). Another advantage of this technique is that apart from applying a reflective coating no special preparations are required even for very rough surfaces. The diameter of the void is about 20% of the aperture diameter so that the void and the

tendon duct can easily be identified when the thickness-sensitive algorithm is applied.

The three-dimensional image is produced according to the principle of the three-dimensional SAFT reconstruction. The intensity maximum correlates with the void position and indicates. No signals are received from the filled tendon duct so that the unfilled area can easily be identified.

2.13.8 EFIT Simulation

The Elastodynamic Finite Integration Technique (EFIT) is an efficient numerical code to model the propagation and scattering of elastic waves in inhomogeneous solids. For applications to concrete a special two-dimensional version has been developed, which allows to model statistical in homogeneities in terms of arbitrarily oriented ellipses of random distributed sizes and material properties. The code produces time frames of spatially propagating wave fronts and time histories of received signals on the specimen surface, so-called A-scans, A set of A- scans along a one-dimensional scan line can be post processed either with the conventional SAFT-algorithm or with a more elaborated EL-FT-SAFT scheme, which accounts for the elastodynamic nature of ultrasound and which includes mode conversion between pressure and shear waves.

2.14 Florida Department of Transportation District 3 (2001) Mid-Bay Bridge Post-Tensioning Evaluation

The post-tensioning system of the Mid-Bay Bridge has undergone a rigorous and testing regiment since the discovery of failed external post-tensioning tendons. FDOT and consultant inspection personnel have worked systematically and aggressively to catalog the condition of the bridge's post-tensioning system. The major inspections and tests conducted were:

- Sounding Post-Tensioning Tendons for Voids
- Bore Scope Inspections of Post-Tensioning Anchors
- Vibrating Testing
- Visual Void Inspections
- Mag-Flux Testing
- Grouting Mock-Up Tests
- Other Corrosion Related Testing

No one inspection or testing procedure is able to provide a complete evaluation of the corrosion of external post-tensioning tendons. Tests that give good results in the free length of external tendons do not give any results in the anchorage zones. Tests that give strong indications of active corrosion in a length of tendon do not necessarily predict the level of force in the tendon or section loss that has occurred. The proper approach for inspecting external post-tensioning tendons is to conduct a battery of tests specifically chosen to develop an understanding of the tendon conditions. This was effectively accomplished for the Mid-Bay-Bridge.

CHAPTER 3

SURVEY OF STATE DEPARTMENTS OF TRANSPORTATION

3.1 Introduction

A survey of Department of Transportation (DOT) was performed to determine their policies toward the use of post-tensioning concrete beams, and to collect information on any guideline on this subject. The survey was distributed to the Department of Transportation's Material Engineers for each state including the District of Columbia and Puerto Rico (52 total); of the 52 departments contacted, 33 responded, (63% response rate). A copy of the survey is shown in Appendix A.

3.2 Results of the Survey:

The raw data representing the results of the survey is shown in Appendix B. Of the 33 state agencies that responded to the survey, 20 states indicated that they use bonded post-tensioning systems, 3 states use unbonded post-tensioning systems, and the 13 do not use any. Figure 3.1 presents the number of states that use different systems of post-tensioning.

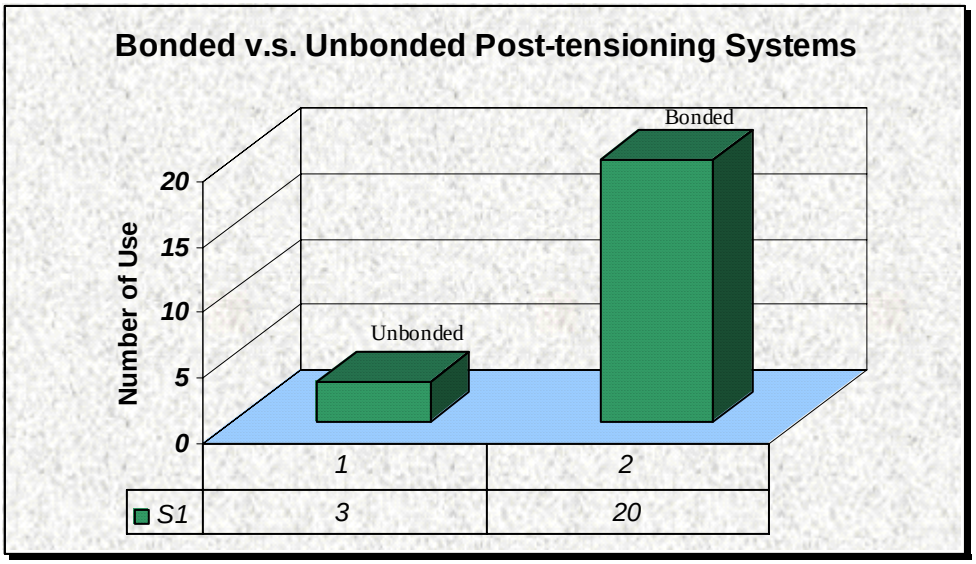

Figure 3.1 Results of Post-Tensioning Systems (Bonded and Unbonded)

Figure 3.2 represents the duct material that is usually used by different DOTs. They were classified into two categories, plastic or metal.

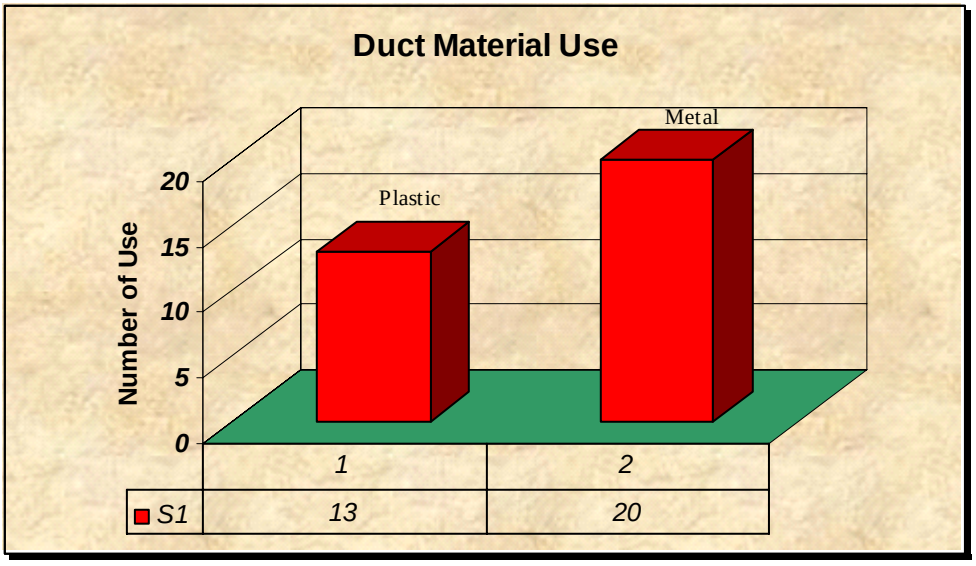

Figure 3.2 Frequency of Duct Material Used in Post-Tensioning

Figure 3.3 includes the different classes of grout used in post-tensioning. Actually they are four classes: A, B, C, D, and others.

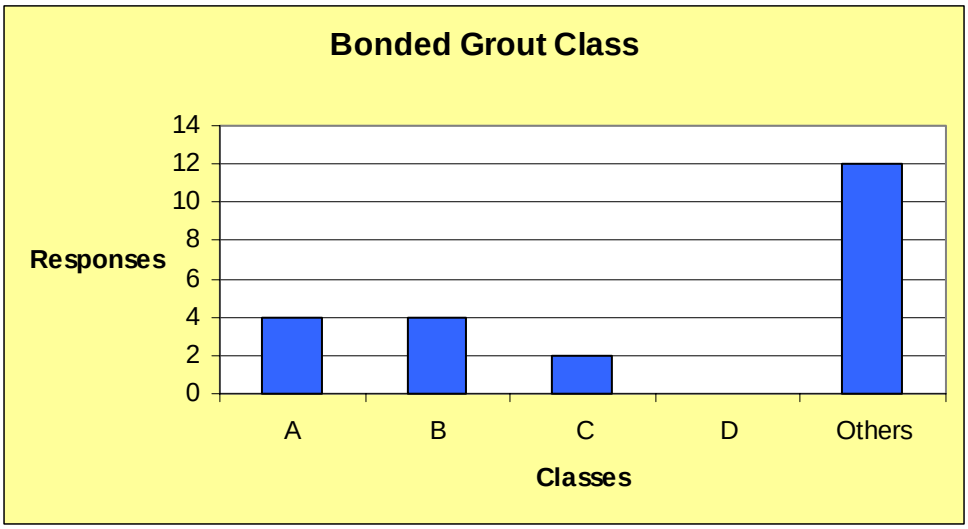

Figure 3.3 Bonded Grout Class Used.

Tables 3.1 and and 3.2 describe the nondestructive inspection method and the failure experienced by the DOTs for the bonded post-tensioning systems respectively.

The results showed that none of the DOTs use nondestructive testing or have even experienced any failure in their bonded post tensioning systems.

Table 3.1 Nondestructive Inspection Method.

Non destructive Inspection	Response
No	23
Yes	0

Table 3.2 Post-tensioning Failures Experienced by DOTs

Tendon's Failure	Response
No	22
Yes	0

CHAPTER 4

RESEARCH METHODOLOGY

4.1 Introduction

Figure 4.1 provides a graphic of the methodology followed for this research. The first step was to generate a literature review of past studies involving testing post-tensioned concrete elements and ducts. A survey was generated and distributed to all state departments of transportation to establish a possible idea about the use of post-tensioning, ducts, failures and the availability of testing procedures for post-tensioned concrete members. The results of this survey were analyzed using a certain statistical analysis. After that, a concrete sample including plastic and metal ducts was cast in the soils laboratory of the School of Building Construction for an experimental purpose of testing it using the various testing techniques.

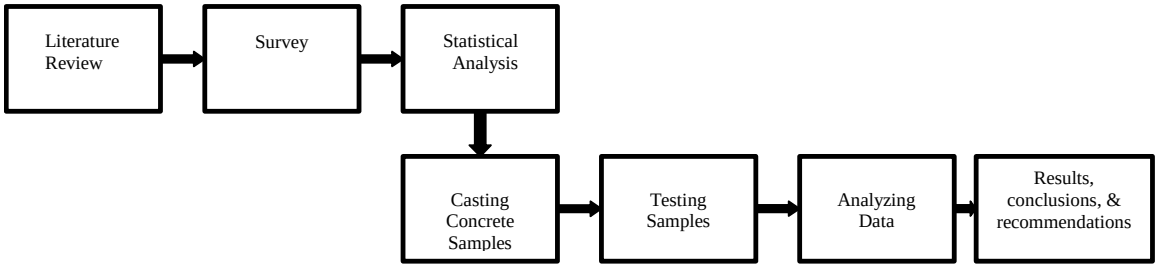

Figure 4.1 Research Methodology Flow Chart

4.2 NDE Technologies to be Evaluated

Ground Penetrating Radar (GPR)

Ground Penetrating Radar was not incorporated in this test series due to the fact that it is primarily used in this application to locate the position of the ducts incorporated in hardened concrete, since this was not a problem with this test series, this test was not performed.

Impact Echo (IE)

Impact Echo has been used successfully since the end of 1980s to detect cracks or voids in concrete slab or beam, and has also been used to detect defects inside of bonded post-tensioned ducts where the ducts are metal. Impact Echo requires only one-side access to the sample and incorporated Olson's new technology of "scanning" impact echo measurements, whereby a data point is taken every 0.8-inches of travel. This improvement allowed for faster testing and also improved the accuracy of the testing. This test was run on our samples, but experienced difficulty maneuvering on the small beam sample sizes, Figures 5 and 6. Data is forthcoming.

Ultrasonic Tomography (UT)

The Ultrasonic Tomography test requires access to 2 sides of a structural element in order to send and receive sound waves at multiple angles above and below ducts that allows imaging of internal concrete and duct conditions. The current technology use a single source and single receiver which results in a slow field testing process. This test was run on the four samples described previously. Olson is in the process of producing a scanning UT device that will be evaluated

during the next round of tests, instead of using a single source and single receiver, an array of sources and receivers will be used. This improvement will tremendously speed up the testing process, Figures 7 and 8. Data is forthcoming.

Spectral Analysis of Surface Waves (SASW)

The SASW method requires only one side access to the structure. In general, the SASW method uses the dispersive characteristics of surface waves to determine the variation of the shear wave velocity (stiffness) of layered system with depth. The SASW test was also performed on the test samples with great difficulty due to the beam sample size. Data was not obtainable using this technique due to beam sample size.

Olson Engineering, Wheat Ridge, Colorado, was identified as an organization that appears to have the necessary technology, know-how and experience to actively take part in this investigation. They have agreed in principle to provide us with the necessary equipment, on a rental basis, and the technical training to operate the equipment to evaluate a variety of NDT techniques on various grouted duct samples. The testing consisted of three phases:

a. Phase I. In phase I of this study, small beam samples (4-in x 4-in x 21-in) and (6-in x 6-in x 21-in) were prepared, incorporating small diameter corrugated metal and plastic ducts, 2-inches in diameter, and 3-inches in diameter respectively, and prefabricated defects. Three types of testing were conducted on these samples that included Impact Echo, Spectral Analysis of Surface Waves, and Ultrasonic Pulse Velocity.

b. Phase II. In phase II of this study, one of the concrete samples was prepared to have an empty section, partially grouted section, and a completely grouted section. Those sections incorporated two types of ducts: Plastic and Metal ducts. Three types of testing were conducted on both ducts: Impact Echo, Spectral Analysis of Surface Waves, and Ultrasonic Pulse Velocity.

c. Phase III. In phase III, the second concrete sample was tested according to the age of grout. Two testing were done daily during the first week of grout, and one testing was done daily during the following two weeks.

Finally, comparisons of the results were made, and conclusions and recommendations were presented.

4.3 Materials

Grout

MASTERFLOW 1205, ChemRex® Commercial Products Division, was used for grout in the ducts. It is specially formulated to produce a pumpable, nonbleeding, high strength fluid product with extended working time for grouting. It provides corrosion protection for highly stressed steel cables, anchorage and rods. To increase corrosion protection, MASTERFLOW 1205 is formulated with a specially graded aggregate that mitigates chloride migration while still allowing the product to be easily pumped long distance through small openings. The technical data guide and the material safety data sheet (MSDS) can be found in Appendices C and D respectively.

Mixing Grout

Since higher shear mixing improves fluidity, a drill with a 950 to 2900 rpm was used. Two gallons of water were added to every cement bag to achieve the necessary placement consistency. Three minutes of mixing with 80% of the required water is recommended for the product to reach a uniform consistency. After adding the remaining water, two additional minutes are required for mixing.

Ducts

Two types of ducts were used in this study. Corrugated metal and corrugated plastic of 3- inches and 2-inches in diameter respectively (Phase I), and corrugated metal and corrugated plastic both of 3-inch ID during Phase II and III.

Tendons

For the purpose of the study, number 8, 1-inch diameter Grade 60 bars (Phase I) and number 3, 3/8-inch Grade 60 bars (Phase II and III) were used instead of tendons which should not make any difference in the testing or analysis of results.

CHAPTER 5

TEST RESULTS AND DISCUSSION

5.1 Introduction

A company was identified, Olson Engineering, Wheat Ridge, Colorado, that has the necessary technology, know-how and experience to actively take part in this investigation. They have agreed in principle to provide us with the necessary equipment, on a rental basis, and the technical training to operate the equipment to evaluate a variety of NDT techniques on various grouted duct samples.

5.2 PHASE I

1. 2- 6x6x21-inch concrete beam samples were prepared incorporating a 3-inch diameter corrugated steel duct. A number 8 steel reinforcing bar was centered in the duct and defects were introduced into both samples prior to grouting the bar in-place, Figures 5.1, 5.2, and 5.3.
2. 2- 4x4x21-inch concrete beam samples were prepared incorporating a 2-inch diameter plastic duct. A number 6 steel reinforcing bar was centered in the duct and defects were introduced into both samples prior to grouting the bar in-place, Figures 5.1 and 5.4.
3. Grout used for the samples was Masterflow 1205, an FDOT approved post-tensioning grout produced by ChemRex® Commercial Products Division.
4. The samples were allowed to cure for 14 days prior to testing.

5. A representative from Olson Engineering performed the testing and training of lab personnel. Tests performed included “scanning” Impact Echo, static Ultrasonic Tomography and Spectral Analysis of Surface Waves.

Figure 5.1 Grouted Beam Samples

Figure 5.2 Grout Beam samples with Defect Locations

A schematic representation of the defect locations for both the grouted 3-inch corrugated metal duct samples and the grouted 2-inch plastic duct samples are shown in Figures 5.3 and 5.4.

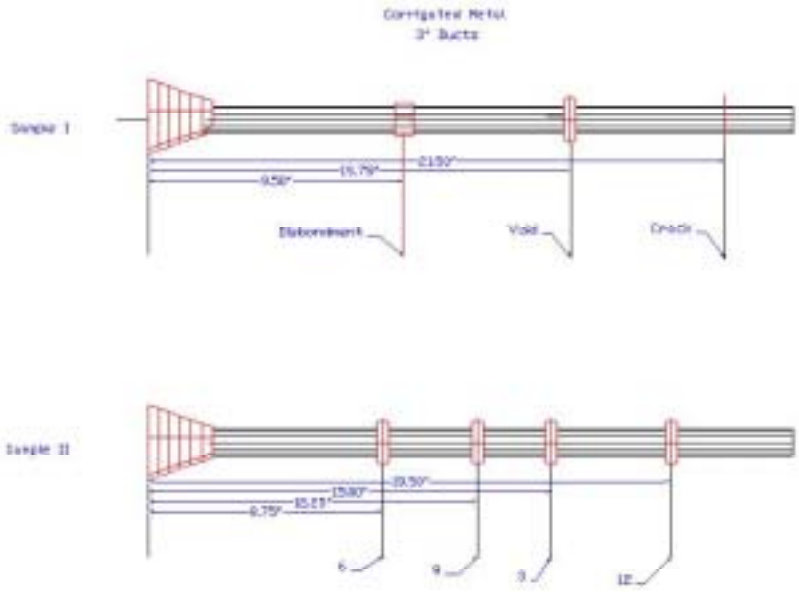

Figure 5.3 Schematic of Defect Type and Location Grouted 3-inch Corrugated Metal Duct Samples

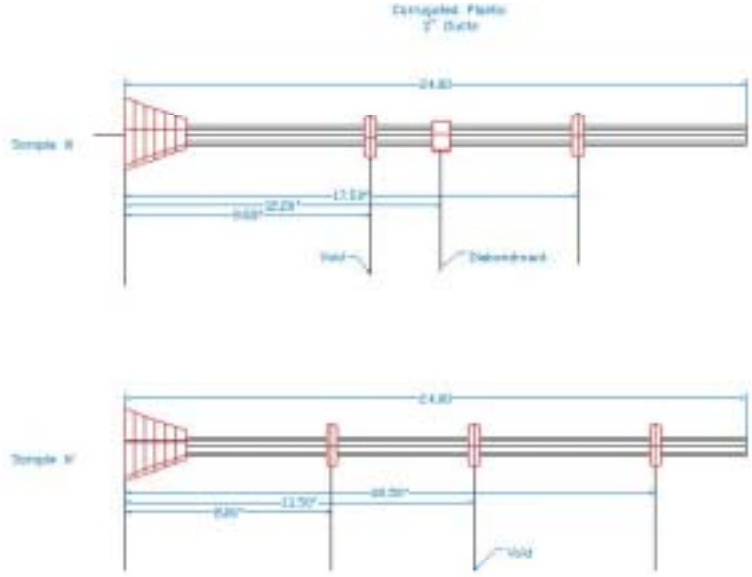

Figure 5.4 Schematic of Defect Type and Location Grouted 2-inch Plastic Duct Samples

5.3 NDE Technologies Evaluated

1. Ground Penetrating Radar (GPR)

   Ground Penetrating Radar was not incorporated in this test series due to the fact that it is primarily used in this application to locate the position of the ducts incorporated in hardened concrete, since this was not a problem with this test series, this test was not performed.

2. Impact Echo (IE)

   Impact Echo has been used successfully since the end of 1980s to detect cracks or voids in concrete slab or beam, and has also been used to detect defects inside of bonded post-tensioned ducts where the ducts are metal. Impact Echo requires only one-side access to the sample and incorporated Olson's new technology of "scanning" impact echo measurements, whereby a data point is taken every 0.8-inches of travel. This improvement allowed for faster testing and also improved the accuracy of the testing. This test was run on our samples, but experienced difficulty maneuvering on the small beam sample sizes, Figures 5.5 and 5.6. Data is forthcoming.

3. Ultrasonic Tomography (UT)

   The Ultrasonic Tomography test requires access to 2 sides of a structural element in order to send and receive sound waves at multiple angles above and below ducts that allows imaging of internal concrete and duct conditions. The current technology use a single source and single receiver which results in a slow field

testing process. This test was run on the four samples described previously. Olson is in the process of producing a scanning UT device that will be evaluated during the next round of tests, instead of using a single source and single receiver, an array of sources and receivers will be used. This improvement will tremendously speed up the testing process, Figures 5.7 and 5.8. Data is forthcoming.

5. Spectral Analysis of Surface Waves (SASW)

   The SASW method requires only one side access to the structure. In general, the SASW method uses the dispersive characteristics of surface waves to determine the variation of the shear wave velocity (stiffness) of layered system with depth. The SASW test was also performed on the test samples with great difficulty due to the beam sample size. Data was not obtainable using this technique due to beam sample size.

Figure 5.5 Scanning IE Device and Data recorder

Figure 5.6 Close-up of Scanning IE Device Relative to Specimen Size

Figure 5.7 Static Ultrasonic Tomography (UT) Test

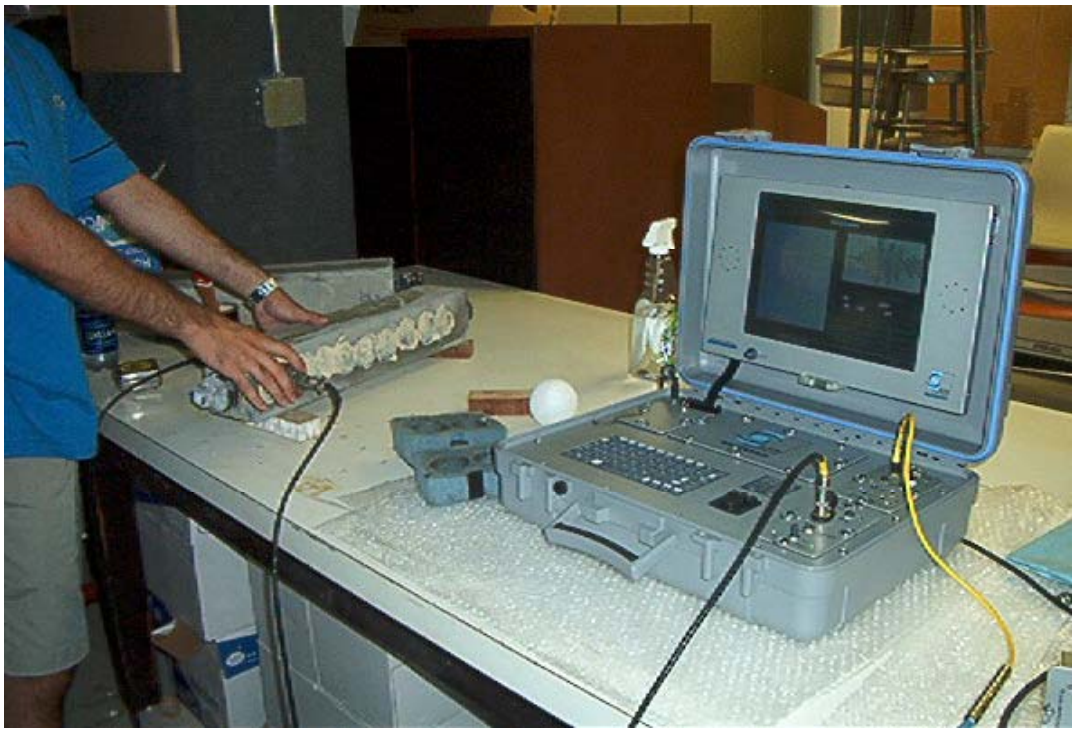

Figure 5.8 UT Test in Progress

5.4 PHASE I RESULTS:

Initially, we produced beams for both 3-inch corrugated metal ducts and 2-inch plastic ducts. The ratio of duct area to concrete area was kept constant as well as steel area to duct area ratios. The problem was that equipment Olson Engineering produced was designed to scan transverse the duct rather than along the duct longitudinally. Therefore, we will embark on producing larger test specimens that would allow for transverse inspection. Transverse detection should not pose a problem for prestressed or post-tensioned double tee beams, inverted tee beams, hollow core slabs, AASHTO I-beams, or AASHTO box beams.

5.5 PHASE II

Two mockup walls, each with one plastic duct (3-inch ID) and one steel duct (3-inch ID), were used in this investigation. The post-tensioning ducts on the first wall (Wall I) were divided into 3 sections. The bottom section of both ducts was fully grouted, the middle section of the ducts was partially grouted and the top section was left empty. Both ducts were filled with grout at the very top of the ducts. The second wall (Wall II) had both steel and plastic ducts inside without any grout, i.e. ungrouted void duct conditions. The pictures of both walls are shown in Fig.5.10. The walls are 9.5 inches thick, 3 ft wide and almost 4 ft high.

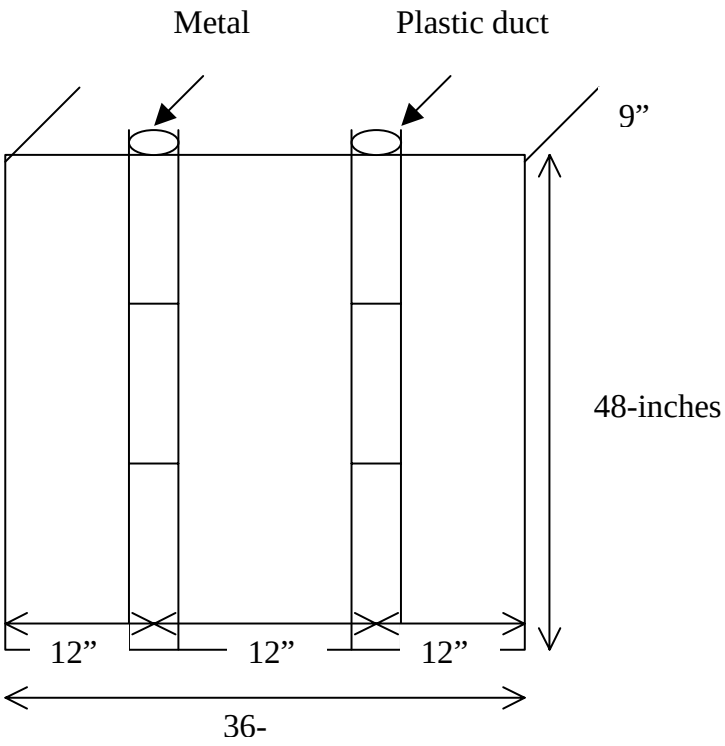

Figure 5.9 Reinforced Concrete Dimensions and Duct Locations

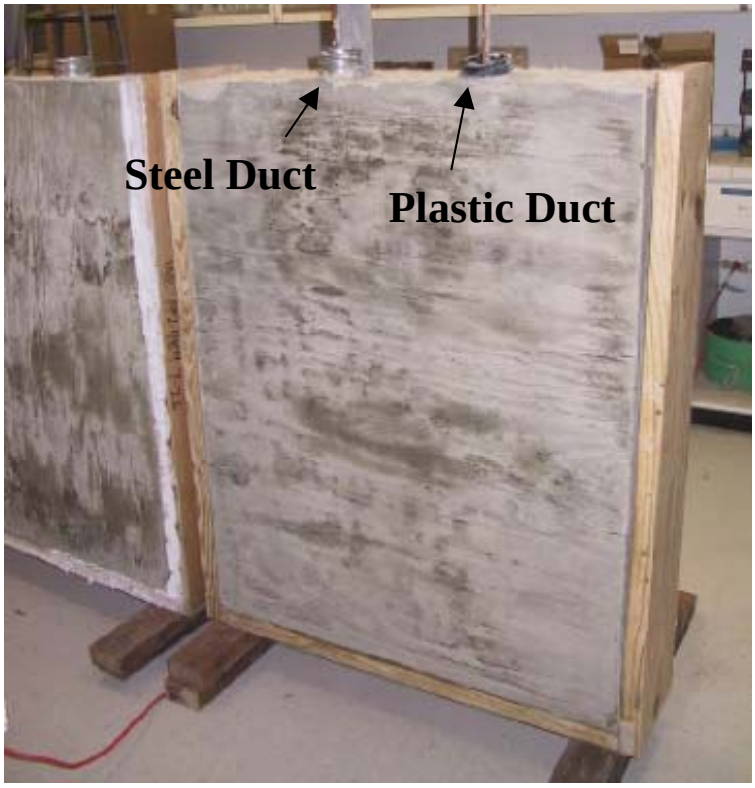

Figure 5.10 Two Concrete Walls with Steel and Plastic Ducts

5.6 Background

Three nondestructive test methods were used to evaluate the internal grout condition of steel and plastic ducts. The methods used in this investigation were Impact Echo (IE) Scanning, Tomography with Ultrasonic Pulse Velocity (UPV) and Spectral Analysis of Surface Waves (SASW). Detailed analysis of the three methods are presented herein.

5.6.1 Impact Echo (IE) Method

The IE tests performed in this investigation involved impacting the concrete wall with a small solenoid operated impactor and identifying the reflected wave energy

with a displacement transducer. Initially, an Olson Instrument IE-1 handheld unit was pressed against the concrete slab as shown in Fig. 5.11 below. The resonant echoes of the displacement responses are usually not apparent in the time domain, but are more easily identified in the frequency domain. Consequently, the linear frequency spectra of the displacement responses are calculated by performing a Fast Fourier transform (FFT) analysis to determine the resonant echo peak(s). The relationship among the resonant echo depth frequency peak (f), the compressional wave velocity (V_P) and the echo depth (D) is expressed in the following equation:

$$D = \beta V_p/(2*f) \qquad (1)$$

where β is a factor equal to 0.96 for a slab/wall shape

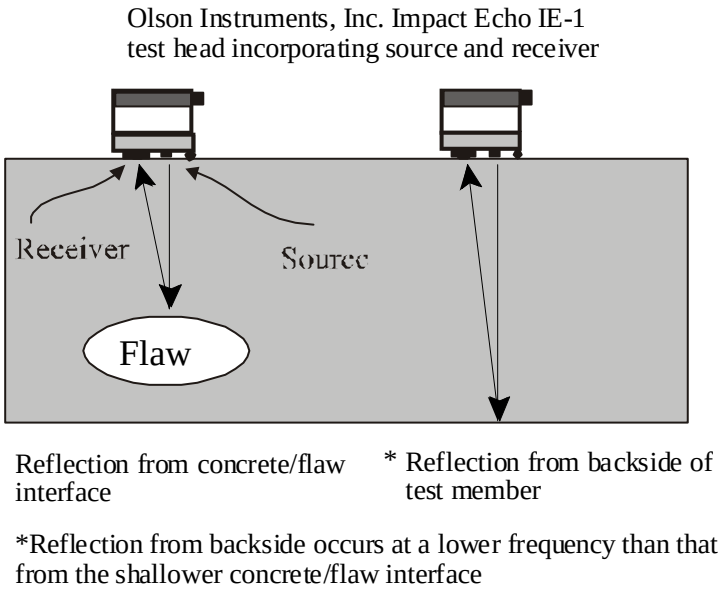

Figure 5.11 Schematic of Impact Echo Method

The IE method can be used for measuring concrete thicknesses, evaluating concrete quality, and detecting hidden flaws such as cracks, honeycombs, etc. The IE test data was recorded on an Olson Instruments Freedom Data PC during the laboratory NDT.

To expedite the IE testing process, Olson Instruments has developed and patented an Impact Echo Scanning device with four wheels and a rolling displacement transducer with 6 sensor elements attached underneath the test unit. As the test unit was rolled along the concrete surface, the central transducer wheel kept track

of the distance. The IE scanner unit is designed to apply an impact every 0.8 inch.

Figure 5.12 Freedom Data PC Acquisition System with IE Scanner

The Freedom Data PC acquisition system and an Impact Echo Scanning unit are shown in Fig. 5.12. The Impact Echo Scanning test is shown in Fig. 5.13.

Figure 5.13 The Impact Echo Scanning test

5.6.2 Spectral Analysis of Surface Waves (SASW) Method

The SASW method uses the dispersive characteristics of surface waves to determine the variation of the surface wave velocity (stiffness) of layered systems with depth. The SASW testing is applied from the surface which makes the method nondestructive and nonintrusive. Shear wave velocity profiles can be determined from the experimental dispersion curves (surface wave velocity versus wavelength) obtained from SASW measurements through a process called forward modeling (an iterative inversion process to match experimental and theoretical results). The SASW method can be performed on any material provided an accessible surface is available for receiver mounting and impacting. Materials that can be tested with the SASW method include concrete, asphalt, soil, rock, masonry, and wood.

Applications of the SASW method include, but are not limited to: 1) determination of pavement system profiles including the surface layer, base and subgrade materials, 2) determination of seismic velocity profiles needed for dynamic loading analysis, 3) determination of abutment depths of bridges, and 4) condition assessments of concrete liners in tunnels, and other structural concrete conditions.

The SASW method requires an accessible surface for receiver attachments. The extent of the accessible surface limits the investigation depth. As a rule of thumb, if one is interested in material properties to a depth of D, then the accessible surface should extend in a line of receivers direction to a distance equal to 1.5D, preferably 2D. Figs. 5.14 and 5.16 show the general field arrangement used in SASW testing. Receiver spacings ranging from 0.25 to +300 ft have been used in the field by our firm to investigate depths from 0.1 ft up to +300 ft.

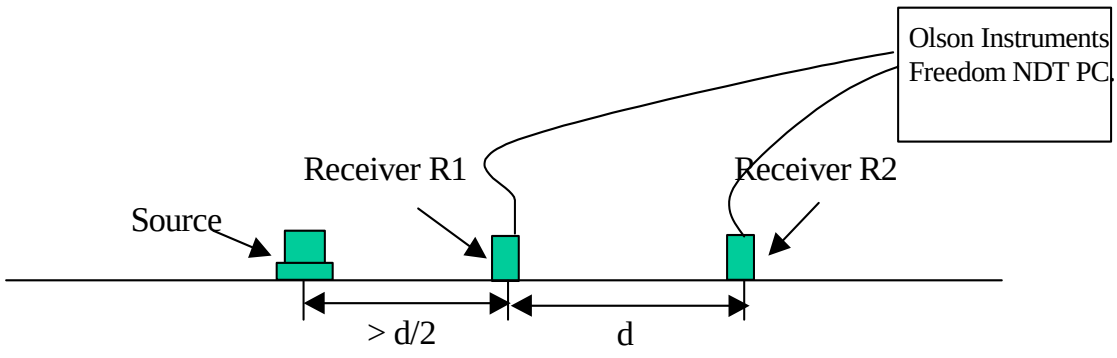

Figure 5.14 Field Setup for SASW Test

Figure 5.15 SASW Test on the Wall

In this case, the SASW method was used to check for possible voids inside the ducts. The SASW method uses the dispersive characteristics of surface waves to evaluate concrete integrity with increasing wavelengths (depths). High frequency or short wavelength waves penetrate through shallow depths, and low frequency or long wavelength waves penetrate through deeper depths. If voids exist in the ducts, longer wavelength waves will not be able to propagate directly through this zone and will show a decrease in velocity at duct wavelengths (depths).

5.6.2.1 Elastic Stress Wave Relationships

The following equations from elastic theory illustrate the relationships between shear moduli (G), mass density (Δ, total unit weight divided by gravitational acceleration), shear wave velocity (Vs), Young's modulus of

elasticity (E), Poisson's ratio (<), compression wave velocity (Vp), and constrained modulus (M):

Direct P- or S- Wave Velocity: Vp = D / tp or Vs = D/ts (1)

Shear Modulus: G = Δ Vs**2 (2)

Young's Modulus: E = 2 (1+<) Δ Vs**2 = Δ Vp**2 [(1+<)(1_2<)/(1-<)] (3)

Constrained Modulus: M = Δ Vp**2 (4)

Poisson's Ratio: < = [0.5 (Vp/Vs)**2 _1]/[(Vp/Vs)**2 - 1] (5)

P- and S-wave Velocities: Vp = Vs [2(1-<)/(1_2<)]**0.5 (6)

(Where D = Distance, tp = P-wave travel time and ts = S-wave travel time).

Values of these parameters determined from seismic measurements (SASW measurements) represent the material behavior at small shearing strains, i.e. strains less than 0.001 percent. Thus, moduli calculated from compression, shear or surface wave velocities represent the maximum moduli of materials because of their low strain levels. It should be noted that the measurement of the surface wave velocity, also called Rayleigh wave velocity, is actually performed in the SASW test. Surface wave velocity (V_R) in a homogeneous half-space is related to shear wave velocity by:

$V_R \sim 0.9\ Vs$ (7)

Surface wave (also termed Rayleigh; R-wave) velocity varies with frequency in a layered system with differing velocities. This variation in velocity with frequency is termed dispersion. A plot of surface wave velocity versus wavelength is called a dispersion curve.

The SASW tests and analyses are generally performed in three phases: (1) collection of data in situ; (2) construction of an experimental dispersion curve from the field data; and (3) inversion (forward modeling) of the theoretical dispersion curve, if desired, to match theoretical and experimental curves so that a shear wave velocity versus depth profile can be constructed. Wavelength (8), frequency (f), and wave velocity (Vr), are related as follows:

$$Vr = f*8 \qquad (8)$$

When the velocity is uniform, the wavelength of the waves is the investigation depth. Forward modeling is used to determine layer thicknesses and velocities when dispersive conditions exist. Forward modeling is most commonly done to determine seismic velocity profiles of soil and rock for earthquake and vibration machine foundation design purposes.

5.6.2.4 SASW Experimental Dispersion Curve Processing

The experimental dispersion curve is developed from the field phase data from a given site by knowing the phase (N) at a given frequency (f) and then calculating the travel time (t) between receivers of that frequency/wavelength by:

$$t = N / 360*f \quad (9)$$

Surface wave velocity (Vr) is obtained by dividing the receiver spacing (X) by the travel time at a frequency:

$$Vr = X / t \quad (10)$$

The wavelength (8) is related to the surface wave velocity and frequency as shown in equation 8. By repeating the above procedure for any given frequency, the surface wave velocity corresponding to a given wavelength is evaluated, and the dispersion curve is determined. The phase data was viewed on the PC data acquisition system in the field to ensure that acceptable data was being collected. The phase data was then returned to our office for processing. The phase of the cross power spectrum (transfer function) between the two receivers and the coherence function were used in creating the dispersion curves. Coherence is related to signal to noise

ratio, and a value near 1.0 indicates good quality data. However, acceptable phase data may have comparatively low coherence.

After masking of all forward and reverse phase record pairs from each receiver spacing, an experimental field dispersion curve is developed that is the plot of surface wave velocity versus wavelength. We used our TFS-SASW software to mask the phase data and generate the experimental field dispersion curves presented in the report.

3.2.4 SASW Theoretical Modeling Processing

To determine the shear wave velocity profile from the "apparent" velocities of the dispersion curve, analytical modeling is necessary. The analytical modeling is a forward modeling process that is iterative and involves assuming a shear wave velocity profile and constructing a theoretical dispersion curve. The experimental (field) and theoretical curves are compared, and the assumed theoretical shear wave velocity profile is adjusted until the two curves match using the WINSASW software of the Geotechnical Engineering Center of University of Texas at Austin. The interactive computer algorithm for both 2-dimensional and 3-dimensional analyses have been developed by Dr. Jose Roesset and his colleagues at the University of Texas at Austin to compute a theoretical dispersion curve based upon an assumed shear wave velocity and layer thickness profile. These algorithms have been in use for some time and

have produced reasonable accuracy when comparing seismic soil and rock velocities determined with the SASW method with seismic boring based crosshole or downhole seismic methods.

5.6.3 Ultasonic Tomographic Imaging (UTI) with Ultrasonic Pulse Velocity

Ultrasonic Tomographic Imaging (UTI) is an imaging method analogous to a CAT-Scan in the medical industry and uses acoustic waves. The testing is often performed on drilled shaft foundations after crosshole sonic testing to obtain more information about the size, shape, location, and severity of a suspected defect or defects in a concrete drilled shaft. This foundation method is known as Crosshole Tomography (CT). A UTI data collection is intense and the procedure is relatively slow. The spatial resolution of Tomography can be high and an actual image of the specimen is produced. A description of the Tomography test method is given below.

In this case the Tomography tests used two ultrasonic transducers (54 KHz), one as a source and the other as a receiver. For Tomography testing, acoustic data are collected for many receiver and source combinations at different depths (Fig. 5.16). For a typical Tomography data set, sound velocity raypaths are generated for tens to thousands of source-receiver location combinations. The term “ray coverage” describes the area through which acoustic wave rays travel from the many source-receiver position combinations.

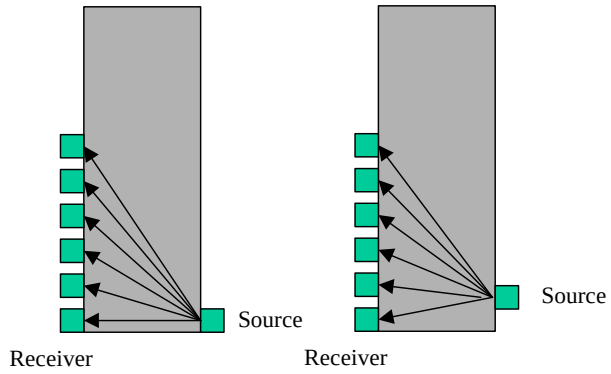

Figure 5.16 Tomography Test - Source and Receiver Combinations at Different Depths

Tomography is an analytical technique which uses an inversion procedure on the first arrival time data of compressional or shear wave energy that can produce ultrasonic pulse-velocity based images of a 2-D or 3-D concrete zone inside a foundation or of the entire foundation. This type of tomography is termed "velocity tomography" and can be used together with amplitude tomography. The test region is first discretized into many cells with assumed slowness values (inverse of velocity) and then the arrival times along the test paths are calculated. The calculated times are compared to the measured travel times and the errors are redistributed along the individual cells using mathematical models. This process is continued until the measured travel times match the assumed travel times within an assumed tolerance. The end result is a 2-D or 3-D velocity image (or contour) of the internal structure of the foundation, revealing sound (fast) versus defective (slow) areas.

5.7 PHASE II RESULTS

This section describes results from all three NDT methods on both mock up walls at the University of Florida Laboratory using the Olson equipment.

5.7.1 Impact Echo Scanning on Wall II (ungrouted ducts)

First, an Impact Echo scan was performed on the solid concrete wall between the ducts where no internal post-tensioned duct was present to allow calibration of the IE velocity of concrete Wall II. The thickness results of the first scan, typical frequency response from the concrete wall are shown in Fig. 5.17. From the calibration, an IE velocity of 11,000 ft/sec (included 0.96∃ factor per Eq (1)) was used in the Impact Echo test. The average wall thickness from Fig. 5.17 is 9.5 inches. The top inset window shows the time domain displacement transducer response at 1 ft from the top of the wall

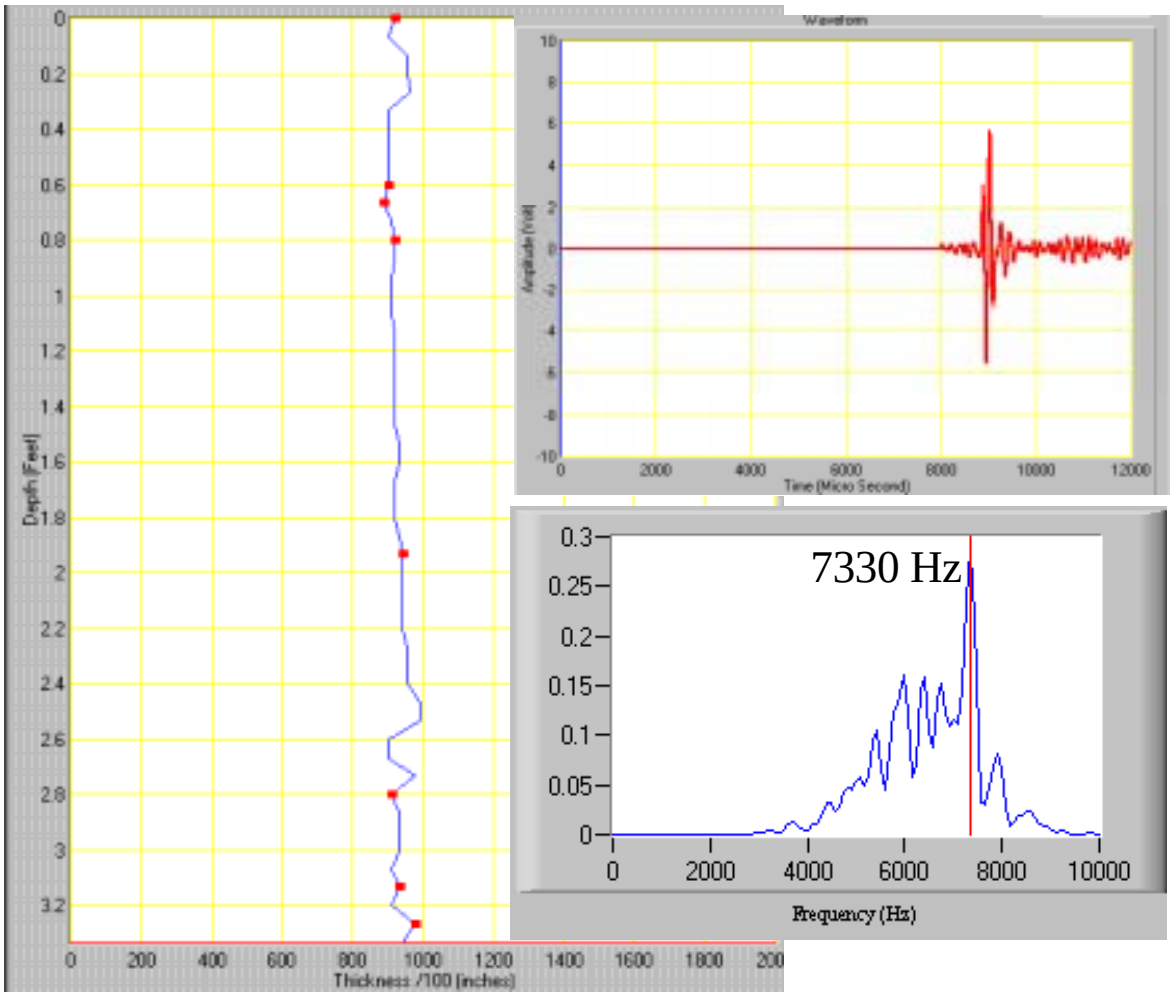

Figure 5.17 Nominal Wall Thickness and its IE frequency response from IE Scanning of Solid Concrete

The bottom inset window shows the linear frequency spectra of the time domain response at 1 ft from the top of the wall. The thickness echo peak is at 7,330 Hz, so by applying Eq. (1), the echo depth is: $D = V_{IE}/(2*f) = 11{,}000/ (2*7{,}330) =$ 0.75 ft = 9 inches.

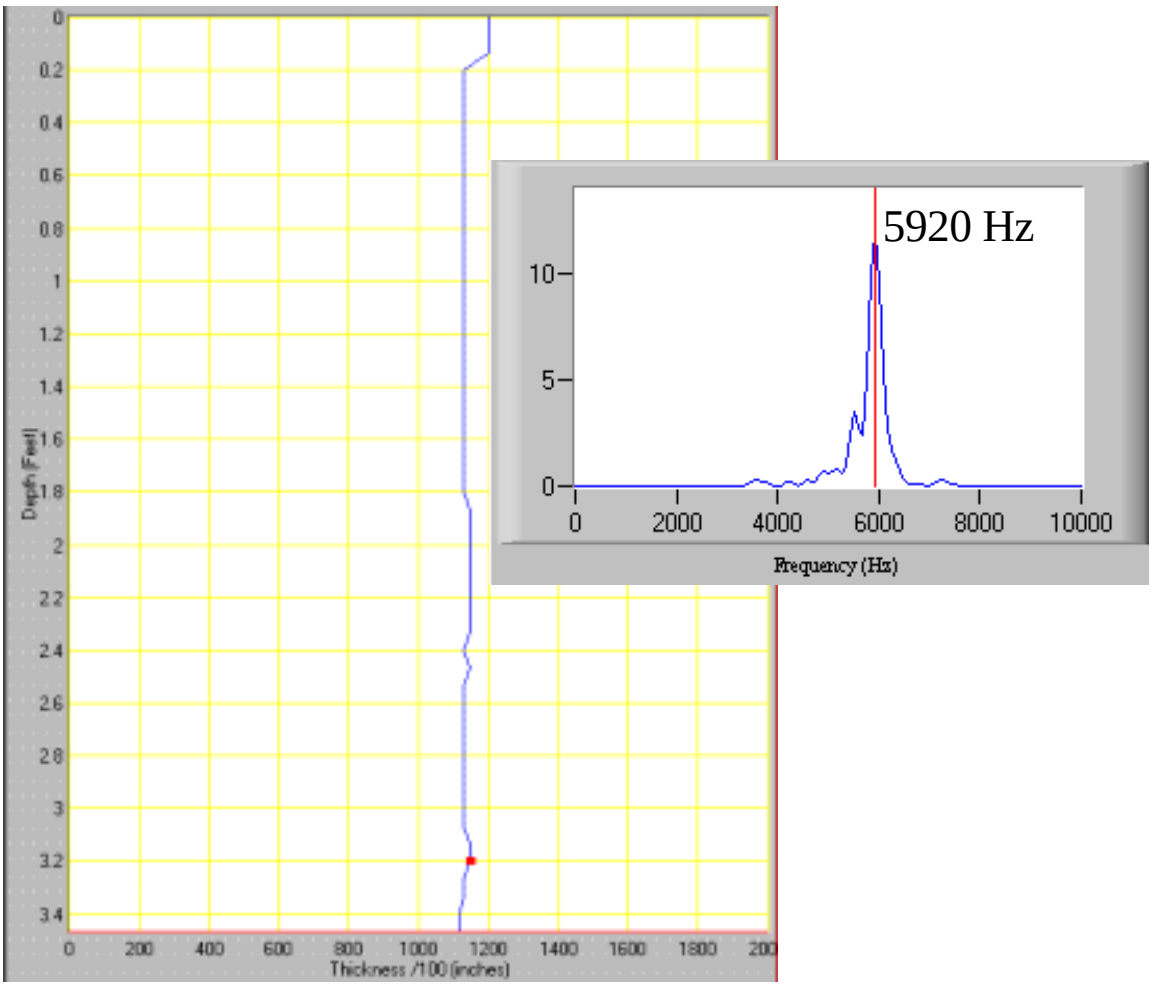

Figure 5.18 IE Thickness Results and Example Frequency Response from the Empty Steel Duct of Wall II (Duct Center Line Scan)

Two Impact Echo scan lines were performed on Wall II along the center lines of empty steel and plastic ducts. The IE thickness results from the empty steel duct are shown in Fig. 5.18.

An average thickness from the empty steel duct (Wall I) was 11.3 inches. Typical frequency response from the data is also shown in the inset in Fig. 5.18. The thickness frequency peak shifted from 7,333 Hz (Fig. 5.17) to 5920 Hz. This

shift in the frequency resulted in a larger thickness response of 11.3 inches due to the decreased resonance as a result of the void of the empty steel duct.

The IE results from the empty plastic duct and a typical frequency response are shown in Fig.5.19. The resonant frequency peak of this data is 5,250 Hz which is slightly lower than the peak response from the empty steel duct (Fig.5.18). Correspondingly, the IE peak results predicted an even greater average thickness of 12.5 inches for the larger diameter (bigger void) empty plastic duct than the 3 inch steel duct.

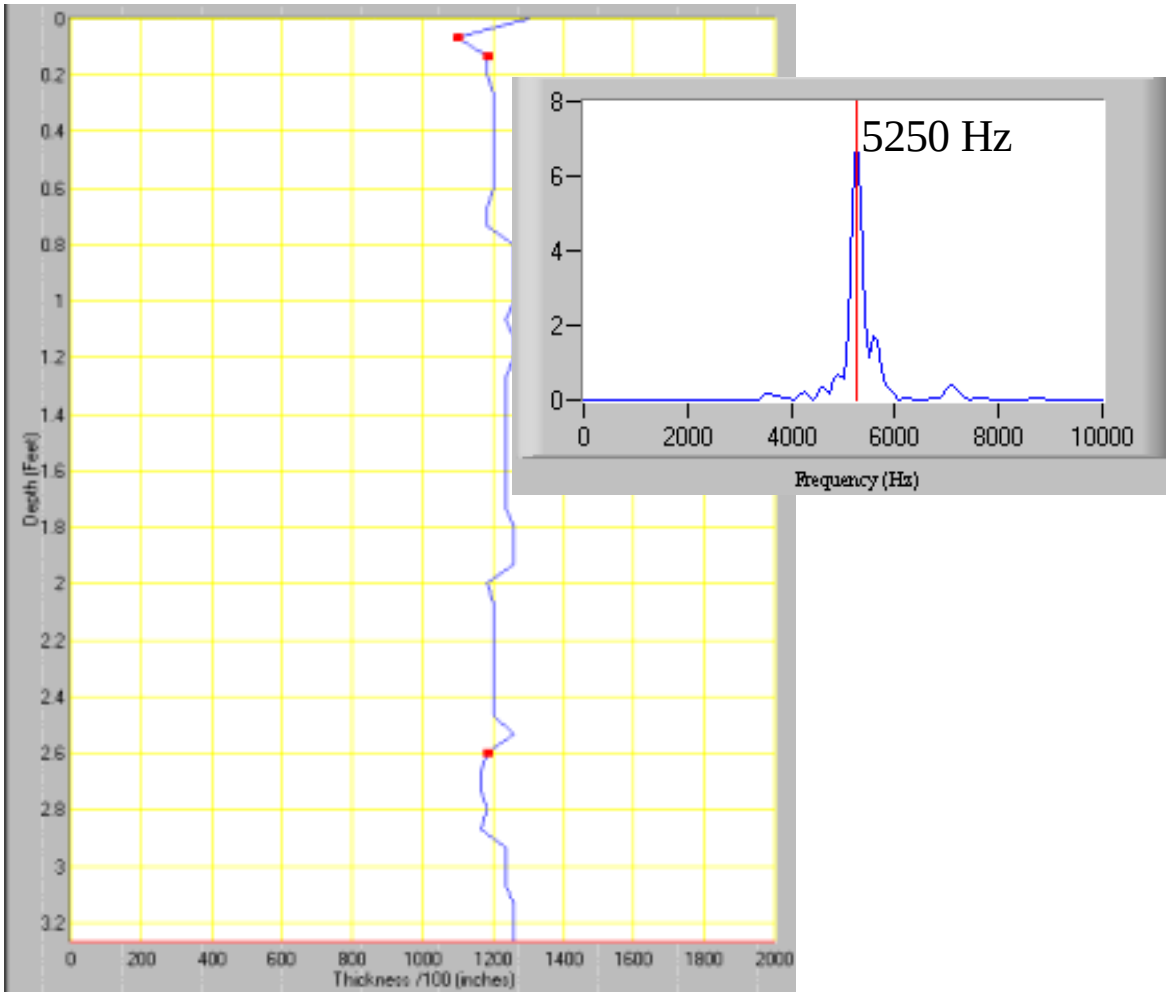

Figure 5.19 IE Thickness Results and Example IE frequency response from the Empty Plastic Duct of Wall II (Duct Centerline Scan)

5.7.2 Impact Echo Scanning on Wall I Scanning of Grouted to Ungrouted Ducts - Scanning along the ducts

After obtaining the base line data for the ungrouted ducts of Wall II, several IE scanning tests were performed on Wall I. In this case, the scan started from near wall bottom (depth of 0 ft). As described in Section 4.0, both ducts in Wall I were divided into 3 sections: the bottom sections with fully grouted ducts, the middle sections with partially grouted ducts and the top sections with empty ducts, plus

grouted cap at the very top. The first IE scan was performed along the center line of the steel duct, starting from near the bottom (3" above the wall bottom) to near the top (~3" below the top wall) of the wall. The IE thickness results and example frequency responses are shown in Fig. 5.20, which shows that the peak frequency shifted to a lower value for the partially grouted and empty steel duct. This resulted in larger apparent thickness results from the partially grouted and empty ducts. An average thickness result from a fully grouted duct section is 9.8 inches and an average thickness result from partially grouted to empty ducts is 10.8 inches. In this case, the results from partially filled duct are similar to the results from the empty duct. This is because the grout was inserted into the duct after hardening to simulate a partially grouted duct situation. Consequently, debonding occurred between the duct and the hardened grout and the IE signal was not able to travel through the debonding. Therefore, the results from both cases (empty duct and partially grouted duct) are similar since the partially grouted duct behaves just as an empty duct in IE tests due to debonding. Review of the IE spectra in the inset figures of Fig. 5.20 shows the resonant echo peaks corresponding to empty to partial to grouted duct results that support this.

The impactechogram, which shows amplitude intensity of frequency data of the IE test result from the steel duct, is presented in Fig. 5.21. The plot presents a shift of frequency to a lower frequency (compared to a fully grouted duct to an empty duct).

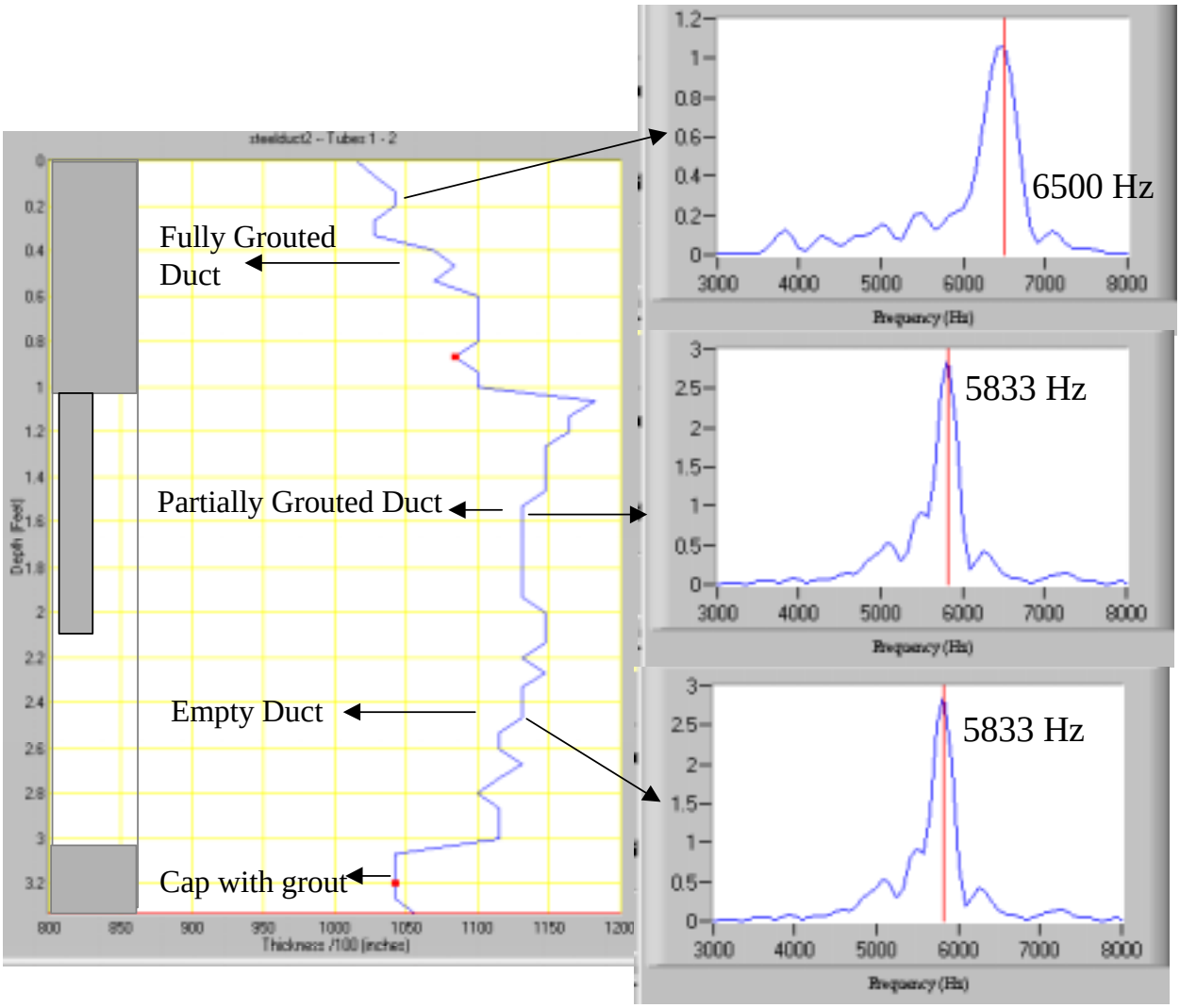

Figure 5.20 IE Thickness and Frequency Results from a Steel Duct - Wall I

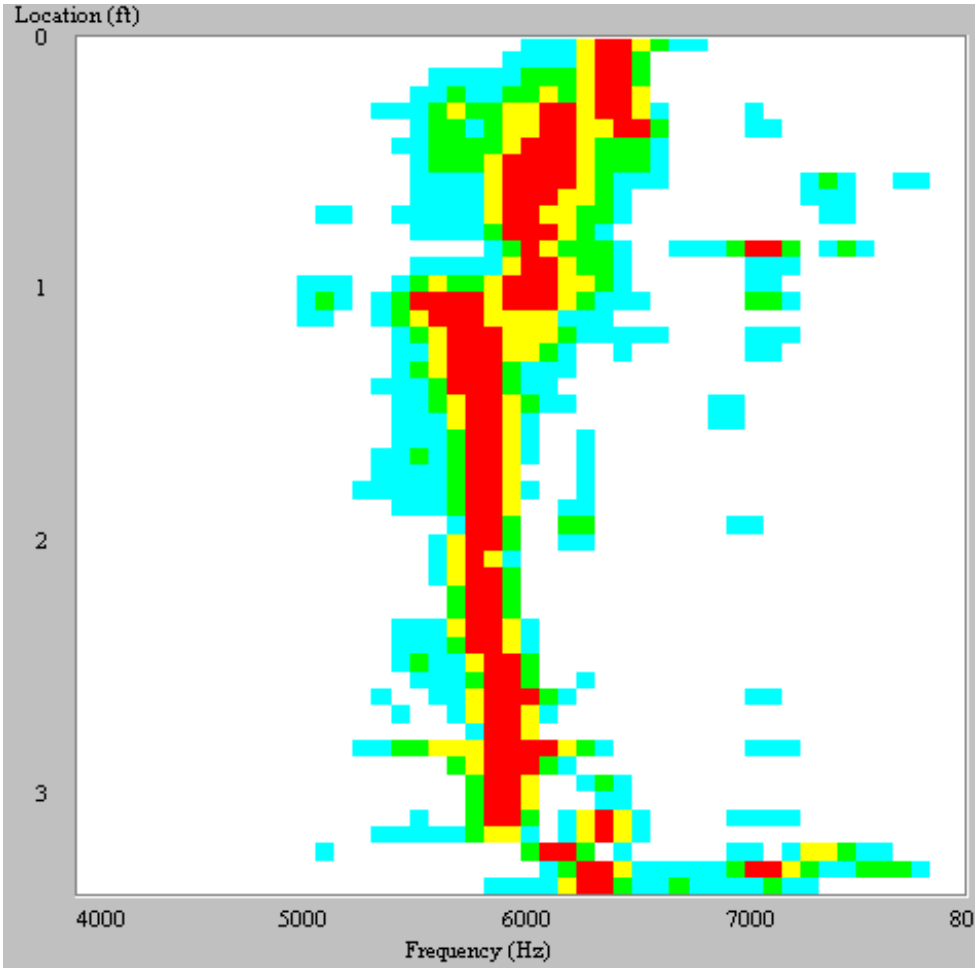

Figure 5.21 Impactechogram of the IE test Results along the Steel Duct

An Impact Echo scan was then performed along the centerline of the plastic duct. The IE thickness and example frequency results are shown in Fig. 5.22. An average thickness reading from a fully grouted plastic duct is 10.6 inches with an average peak frequency of 5916 Hz. An average thickness of a partially filled plastic duct is 11.4 inches with an average peak frequency of 5416 Hz. For an empty plastic duct, an average thickness is 11.2 inch with an average peak

frequency of 5583 Hz. Thus, the IE method showed about an 85% increase in thickness for an ungrouted duct.

An impactechogram of the IE frequency data from the plastic duct is presented in Fig. 5.23. It is noticed that for the fully grouted plastic duct section (the top section), both lower frequency peak (~ 5,400 Hz) and a higher frequency peak (~5,900 Hz) appears in the impactechogram plot. This lower frequency peak corresponds to lower stiffness from plastic ducts inside the wall. However, the higher peak frequency can still be used to indicate that the plastic duct in the top section is fully grouted.

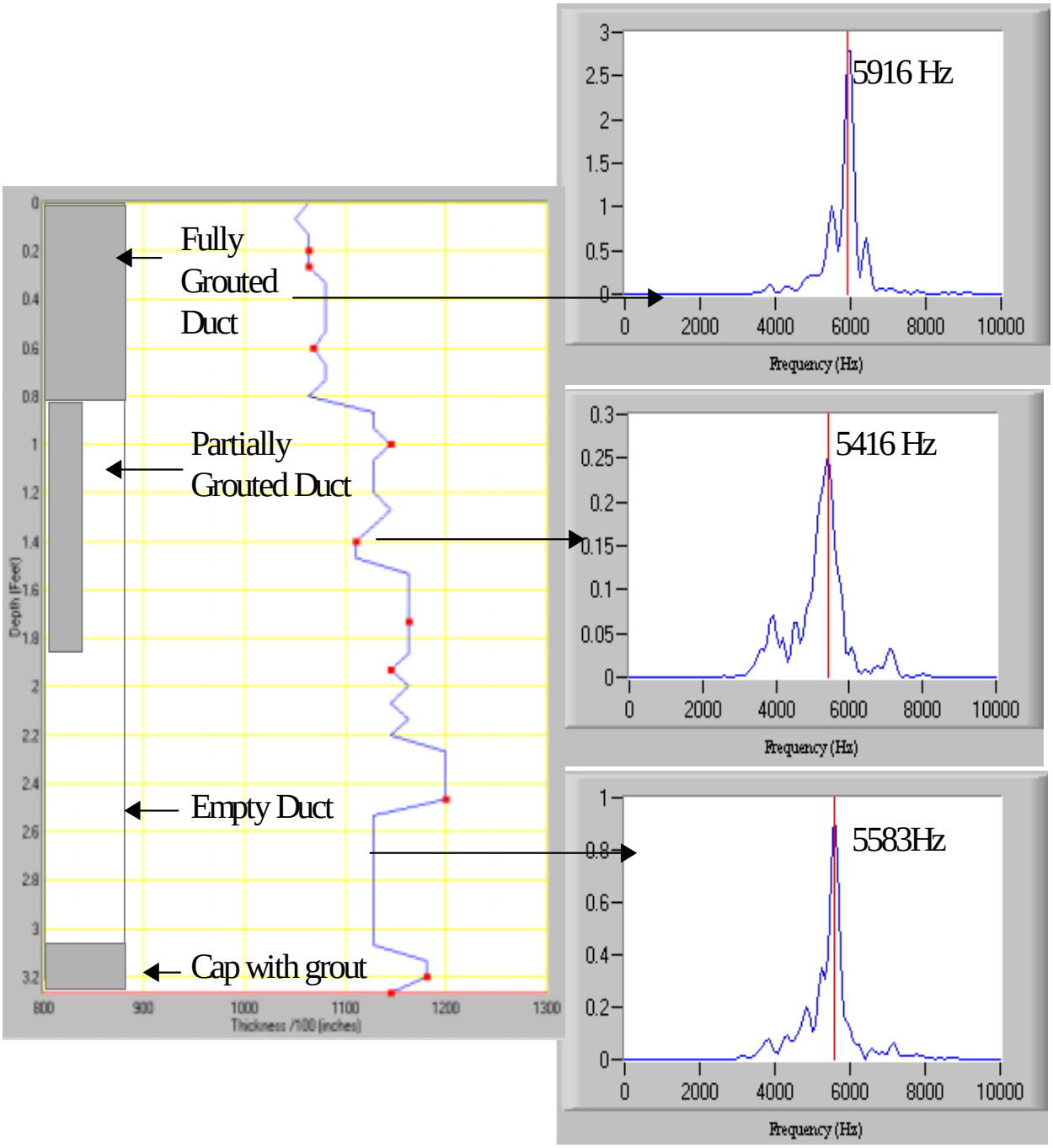

Figure 5.22 IE Thickness and Example Frequency Results from a Plastic Duct

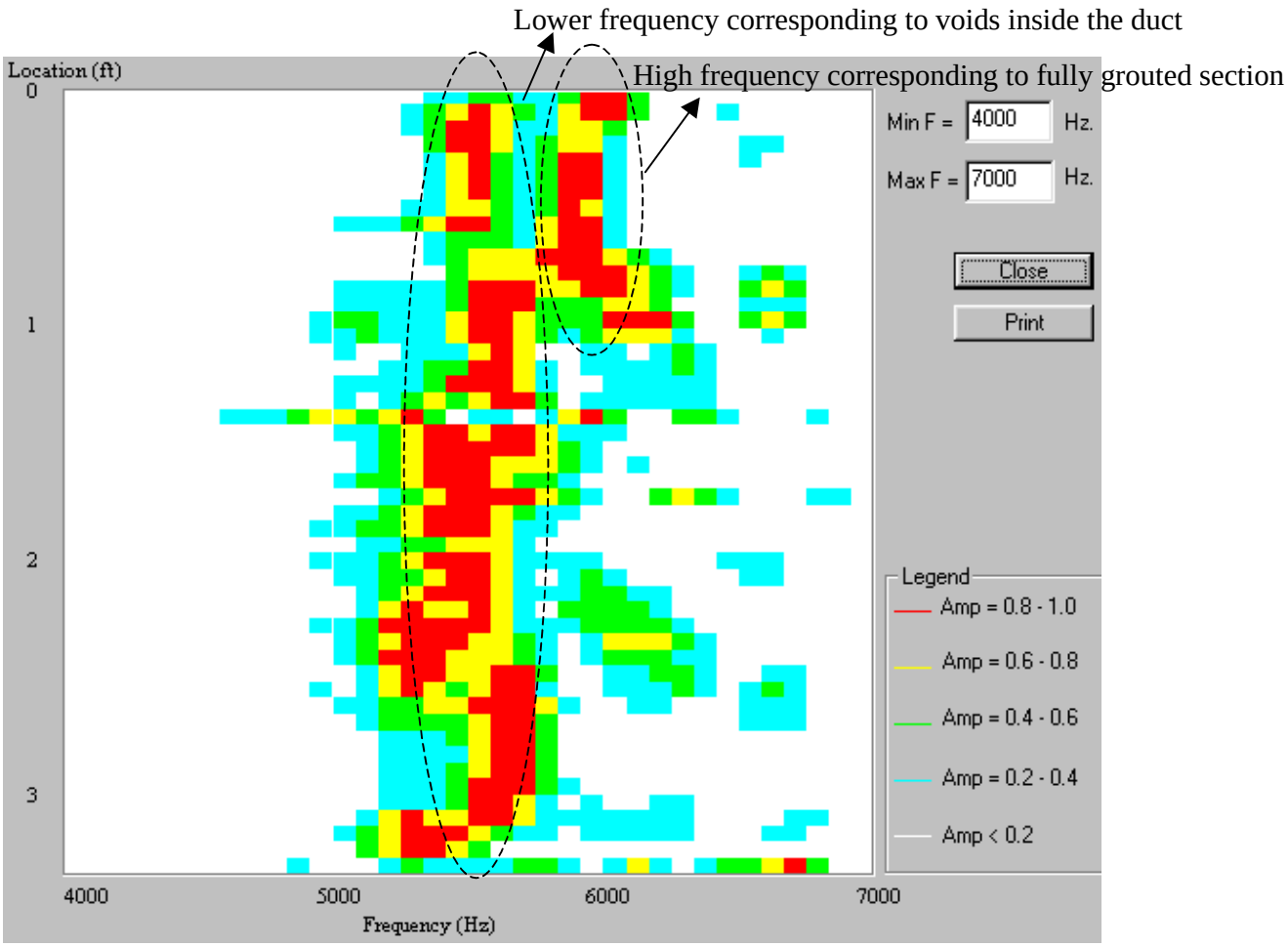

Figure 5.23 Impactechogram of Frequency Data from a Plastic Duct

5.7.3 Results from IE Scanning when the Scanning is off the Center Line - Wall I

This section describes the test setup and results when IE scanning was performed off the centerline of the duct. The first scan was performed along the centerline of the steel duct (see Fig. 5.16), The second, third and fourth scans were performed 1, 2 and 3 inches off the centerline of the steel duct. The thickness results from all four scans are presented in Fig. 5.24. It is interesting to see that the first three scans (on the centerline, 1 inch off the centerline and 2 inches off the centerline) yielded almost identical thickness results. The last scan (3 inches off the duct) yielded the nominal thickness of the concrete wall. Note that the diameter of the steel duct was 3 inches.

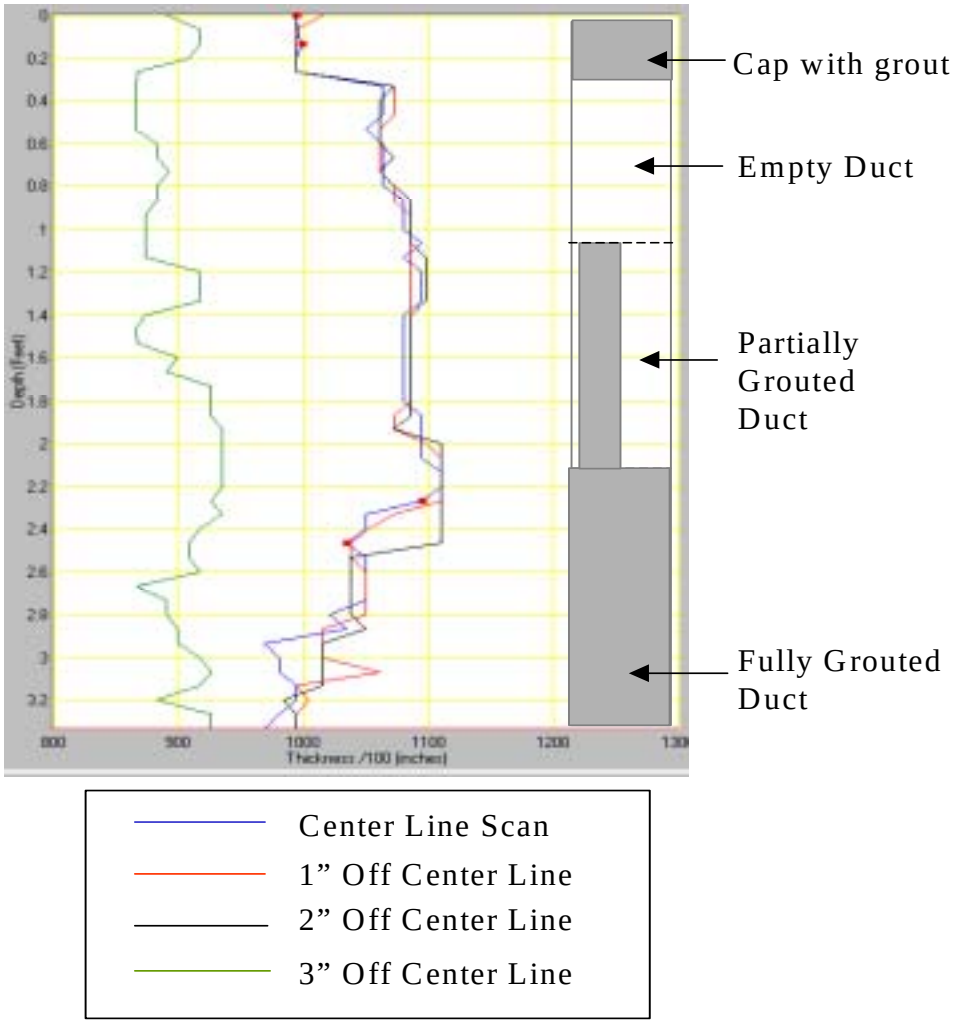

Figure 5.24 IE Thickness Results from IE Scanning off the Center Line of Steel Duct

5.7.4 Impact Echo Scanning on Wall I - Scanning across the Ducts

Several IE scans were performed transversely (horizontally) across both steel and plastic ducts. The first scan was performed at the bottom of the wall where both ducts were fully grouted. The results from the first scan are presented in Fig. 5.25 and the wall nominal thickness was 9.7 inches. The thickness from fully grouted steel duct section was 11.1 inches and the thickness from the fully grouted plastic

duct was 12.5 inches. The second scan was performed at the middle of the wall where both ducts were partially grouted and the results of the test are shown in Fig. 5.26. In the partially grouted case, an average thickness of the partially grouted steel duct was 11.8 inches and an average thickness of the partially grouted plastic duct was 12.9 inches. Finally, the last scan was performed toward the top of the wall where both ducts were left empty and the thickness results are shown in Fig. 5.27. In the empty case, an average thickness of the empty steel duct was 11.4 inches and an average thickness of the empty plastic duct was 12.3 inches.

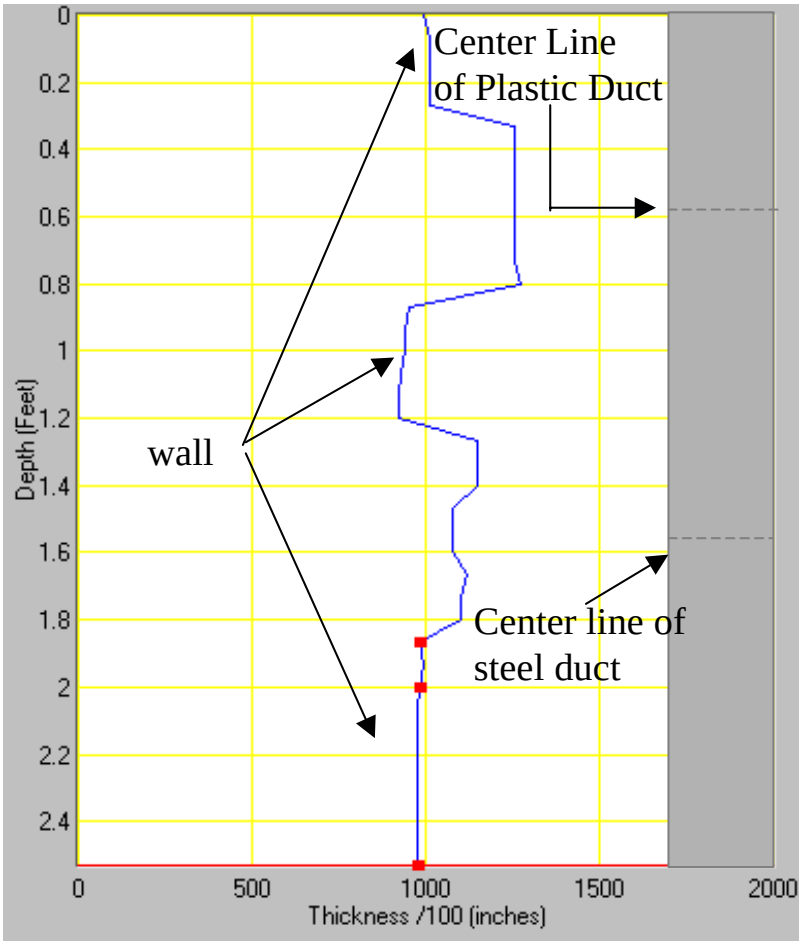

Figure 5.25 IE Thickness Results from IE Scanning across Steel and Plastic Ducts - Fully Grouted Ducts

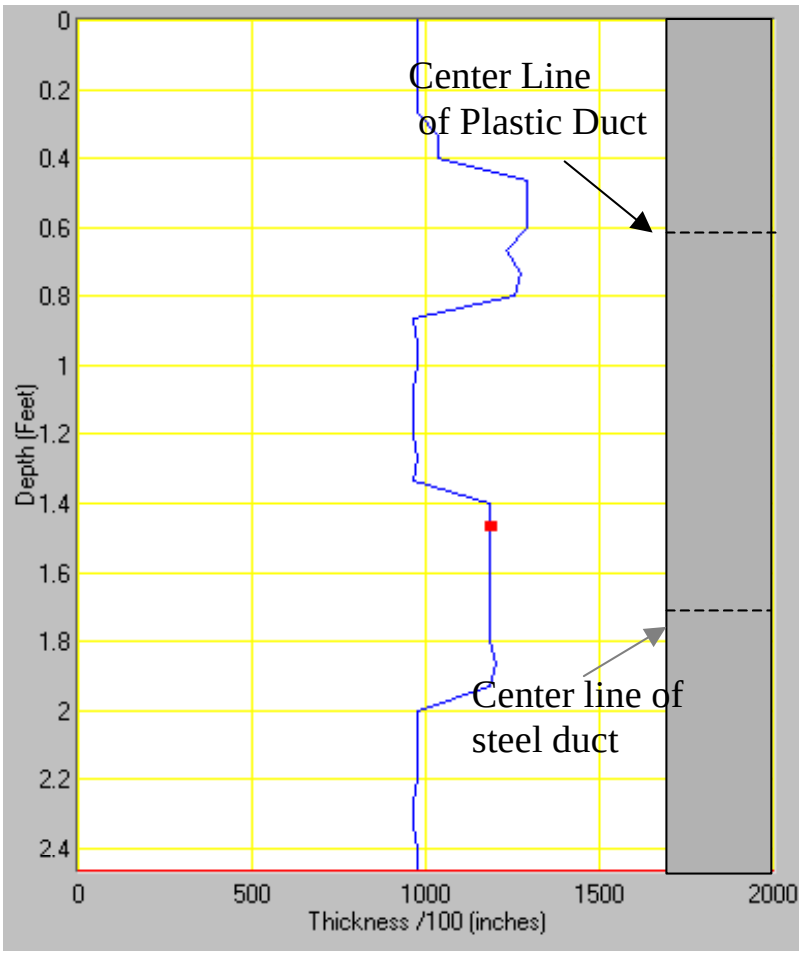

Figure 5.26 IE Thickness Results from IE Scanning across Steel and Plastic Ducts - Partially Grouted Ducts (Debonded)

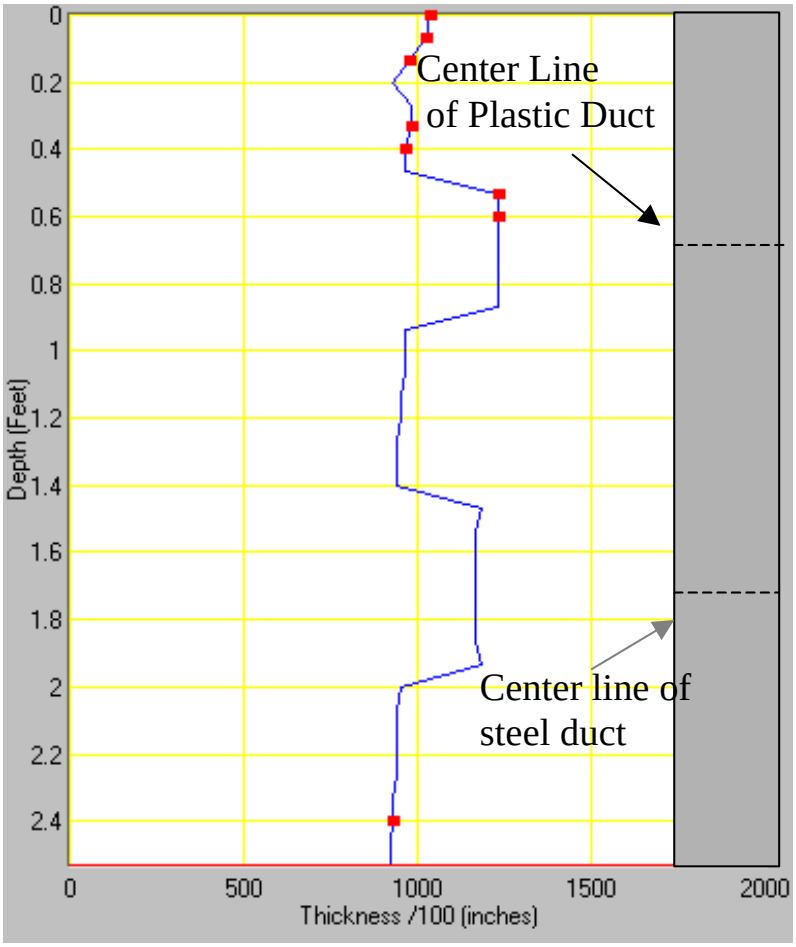

Figure 5.27 IE Thickness Results from IE Scanning across Steel and Plastic Ducts - Empty Ducts

5.7.5 Ultrasonic Tomography Imaging (UTI) Results

Three UTI tests were performed with UPV transducers (54 Kilo Hertz). The first test was performed across the fully grouted ducts (plastic and steel) and the velocity tomogram image result is shown in Fig. 5.28. The second test was performed across the partially grouted ducts and the tomography image result is

shown in Fig. 5.29. The last test was performed across the empty ducts and the result is shown in Fig.5.30.

The image results from all three cases showed locations of the top plastic and bottom steel ducts. However, the images did not show the details inside the ducts. This is likely due to the 3 inch long ultrasonic waves going around rather than through the ducts. A further complication may be due to the acoustic impedance (velocity times density) contrast between concrete, steel and plastic, which can result in most of the energy being reflected back from the ducts. Consequently, only a very weak signal may emerge from a duct.

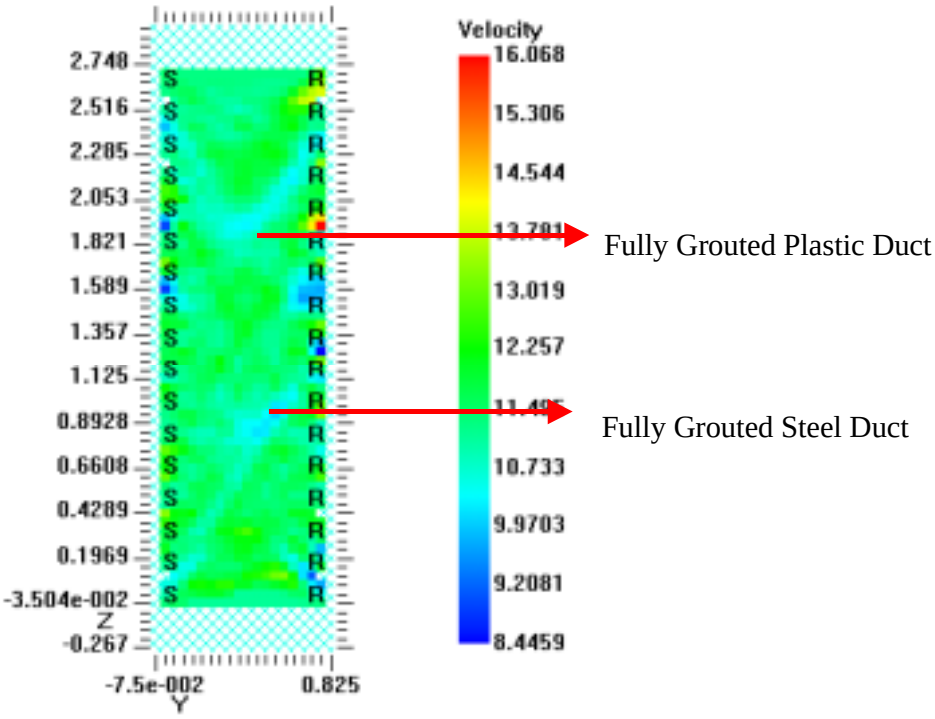

Figure 5.28 Velocity Tomogram Image from Fully Grouted Steel and Plastic Ducts

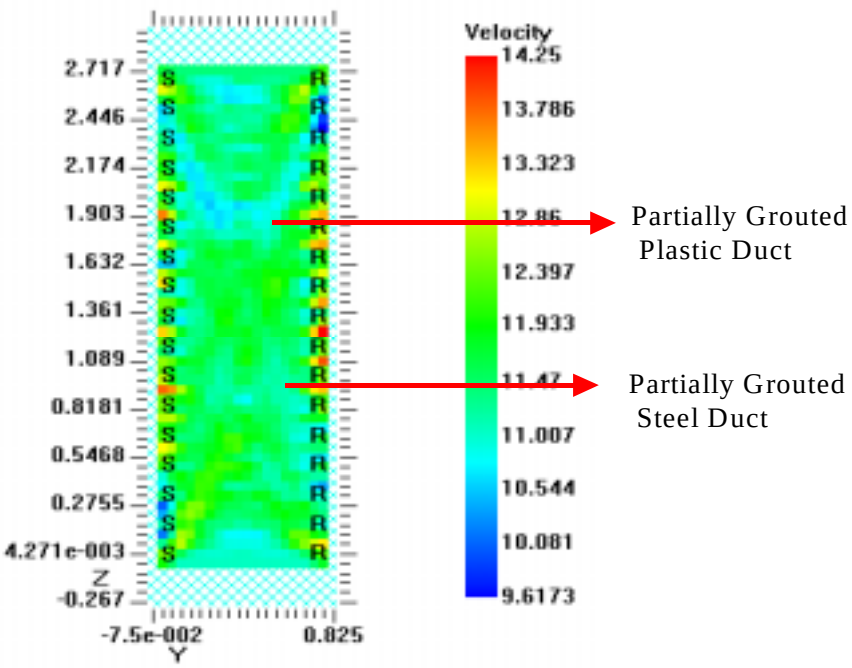

Figure 5.29 Velocity Tomogram Image from Partially Grouted (Debonded) Steel and Plastic Ducts

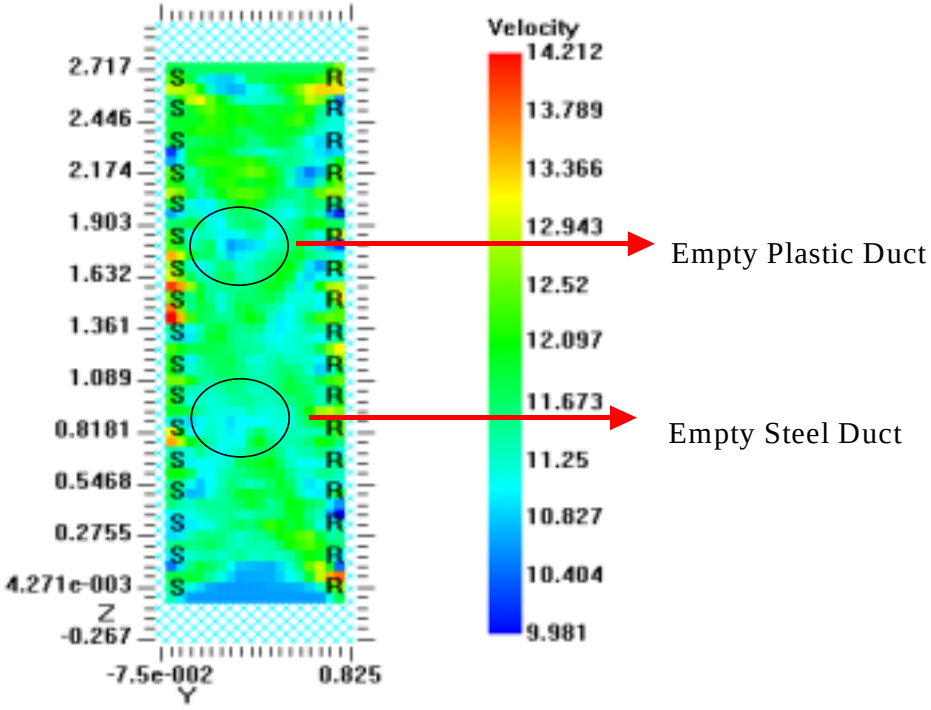

Figure 5.30 Velocity Tomogram Image from Empty Steel and Plastic Ducts

5.7.6 Spectral Analysis of Surface Waves (SASW) Test Results

Several SASW tests were performed across the ducts with a receiver - receiver spacing of 20 cm. The surface wave velocity vs. wavelength results from empty, partially grouted and fully grouted steel duct are shown in Fig. 5.31. Review of this figure shows that the surface wave velocities at shallow depths (0 - 0.4 ft or 0 - 4.8 inches) from all three cases are similar. At deeper depths, it is apparent that the surface wave velocity from the fully grouted duct is slightly higher than the velocity obtained from partially grouted duct. The velocity from the partially grouted duct is also slightly higher that the velocity from the empty, ungrouted duct.

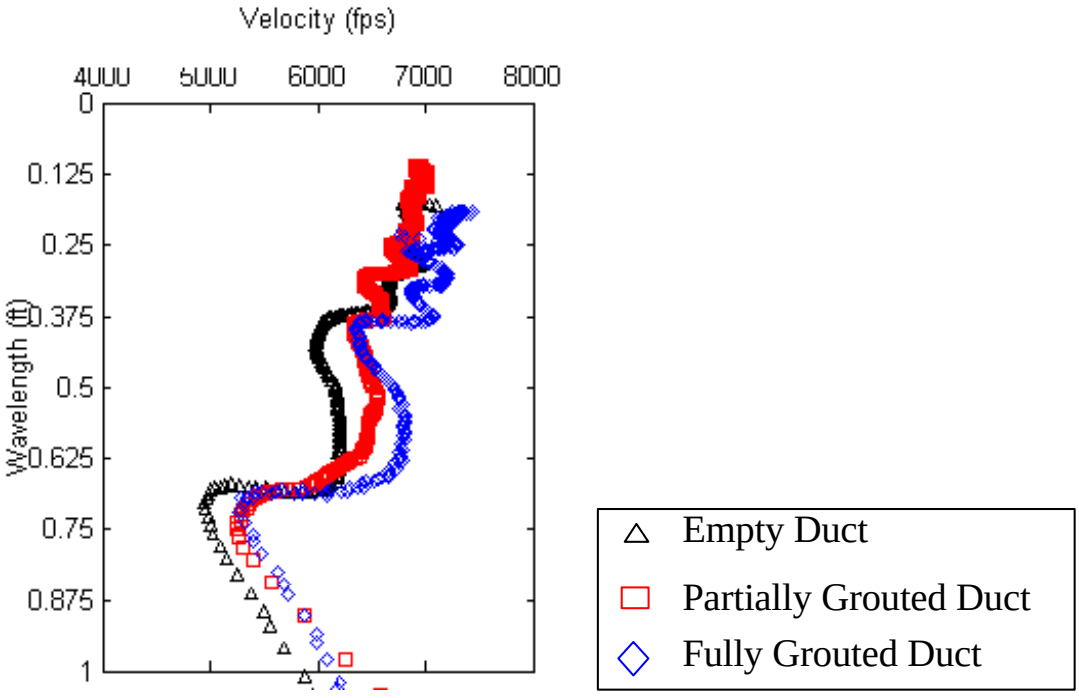

Figure 5.31 Surface Wave Velocity Dispersion Curve Results from Steel Duct

Next, the SASW tests were performed across the plastic duct with the same receiver- receiver spacing of 20 cm. The surface wave velocity results from empty, partially grouted and fully grouted steel duct are shown in Fig. 5.32. In this case, the surface wave velocity from an empty plastic duct is slightly higher than velocity from the partially grouted plastic duct. The velocity from the fully grouted duct seems to be the lowest among the three.

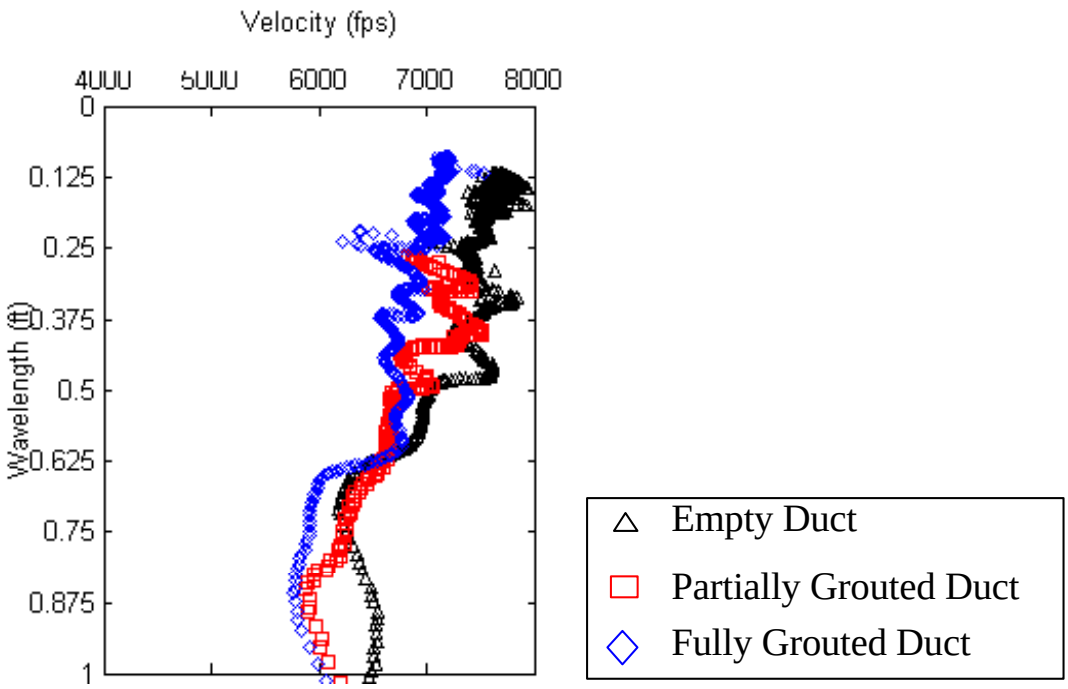

Figure 5.32 Surface Wave Velocity dispersion Curve Results from Plastic Duct

5.8 PHASE III RESULTS

5.8.1 Research Investigation Scope

This portion of the research focuses on Impact Echo (IE) with a scanning technology to expedite the field procedure. The Impact Echo Scanning technique requires only one-sided access. The results of this investigation are to provide data on the potential use of the methods in the field. The tests were performed by University of Florida personnel using an Olson Instruments Freedom Data PC system.

5.8.2 Summary Of Findings

1. **Laboratory NDE.** Several IE scans were performed along and across the steel and plastic ducts over a period of 24 days. The purpose of this was to observe the effects of the curing grout within the ducts. Also, the IE scans were performed off the centerline of the duct to see duct diameter effects. Each day a calibration scan was also recorded of a sound wall section (no ducts).

2. **Results from IE Scanning.** At Day 1, the grout inside the ducts produced IE Scan results similar to the void section of duct in both the plastic and steel ducts. At day 4 and the first indication of a difference between true void and grouted section of the ducts could be seen. At day 24, scanning along the steel duct showed a change in thickness measured

at approximately 2.1 ft, shifting from 11.6 in to 12.3 in. Scanning along the plastic duct showed a change in thickness measured at approximately 1.6 ft, shifting from 12.4 in to 13.0 in.

5.8.3 Background

During this portion of the research, only Impact Echo (IE) Scanning was used to evaluate the internal grout condition of steel and plastic ducts. The IE Scanning system is shown in Fig. 5.33 below. The results from IE Scanning tests during the first phase of the research proved to be most promising among the technologies of IE Scanning, Ultrasonic Pulse Velocity (UPV) / Tomography and Spectral Analysis of Surface Waves (SASW).

Figure 5.33 Data Acquisition System with IE Scanning Device

5.8.4 Wall Specimen II

Only one mockup wall (Wall II), with one plastic duct (3.5 “ ID.) and one steel duct (3" ID.), was used in this investigation. Wall II had both steel and plastic ducts inside which were half filled with grout. A picture of the walls is shown in Fig. 5.34. The walls are 3 ft wide, almost 4 ft high and about 9 ½ inches thick.

(Wall II) (Wall I)

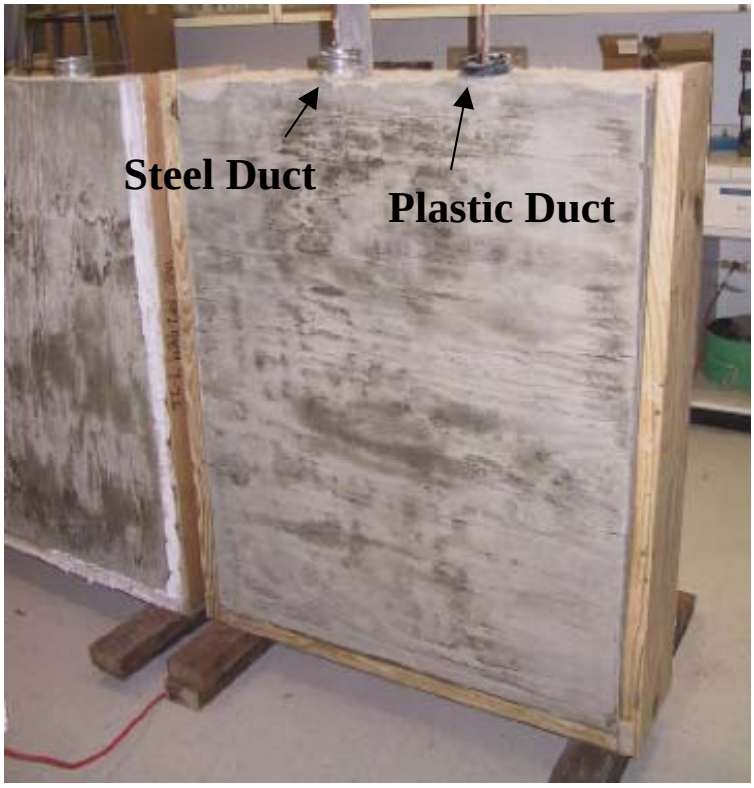

Figure 5.34 Concrete Walls with Steel and Plastic Ducts

5.8.5 Field Investigations And Test Results

This section describes the field investigation and the test results from IE Scanning on both the mock up wall. Each duct was half filled from the bottom of the duct. Please note that the vertical IE Scan results are shown inverted. Note that 0-ft is at the top of the scan, but actually represents the beginning point of the scan, or the bottom of the wall. Scans were performed starting from the bottom (~3" above the bottom of the wall) to the top of the wall (~3" below the top of the wall**)**.

1. Impact Echo Scanning Calibration on Wall II

First, an Impact Echo scan was performed at a location on the concrete wall with no duct inside to calibrate for the IE velocity of the concrete wall. The thickness results of the first scan, with a typical frequency response from the concrete wall are shown in Fig. 5.35. From the calibration, an IE velocity of 12,000 ft/sec was use in the Impact Echo test. The average wall thickness from Fig. 5.35 is just under 10 inches. A value of 11,000 ft/sec was used during Phase I research, which yields slightly lower thickness.

At 24 days, the calibration test is roughly identical to the calibration test at day 1, as shown in Fig. 5.36 below. This indicates the velocity of the several month old wall was basically constant during the test period.

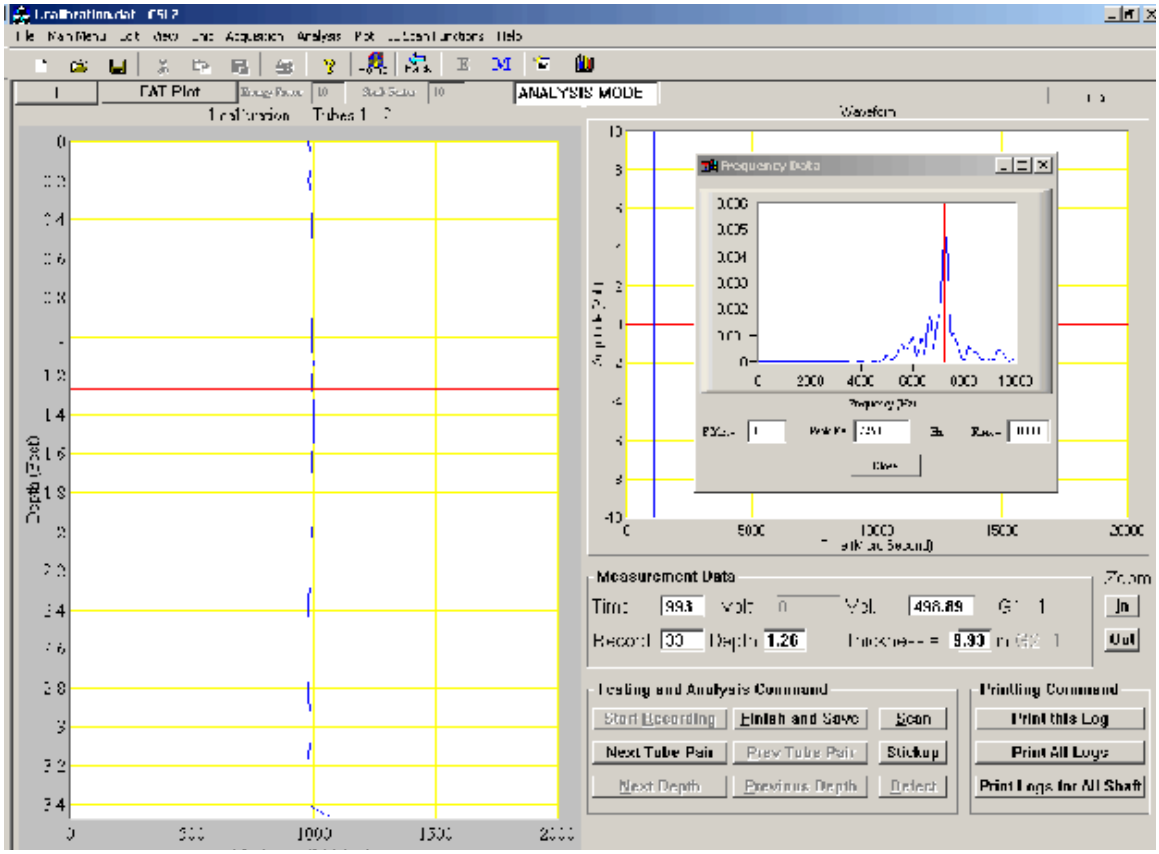

Figure 5.35 Calibration Scan from Sunday, 12/29/02

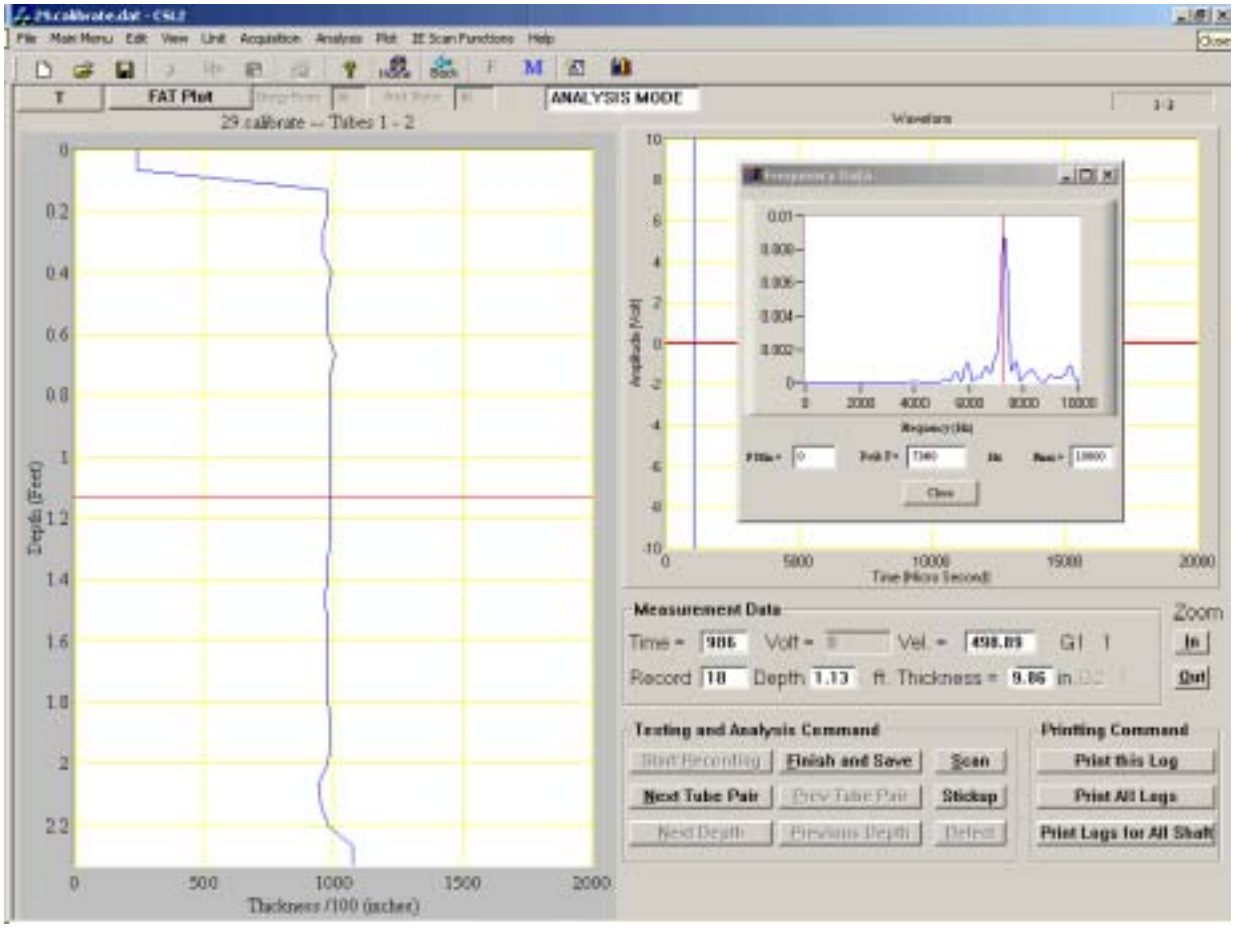

Figure 5.36 Calibration Scan from Tuesday, 1/12/03

2. Impact Echo Scanning across the ducts

IE scans were run across both steel and plastic ducts. The scans were performed at the bottom half of the wall where both ducts were grouted. The results from the first scan (day 1) is presented in Fig. 5.37. From Fig. 5.37, the wall nominal thickness was 10 inches. The thickness from fully grouted steel duct was 12.4 inches and the thickness from the fully grouted plastic duct was 13.0 inches.

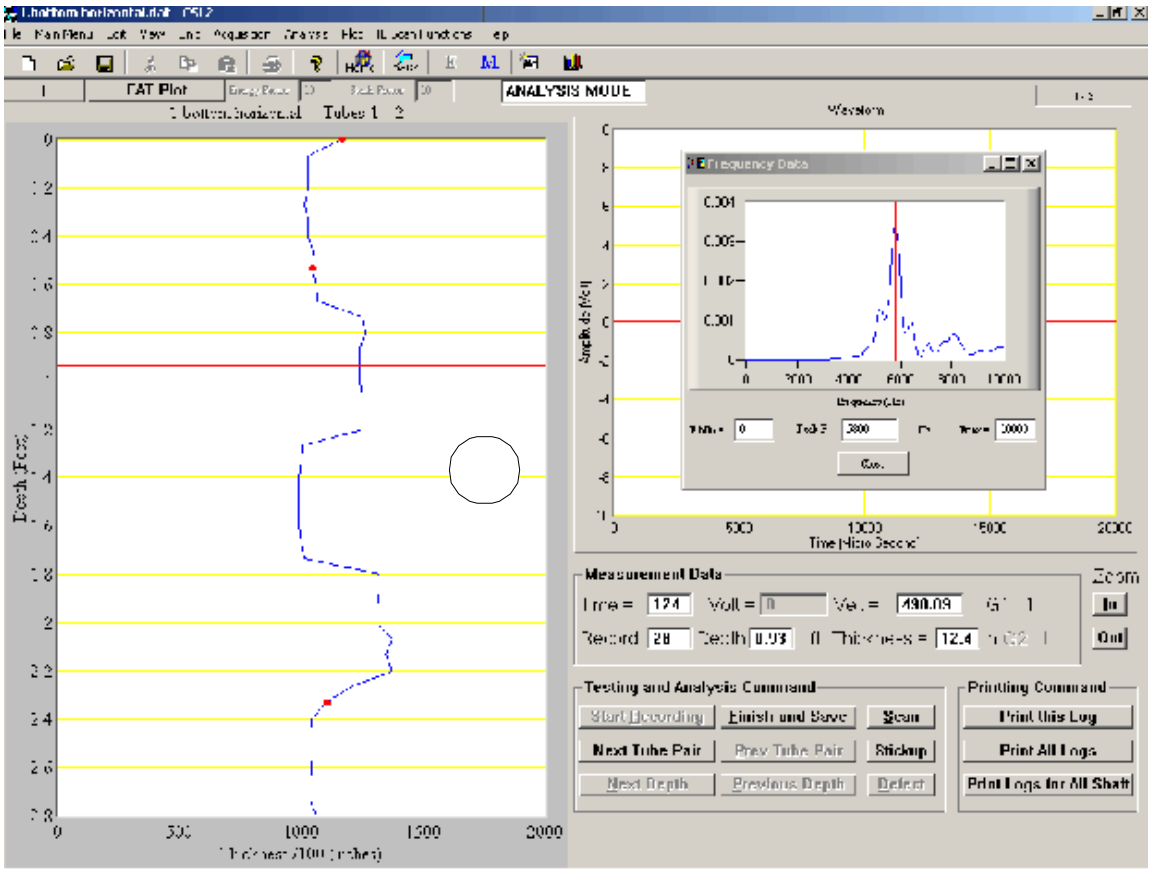

Figure 5.37 Horizontal Scan from Sunday, 12/29/02 – Day 1

At 24 days, the horizontal test across the grouted ducts is similar to the horizontal test at day 1, as shown in Fig. 5.38 below. The thickness from fully grouted steel duct now measures 11.6 inches, down from 12.4 inches. The thickness from the fully grouted plastic duct measures 12.4 inches, down from 13.0 inches.

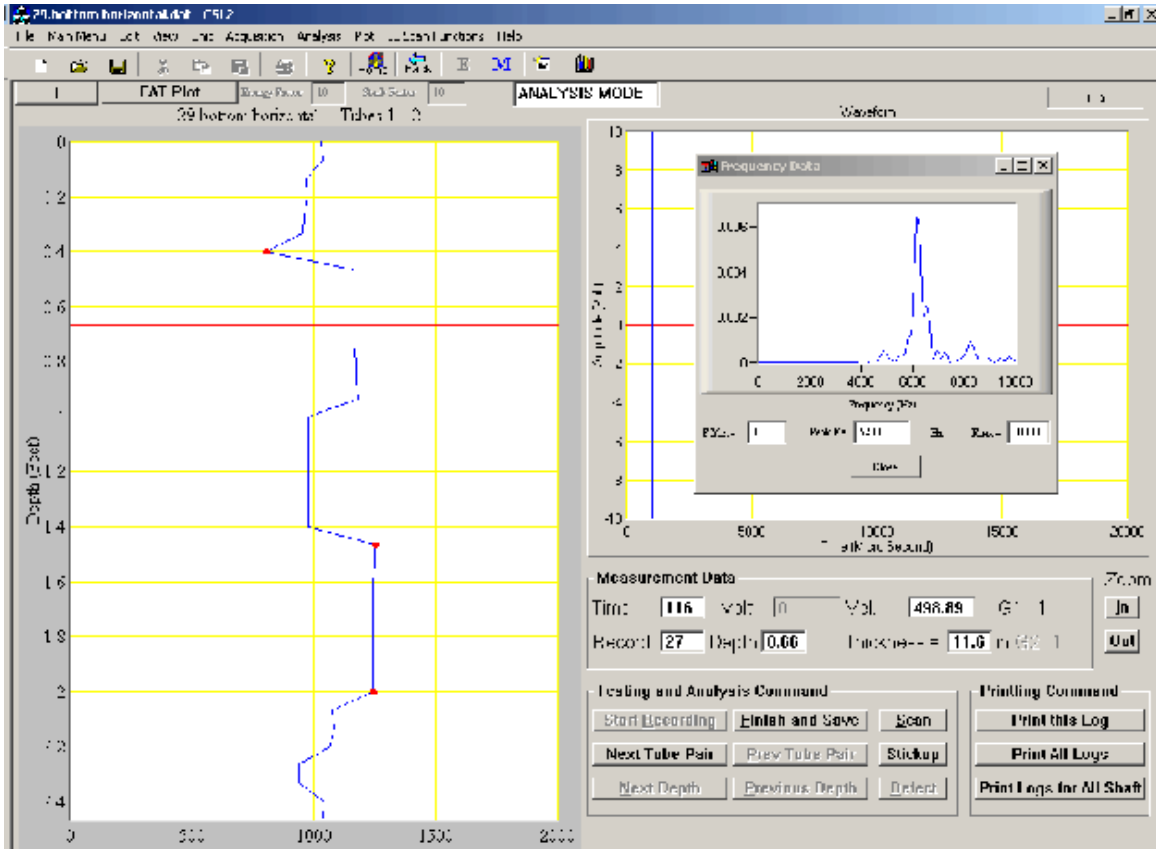

Figure 5.38 Horizontal Scan from Tuesday, 1/21/03 – Day 24

3. Impact Echo Scanning along the ducts

Several IE scan tests were performed on Wall II along each duct. The IE scan below was performed along the center line of the steel duct, starting from the bottom (~3" above the bottom wall) to the top of the wall (~3" below the top wall). The thickness results and an example frequency response are shown in Fig. 5.39. From the frequency and thickness results in Fig. 5.39, it is seen that the

peak frequency shifted to a lower value for the duct as compared to the calibration scan shown in Fig. 5.35. This resulted in higher thickness value, 12.4 inches, from the nominally 10 inch thick wall. There is, however, no indication that the duct is grouted in the bottom half of the duct at day 1.

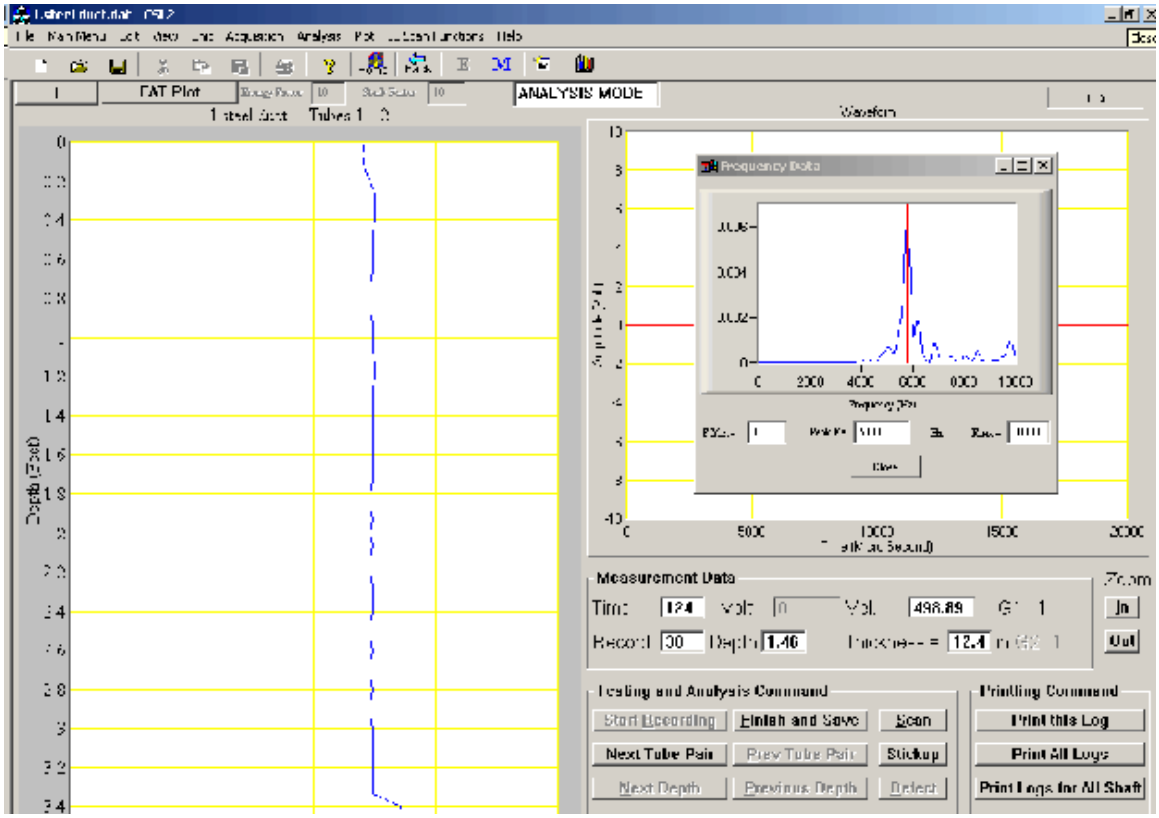

Figure 5.39 Scan along Steel duct from Sunday, 12/29/02 – Day 1

At 24 days, the vertical test along the steel duct does show an indication of the grout in the bottom half of the duct, as shown in Fig. 5.40 below. At approximately 2 feet, there is a break in the plot, indicating the beginning of the un-grouted section. The thickness from the un-grouted section of duct now measures 12.3 inches, as compared to 11.6 inches for the grouted section.

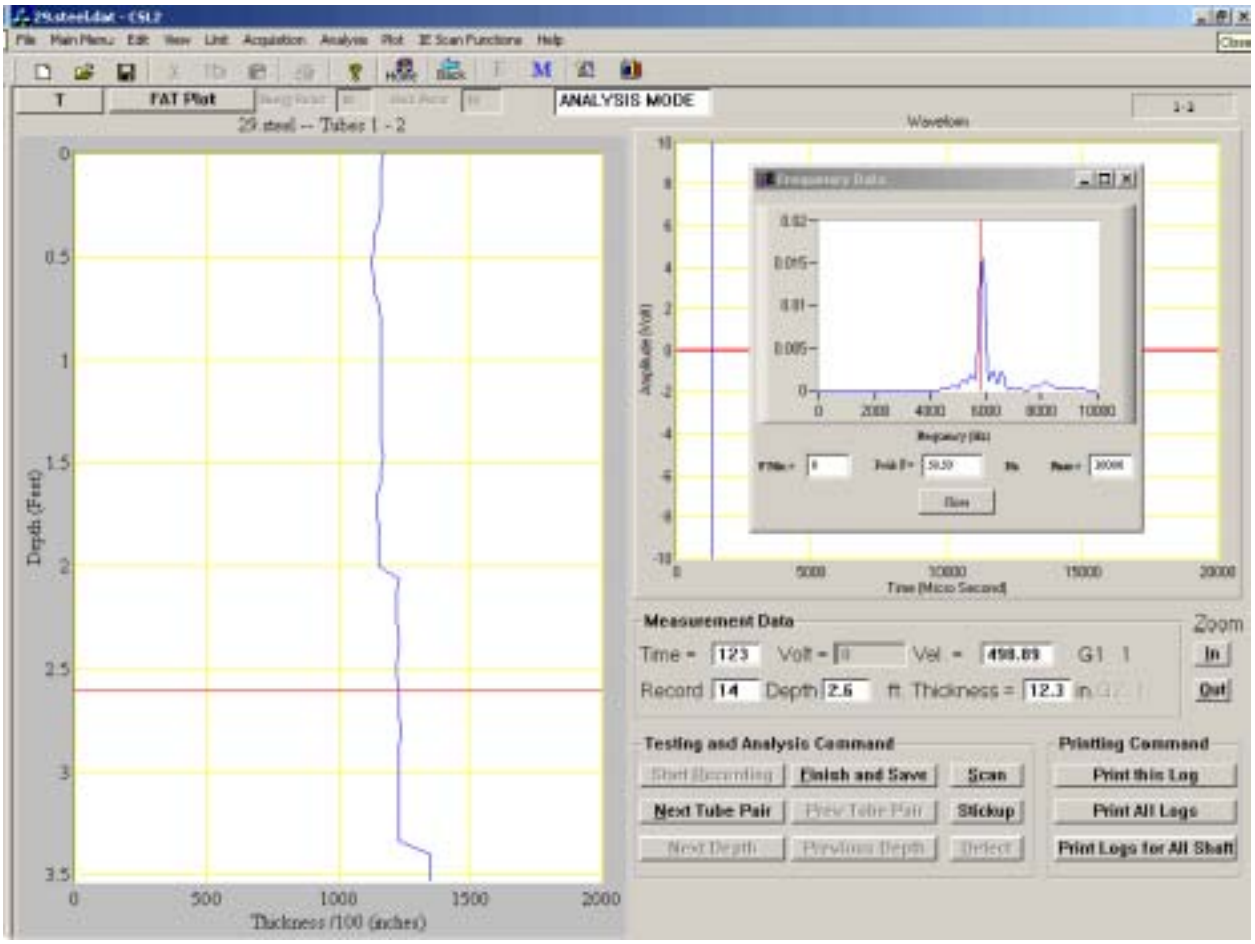

Figure 5.40 Scan along Steel duct from Tuesday, 1/21/03 – Day 24

An Impact Echo scan was then performed along the center line of the plastic duct. The thickness and example frequency results are shown in Fig. 5.41. An average thickness reading from the plastic duct is 13.4 inches with an average peak frequency of 5350 Hz. This example also shows the frequency and thickness shift as compared to typical values for the concrete wall by itself. There is, however, no indication that the duct is grouted in the bottom half of the duct.

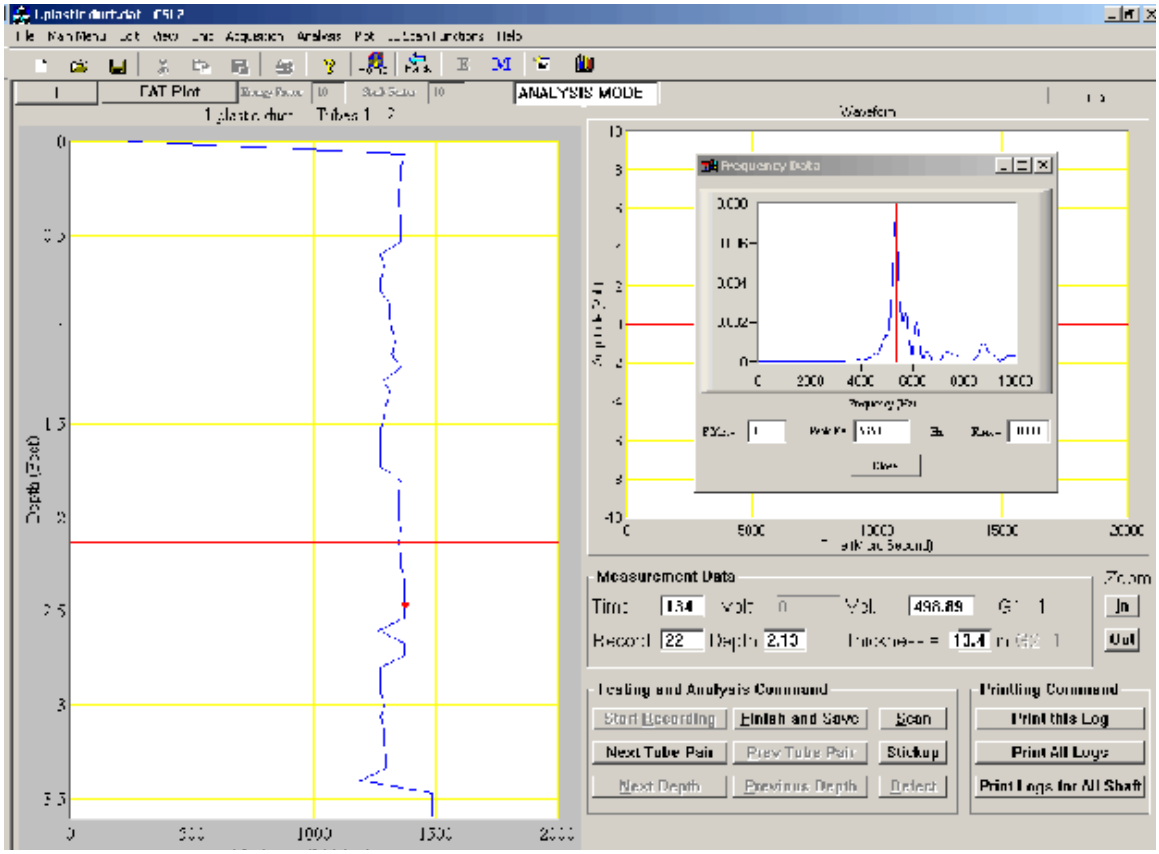

Figure 5.41 Scan along Plastic duct from Sunday, 12/29/02 – Day 1

At 24 days, the vertical test along the plastic duct does show an indication of the grout in the bottom half of the duct, as shown in Fig. 5.42 below. At approximately 1.6 feet, there is a break in the plot, indicating the beginning of the grouted section. The thickness from the un-grouted section of duct now measures 13.0 inches, as compared to 12.5 inches for the grouted section.

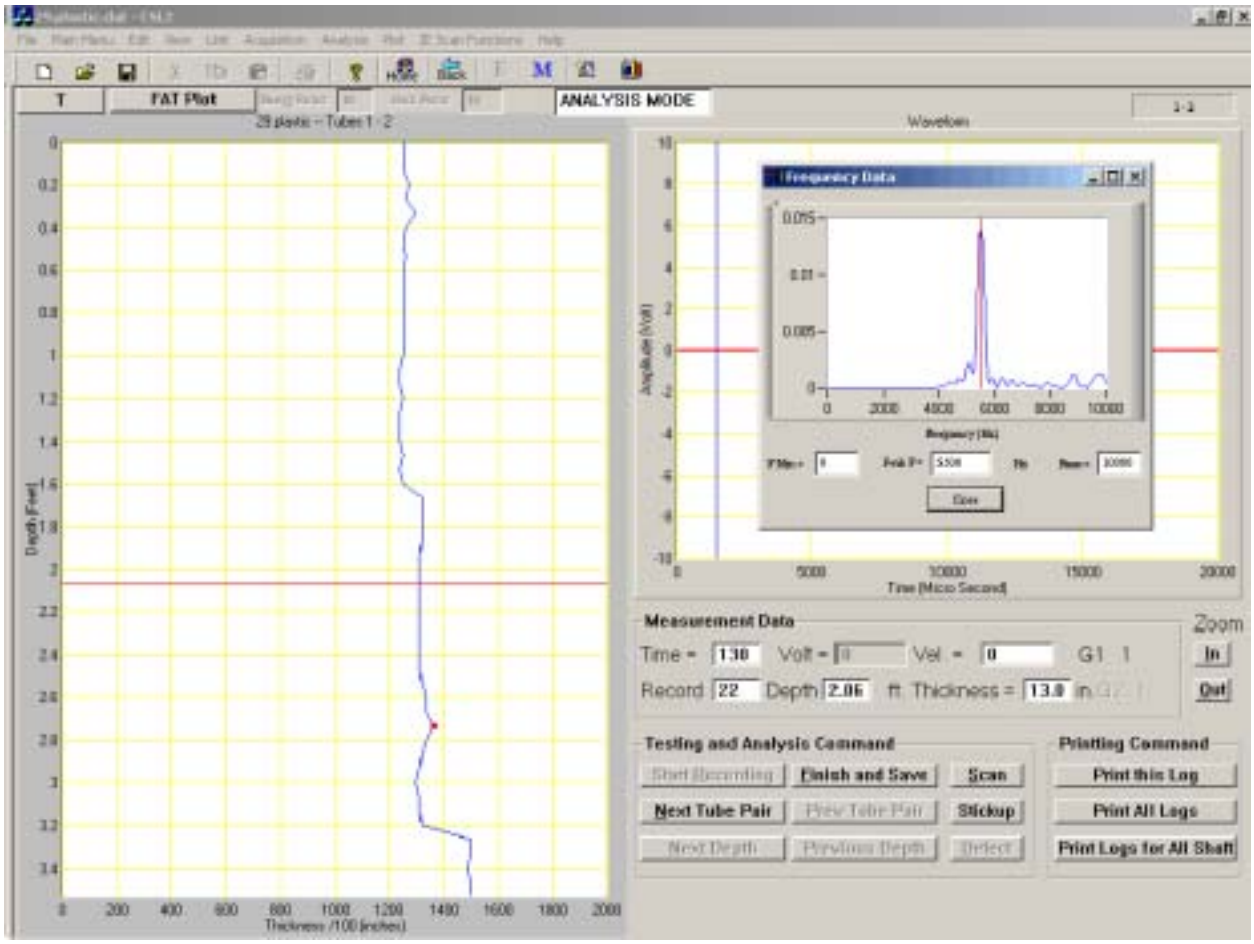

Figure 5.42 Scan along Plastic duct from Tuesday, 1/21/03 – Day 24

4. IE Scanning off the Center Line

Further testing was performed to see the effects of IE scanning when performed off the center line of the duct. Results from testing performed on 12/29/02 off the centerline of the steel and plastic ducts are shown in Figs. 5.43 and 5.44, respectively. Testing was performed 3 inches off the centerline of the ducts. From Figs. 5.43 and 5.44, there are no clear indications of grouted versus un-grouted ducts from these tests on day 1.

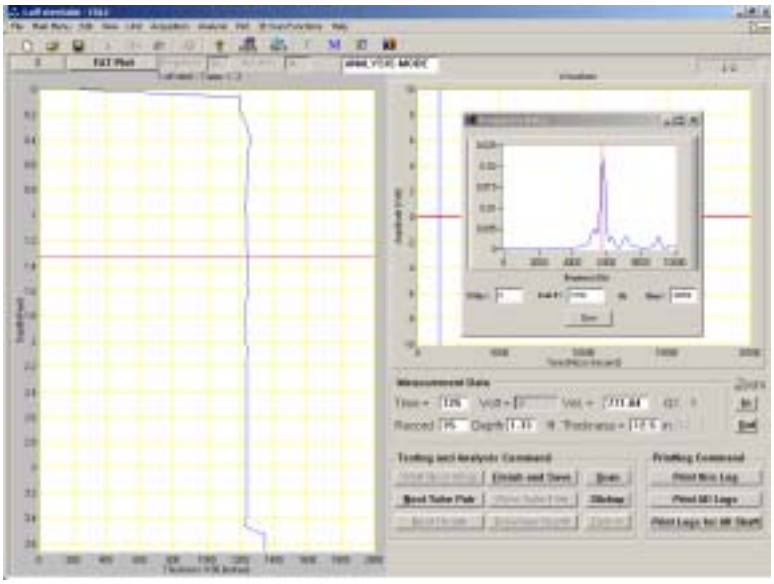

Figure 5.43 Off Centerline of Steel Duct from 12/29/02 – Day 1

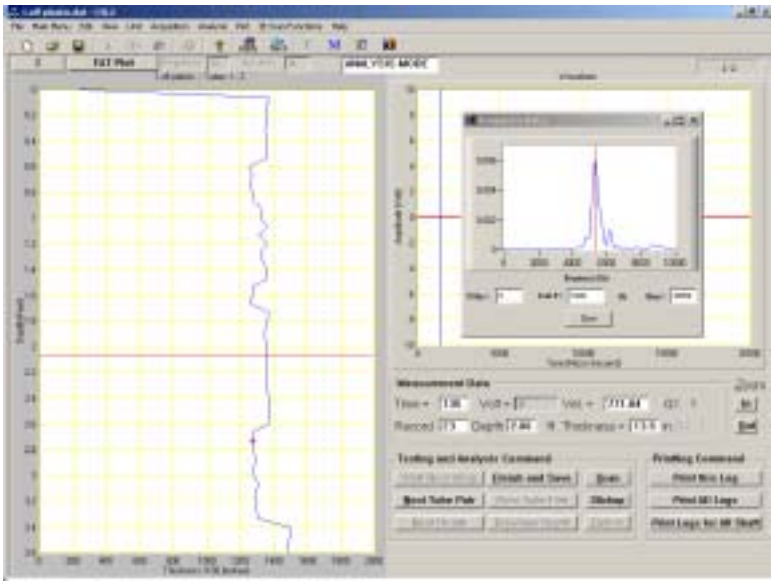

Figure 5.44 Off Centerline of Plastic Duct from 12/29/02 – Day 1

Results from testing performed on 1/21/03 off the centerline of the steel and plastic ducts are shown in Figs. 5.45 and 5.46, respectively. At the steel duct, a change in thickness is measured at approximately 2.1 ft, shifting from 11.6 in to 12.3 in. At the plastic duct, a change in thickness is measured at approximately 1.6 ft, shifting from 12.4 in to 13.0 in. The thickness measurements above and below each shift are consistent.

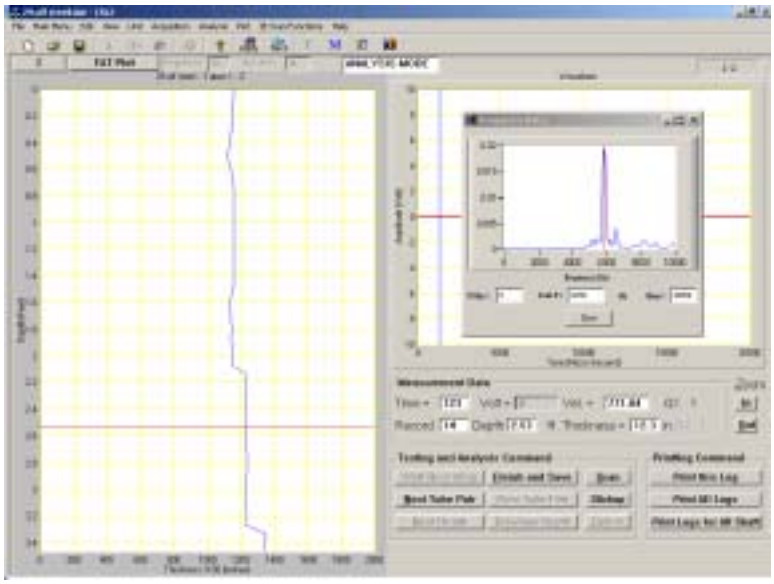

Figure 5.45 Off Centerline of Steel Duct from 1/12/02 – Day 24

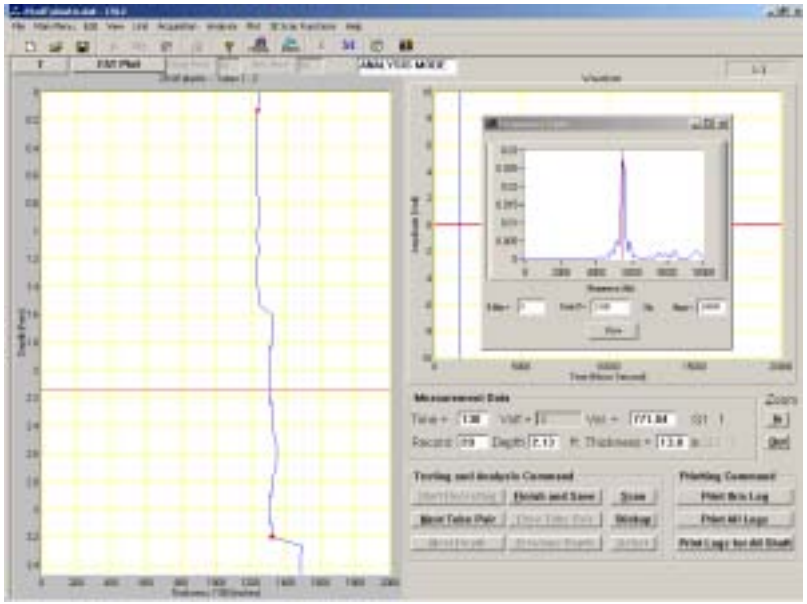

Figure 5.46 Off Centerline of Plastic Duct from 1/21/03 – Day 24

CHAPTER 6

CONCLUSIONS

Apparently, the results of the Survey of State DOTs including the District of Columbia and Puerto Rico showed that none of the DOTs that responded (63%) use nondestructive testing to evaluate their bonded post-tensioning systems, or have even experienced any failure with them.

Scanning Impact Echo, IE, tests showed the most promise for assessing internal grout conditions of the steel duct. For a plastic duct, it was more difficult to identify grout conditions due to partial debonding conditions between the plastic duct and concrete wall. In this investigation, internal conditions of grouted ducts were successfully evaluated using the IE thickness results together with a shift in the IE peak frequency and an impactechogram. The impactechogram was particularly useful for the internal grout evaluation of the fully grouted plastic duct where multiple fundamental frequencies occurred.

The Spectral Analysis of Surface Waves, SASW, tests showed good promise for steel ducts. The surface wave velocity results from the fully grouted steel duct showed the highest velocity while the velocity results from the empty steel duct showed lowest velocity. However, the test results from the plastic duct did not yield similar results.

The image results from the Ultrasonic Tomography Imaging, UTI, tests showed locations of the ducts. Unfortunately, the image results did not show grout condition details inside the ducts. This was because the frequency of the transducers used in this investigation was 54 kHz, which is standard for concrete. This range of frequency yielded a wavelength longer than the diameter of the ducts, therefore higher frequency/shorter wavelength transducers, should be used on 3-inch I.D. ducts.

Only Impact Echo (IE) Scanning was used to evaluate the internal grout condition of steel and plastic ducts as a function of time. By day 4, 96 hours after grout had been introduced into the duct, the first indication of a difference between true void and grouted section of the ducts could be seen. By day 24, scanning along the steel duct showed a significant difference between the grouted and empty ducts. Scanning IE results of the plastic duct were considered to be inconclusive due to debonding between the plastic duct and the concrete matrix.

CHAPTER 7

RECOMMENDATIONS

Further Research:

Research recommendations include study of the effects of various size defects ranging from ½ the cross-section to ¼ or less of the cross-section on IE scanning. We further recommend further studies be conducted to determine the sensitivity of IE Scanning to varying size void defects ranging from ½ the cross-section to ¼ the cross-section or smaller. Voids in PT ducts are typically found at the top of the drape, and then only the top half or less of the duct is missing grout. The ability to identify this type of defect in the field is critical to the life span of any structure utilizing post-tensioning to mitigate the risk of long-term strand corrosion. Finally, we recommended applying a higher frequency source to attempt to "image" conditions in the duct with IE Scanning, Ultrasonic Tomography and/or SASW.

Impact on FDOT Specifications:

Based on the results from all three tests, we suggest that scanning Impact Echo should be incorporated as a practical method to evaluate the internal condition of the grout in actual field conditions for bonded post-tensioning systems. Impactechograms may also be used as a way to present the results since the plot provides more information in IE frequency data. Also, based on this investigation, the use of plastic ducts for bonded post-tensioning systems should be discouraged, since scanning IE verification of fully grouted tendons is not reliable for plastic duct systems.

REFERENCES

Aouad, M.F., "Evaluation of Flexible Pavements and Subgrades Using the Spectral Analysis of Surface Waves Method", Dissertation Submitted in Partial Fulfillment of the Doctor of Philosophy Degree, The University of Texas at Austin, 1993.

Chang, Y., Wang C., and Hsieh, C., Feasibility of Detecting Embedded Cracks in Concrete Structures by Reflection Seismology. *NDT & E International*. Vol. 34, 2001.

Florida Department of Transportation District 3,Mid-Bay Bridge Post-Tensioning Evaluation, 2001

Halabe, U., and Franklin, R., Detection of Flaws in Structural Members Using Spectral Analysis of Ultrasonic Signals. *Nondestructive Testing and Evaluation.* Vol. 15, No. 3, 1999.

Karagouz, M., Bilgutay, N., Akgul, T., and Popovics, S., Ultrasonic Testing of Concrete Using Split Spectrum Processing. *Materials Evaluation*. Vol. 57, No. 11, 1999.

Koehler, B., Hentges, G., Mueller W., A Novel Technique For Advanced Ultrasonic Testing Of Concrete By Using Signal Conditioning Methods And A Scanning Laser Vibrometer, 2001.

Martin, J., Broughton, K.J., Giannopolous, A., Hardy, M.S.A., and Forde, M.C., Ultrasonic Tomography of Grouted Duct Post-tensioned Reinforced Concrete Bridge Beams. *NDT & E International*. Vol. 34, No. 2, 2001.

Nazarian, S., and Stokoe, K.H., II, In Situ Determination of Elastic Moduli of Pavement Systems by SASW Method (Practical Aspects), Report 368_1F, Center For Transportation Research, The University of Texas at Austin, 1985.

Nazarian, S., and Stokoe, K.H., II, In Situ Determination of Elastic Moduli of Pavement Systems by SASW Method (Theoretical Aspects), Report 437_2, Center For Transportation Research, The University of Texas at Austin, 1986.

NDTnet, Comparison of Pulse-Echo-Methods for Testing Concrete (1996)

"Nondestructive Test Methods for Evaluation of Concrete in Structures", reported by ACI Committee 228, ACI 228.2R-98 (Section 2.2.4).

Rens, K., Transue, D., and Schuller, P., Acoustic Tomographic Imaging of Concrete Infrastructure. *Journal of Infrastructure Systems*, March 2000.

Roesset, J.M., Chang, D.W., and Stokoe, K.H., "Comparison of 2-D and 3-D Models for Analysis of Surface Waves Tests", Proceedings, Fifth International Conference on Soil Dynamics and Earthquake Engineering, Karlsruhe, Germany, 1991, pp. 111-126

Schokker, A., Koester, B., Breen, J., and Kreger, M. Development of High Performance Grouts for Bonded Post-tensioned Structures, June, 1999.

Titman,T.J., Applications of Thermography in Non-destructive Testing of Structures. *NDT & E International*. Vol.34, No. 2, 2001.

Wang, X., Chang C., and Fan L., Nondestructive Damage Detection of Bridges: A Status Review. *Advances in Structural Engineering*. Vol. 4, No. 2, 2001.

Watanabe, T., Ohtsu, M., and Tomoda, Y. Impact-Echo Technique for Grouting Performance in Post-Tensioning Duct. *j. Soc. Mat. Sci., Japan*, Vol. 48, No.8, Aug. 1999.

Yeih, W., and Huang, R., Detection of the Corrosion Damage in Reinforced Concrete Members by Ultrasonic Testing. *Cement and Concrete Research*. Vol. 28, No. 7, 1998.

APPENDIX A

Sample Survey
Date: November 30, 2001

Alabama Department of Transportation
Paul Bowlin, Transportation Director
Alabama Department of Transportation
1409 Coliseum Blvd.
Montgomery, AL 36130
(334) 242-6311
(334) 262-8041 Fax
(334) 242-6319 Donald W. Vaughn, Administrative Engineer
(334) 242-6318 Ray D. Bass, Chief Engineer
Web Site: http://www.dot.state.al.us

Dear Mr. *Bowlin*

A team at the University of Florida's School of Building Construction is currently involved in a research project aimed at identifying an accurate, convenient, and rapid non-destructive method of detecting defects in bonded post-tensioned ducts.

It would be beneficial to our research if you would take a few moments to complete the attached survey. The survey is designed to inform us of the standard procedures that are incorporated by your organization. Your professional knowledge will help us in our future efforts, and we greatly appreciate your time and support.

Please complete the enclosed questionnaire and mail your response by 31 Dec. 2001. A self-addressed envelope is provided for the convenient return of this information. Results of the survey will be provided to you upon completion of the project if you so desire.

Sincerely,

Dr. Larry C. Muszynski
Assistant Professor

Mr. Elie Andary
Graduate Research Assistant

Name_____ Date_____

Position_____

Agency_____

Phone No._____

E-mail Address_____

Agency's WWW Address: http://_____

The following survey contains five items and should take no more than 10 minutes to complete. Once again, thank you for your participation. Please check the following box if you would like the results of the survey sent to you. ☐

1. Do you use post-tensioning systems in bridge construction in your state and what type?

   Unbonded yes ☐ no ☐

   Bonded yes ☐ no ☐

2. What type of duct material is generally used in your systems?

Smooth plastic ☐ corrugated plastic ☐ smooth metal ☐ corrugated metal ☐

3. If you are using <u>bonded</u> post-tensioning systems, what class of grout do you typically use?

   Class A ☐ Class B ☐ Class C ☐ Class D ☐ Other ☐

4. Have you ever experienced failure of <u>bonded</u> post-tensioning tendons?

   Yes ☐ No ☐ if yes what was/were the cause(s)_____

   _____

5. Do you use Non-destructive inspection and/or testing methods to assess the integrity of the grout in your <u>bonded</u> post-tensioning systems? Yes ☐ No ☐

   If yes, what type(s)_____

_____

_____

Thank You!

APPENDIX B

Raw Data from State Departments of Transportation Survey

										Bonded Post-tensioning Grout class								
				Post-tensioning systems		Duct material									Non-destructive inspection		Tendon's	Failure
DOT Name	Symbol	Respond	Results	Unbonded	Bonded	SP	CP	SM	CM	A	B	C	D	Other	Yes	No	Yes	No
Alabama	AL																	
Alaska	AK	x	x															
Arizona	AZ	x	x		x				x		x					x		x
Arkansas	AR	x																
California	CA	x	x		x				x					x		x		x
Colorado	CO	x	x		x		x		x	x						x		x
Connecticut	CT	x	x		x				x					5000psi		x		x
Delaware	DE	x																
Florida	FL																	
Georgia	GA	x	x		x				x	x						x		x
Hawaii	HI	x	x		x				x		x					x		x
Idaho	ID	x	x		x		x			x						x		x
Illinois	IL	x	x		x		x		x					x		x		x
Indiana	IN																	
Iowa	IA	x	x															
Kansas	KS	x	x		x		x							x		x		x
Kentucky	KY	x	x															
Louisiana	LA	x	x		x				x		x	x				x		x
Maine	ME																	
Maryland	MD																	
Massachusetts	MA	x	x	x		x												
Michigan	MI	x			x	x			x					E-1		x		x
Minnesota	MN																	
Mississippi	MS	x	x	x	x	x		x								x		x
Missouri	MO																	
Montana	MT	x	x															
Nebraska	NE																	
Nevada	NV																	
New Hampshire	NH	x																
New Jersey	NJ																	
North Carolina	NC																	
District of Columbia	DC																	
New Mexico	NM																	
New York	NY	x	x	x	x	x	x		x					x		x	x	
North Dakota	ND	x														x		x
Ohio	OH																	
Oklahoma	OK																	
Oregon	OR																	
Pennsylvania	PA	x				Rigid plastic			x					x		x		x
Puerto Rico	PR	x																
Rhode Island	RI																	
South Carolina	SC	x	x		x	x		x						5000psi		x		x
South Dakota	SD																	
Tennessee	TN	x			x				x	attached						x		x
Texas	TX	x	x		x	x	x	x	x	x		x				x		x
Utah	UT	x	x		x		x				x					x		x
Vermont	VT	x																
Virginia	VA																	
Washington	WA	x			x				x	specify recipe						x		x
West Virginia	WV	x			x			x	x					x		x		x
Wisconsin	WI	x														x		x
Wyoming	WY	x			x				x					x		x		x

MASTERFLOW®'1205

High-performance grout for highly stressed steel

Cementitious Grouts

Description

MASTERFLOW 1205 is specially formulated to produce a pumpable, nonbleeding, high-strength fluid product with extended working time for grouting. It provides corrosion protection for highly stressed steel cables, anchorage, and rods. MASTERFLOWO 1205 is formulated with a specially graded aggregate, which mitigates chloride migration while still allowing the product to be easily pumped long distance through small openings.

Features/Benefits

Nonshrink materials - Enhances flow and protects stress tendons, bolts, or bars from the threat of corrosion

- Easy to pump or pour grout- Hardens without bleeding or settlement shrinkage and formation of voids
- Can be pumped and/or recirculated for relatively long periods of time-Can be used at temperatures ranging from 40°F to 90°F (4°C to 32°C)
- Hardens without settlement shrinkage within the grout duct - Ensures maximum bond and long-term protection against ingress of water and chlorides
- Meets all the compressive strength and nonshrink requirements of CRD C 621 and ASTM C 1107, at a fluid consistency
- Does not contain components that are detrimental to high strength steel; does not form hydrogen gas, carbon dioxide, or oxygen as an early expansion mechanism
- Meets requirements of PTI guide specifications
-

Where to Use MASTERFLOW® 1205

- Pumping into areas around post-tensioned cables and rods to encapsulate the steel, protecting it against corrosion and providing maximum anchorage
- 1 Placing around end sections of unanchored cables and rods, providing anchorage for subsequent tensioning
- Filling voids in restricted spaces between wall panels, beams, and columns where grout will be in contact with highly stressed steel
- Grouting cable anchor plates or other types of plates where grout will be in contact with highly stressed anchorages

Important: read this first

ChemRex' does not warrant the performance of this product unless the instructions of this document and other related ChemRex• documents are adhered to in all respects

Pre job conference and Job service

Conferences prior to the installation of the product should be held as early as practical. Such conferences are important to review the following recommendations (for a given grouting project) to ensure the placement of highest quality and lowest in-place cost.

How to Apply MASTERFLOW° 1205

Preparation

Clean cables/strands of all oxidation, dirt, oil, or any loose materials. Ducts should be clean and free of any defects.

Check proposed method of mixing and pumping to ensure continuous placement once pumping starts. It is recommended to have a source of high pressure water with connections for flushing grout hoses or partially grouted cable ducts in case the pumping must be interrupted.

Test the pump and grout lines with water or pressurized oil-free air to confirm they are capable of providing and withstanding the required pressure, and to see that all connections are tight, without leaks. Loss of water from slow or nonmoving grout can result in a blocked line.

Plug, ball or gate valves should be provided at the pump outlet, at the inlet ends of vertical cable ducts, and at both ends of the horizontal ducts. Also, a valued by-pass hose or pipe from the pump discharge line back to its hopper is strongly recommended. This will ensure grout recirculation from pump to hopper can be maintained during connection changes and other pumping delays.

The inside diameter of the pipe, hose and valves, through which MASTERFLOW 1205 is to be pumped, should be at least 3/4 inches (19 mm) inside diameter to 2 inches (51 mm) inside diameter, consistent throughout the system. Avoid elbows if possible.

The pump lines and grout line, if needed, may be flushed with high pH lime saturated water to lubricate and cool the ducts. This water will be displaced by the oncoming grout and discharged at the outlet end prior to obtaining the air free mixed grout. Collect the lime saturated water and use as mix water if needed. Collect the transitional grout and discard.

Temperature

The recommended temperature range of the grout as mixed should be 40°F to 90°F l4°C to 32°C). The duct temperatures should also be within the same temperature range. Special precautions should be followed for hot or cold weather. Higher temperatures increase the amount of mixing water needed for a given fluidity and limit working time. Lower temperatures induce bleeding, retard set and impede early strength gain, but permit reducing mixing water content for a given fluidity and increase ultimate strength.

When duct temperatures are above 90°F (32°C), employ techniques to produce lower mixed grout temperature. Cool bags of MASTERFLOW• 1205 by storing in a shaded area or a cool place. Use cold potable water to attain the mixed grout at proper temperature. Be careful that you do not drop the grout temperature below 50°F (4°C). Ducts can also be cooled by circulating cold water. Lime ($Ca\ OH,$) can be added to the circulating water to increase pH to 12.4 to help passivate the steel and reduce the potential for steel oxidation prior to grouting.

When duct temperatures are 40°F (4°C), the temperature of the mixed grout should be increased by mixing in warm potable water. Ducts can be heated by circulating warm water throughout ducts. Lime (Ca OH,) may be added to the mixing water to increase pH and lubricate duct. Do not exceed 90°F (32°C) temperatures when warming both the mixed grout and the duct.

Mixing

MASTERFLOW 1205 is a ready-to-use product requiring only the addition of potable water. Normal mixing water content is determined by the ASTM C 939 Grout Efflux Time of 20 to 30 seconds immediately after mixing, and attaining '0' bleeding in the modified ASTM C 940 Wick Induced Bleeding Test, using the specified mixer for mixing the grout at the job. Charge mixing vessel with 80% of the required water and add MASTERFLOW 1205 with mixer running. Mix a minimum of 3 minutes or until product has reached a uniform consistency. Add additional water as needed to attain correct efflux and mix an additional 2 minutes. Consult your ChemRex° representative for special mixing instructions. Do not use water in an amount or at a temperature that will produce a flow of less than 20 seconds on the flow cone (ASTM C 939), or that will cause mixed grout to bleed or segregate. Jobsite conditions such as the size and complexity of the space to be grouted, pumping line diameters, height, mixing and pumping methods, and temperatures are factors that determine the actual amount of water needed.

Have one or more mixers available with the capacity to allow mixing and pumping to proceed simultaneously and continuously.

Place water in the mixer first, then steadily add the grout with mixer operating. Mix until the grout is homogeneous and free of lumps, which should be approximately 3 to 5 minutes, making sure all of the dry material is scraped from the mixer sides. Convey the mixed grout into the pump surge hopper and pass through a screen with 0.125 to 0.188 in. (3 mm to 5 mm) openings to catch possible lumps and then start pumping grout, after verifying grout efflux, into the duct.

Note: Do not mix more grout than can be placed through a pump in 30 to 45 minutes, depending on temperature.

Application

Place MASTERFLOW 1205 in accordance with section C5.6.3 Grouting Operations as stated in the 'Guide Specification for Grouting of Post-Tension Structures' prepared by the PTI Committee on Grouting Specifications.

Curing

Cure all exposed grout areas by wet curing for 24 hours with clean, wet rags (do not use burlap), followed by the application of an ASTM C 309 compliant curing compound. In cold weather, keep grout temperature above 40°F (4°C) until final set. Thereafter, keep temperature above freezing until a compressive strength of 1500 psi (10 MPa) is attained prior to the first freeze.

For Best Performance

- The walls of the space being grouted should be between 40°F and 100°F (4°C and 38°C) and should be saturated with lime water for optimum results. For use at temperatures above the range, consult ChemRex• Technical Service.
- DO NOT use mixing water in an amount or at a temperature that will produce a flow of less than 20 seconds (CRD C 611 or ASTM C 939) or cause the mixed grout to bleed or segregate when tested by the Modified Wick Induced Bleeding Test (ASTM C 940).
- ChemRex* is not responsible for stress corrosion caused by ingredients in the flushout, saturation or mixing water, or for contaminants either in the space being grouted or from other materials used in the system.
- The product contains Portland cement. Portland cement, in combination with water, may cause skin irritation, rash, and alkali burn. Do not wear contact lenses when working with this product. Remove soiled clothing and wash before reuse.
- Make certain the most current version of this data guide is being used; call Customer Service (1-800-433-9517) to verify the most current version.
- Proper application is the responsibility of the user. Field visits by ChemRex° personnel are for the purpose of making technical recommendations only and are not for supervising or providing quality control on the jobsite.

Technical Data

Compliances

- Meets all compressive strength and settlement shrinkage requirements of CRD C 621 and ASTM C 1107 at a fluid consistency.
- Complies with Post Tensioned Institute recommendations for a prepackaged post tensioned steel duct grout.

Typical Performance Data 0 70°F (21"C)

Flow (ASTM C 939)	20 - 25 sends
Final set (ASTM C 953)	<10 hours
Volume change (ASTM C 1090)	
1 day	> 0.0%
28 davs	>0.0% and <0.2%
Prehardened expansion height change @ 3 hours (ASTM C 940)	<0.2%
Compressive strength (ASTM C 942)	
1 day	)2,000 Psi (13.8 MPa)
3 days	)4,000 PSI (27.6 MPa)
7 days	)5.500 Psi (37.9 MPa)
28 davs	)8,000 PSI (55.2 MPa)
Chloride permeability (ASTM C 1202) Modified PTI 30 Volts	<2,500 coulombs
Acid soluble chloride content (ASTM C 1157)	<0.08% by weight of cement
Gelman Pressure Bleed 10 minutes @ 30 psi 0 vertical rise of 6 ft. (1.6 m) maximum pressure	
Wick induced bleeding (ASTM C 940. modified per PTD	% bleed 0 3 hrs.
FHWA acce erated corrosion test	)1.600 hrs.

Reasonable variations from the results shown above can be expected. Field and laboratory tests should be controlled on the basis of the desired plating consistency rather than strictly on water content.

Order Information

Packaging

MASTERFLOW 1205

- 55 lb. (25 kg) bags
- 2,500 lb. (1,134 kg) bulk bags also available by special order

Shelf Life

- Shelf life is 6 months in original, unopened bags'stored under normal conditions.

Coverage

- One 55 Ib. l25 kg) bag yields approximately 0.55 ft.' (0.016 m°)

Caution

MASTERFLOW' 1205

Risks

Eye irritant. Skin irritant. Causes burns. Lung irritant.

Precautions

KEEP OUT OF THE REACH OF CHILDREN. Avoid contact with eyes. Wear suitable protective eyewear. Avoid prolonged or repeated contact with skin. Wear suitable gloves. Wear suitable protective clothing. Do not breathe dust. In case of insufficient ventilation, wear suitable respiratory equipment. Wash soiled clothing before reuse.

First Aid

Wash exposed skin with soap and water. Flush eyes with large quantities of water. If breathing is difficult, move person to fresh air.

Waste Disposal Method

This product when discarded or disposed of is not listed as a hazardous waste in federal regulations. Dispose of in a landfill in accordance with local regulations.

For additional information on personal protective equipment, first aid, and emergency procedures, refer to the product Material Safety Data Sheet (MSDS) on the job site or contact the company at the address or phone numbers given below.

Proposition 65

This product contains materials listed by the state of California as known to cause cancer, birth defects, or reproductive harm.

VOC Content

This product contains 0 g/L or 0 lbs./gallon.

For medical emergencies only, call ChemTrec (1/800/424-93001.

Limited Warranty Notice

Every reasonable effort is made to apply ChemRex• exacting standards both in the manufacture of our products and in the information which we issue concerning these products and their use. We warrant our products to be of good quality and will replace or, at our election refund the purchase price of any products proved defective. Satisfactory results depend not only upon quality products, but also upon many factors beyond our control. Therefore, except for such replacement or refund, CHEMREX° MAKES NO WARRANTY OR GUARANTEE, EXPRESS OR IMPLIED, INCLUDING WARRANTIES OF FITNESS FOR A PARTICULAR PURPOSE OR MERCHANZ4BILITY, RESPECTING ITS PRODUCTS, and CHEMREX* shall have no other liability with respect thereto. Any claim regarding product defect must be received in writing within one (1) year from the date of shipment. No claim will be considered without such written notice or after the specified time interval. User shall determine the suitability of the products for the intended use and assume all risks and liability in connection therewith. Any authorized change in the printed recommendations concerning the use of our products must bear the signature of the ChemRek Technical Manager.

Corporate office:
889 Valley Park Drive: Shakopee, MN 55379

Customer Service: 1/800/433-9517
Technical Services: 1/800/ChemRex (1/800/243-6739)

Web Site: www.chemrex.com

Form No. 1019403

For professional use only.
Not for sale to or use by the general public.

7M 1/02
Replaces 1/01

® Printed on recycled paper including 10% post-consumer fiber

APPENDIX D
Material Safety Data Sheet

MATERIAL SAFETY DATA SHEET

ChemRex, Inc.
Commercial Construction Products Division
889 Valley Park Drive
Shakopee, MN 55379
Prepared by: Regulatory Affairs Department (612) 496-6000
Revision Date: 03/29/00

24-Hr Emergency
CHEMTREC (800) 424-9300

Page: 1 of 4
Reason for revision: Manufacturer name change

This document is prepared pursuant to the OSHA Hazard Communication Standard (29 CFR 1910.1200). Where a proprietary ingredient is shown, the identity may be made available as provided in this standard.

All components of this product are included in the EPA Toxic Substances Control Act (TSCA) Chemical Substance Inventory.

1. PRODUCT NAME: MASTERFLOW 1205 GROUT (Formerly: GS 1205)

Chemical Family: Hydraulic Cement Compounds

2.

		EXPOSURE LIMITS*			
HAZARDOUS INGREDIENTS:	CASNO	TLV	STEL	PEL	CONTENT
Portland cement	65997-15-1	10 mg/m3	None	None	55-65%
Silica, Crystalline Quartz"	14808-60-7	3 mg/m3***	None	****	1-7%
Calcium Oxide	1305-78-8	2 mg/m3	None	5 mg/m3	1-7%
Silicon Dioxide, Amorphous	7631-86-9	3 mg/m3*****	None	None	1-7%

*) Refer to Section 7 for available LD/LC(50) Health Hazard Data.
**) Contains less than 0.1% w/w 53 micron or smaller Crystalline Quartz. (***) 0.1 mg/m3 respirable quartz
(****) 10 mg/m3 divided by %Si02+2 (respirable quartz) (*****)
Particulates NOC - Respirable fraction.

3. PHYSICAL DATA:

Boiling Point (oC):	N/Ap	Water/Oil Distribution	
Percent Volatile:	0	Coefficient:	N/Ap
Freezing Point (oC):	N/Ap	Solubility in Water:	Slight
Vapor Pressure mmHg @20 (oC):	N/Ap	Density:	93 Lb/Ft3
Vapor Density:	N/Ap	pH: N/Ap	
Odor Threshold: (ppm)	N/Ap	Evaporation Rate:	N/Ap
Appearance: Grayish granular powder		Odor: Odorless	
N/Av = Not Available	N/Ap = Not Applicable		ca. = Approximate

4. FIRE AND EXPLOSION HAZARD DATA: HMIS Hazard Rating No. 0 (Minimal)

4. FIRE AND EXPLOSION HAZARD DATA: (cont'd)

Auto-Ignition Temperature: Not Applicable

Limits Of Flammability: LEL: Not Applicable UEL: Not Applicable

Extinguishing Media: This material is non-flammable. Use extinguishing agent suitable for type of surrounding fire.

Special Fire & Unusual Hazards: None known.

5. REACTIVITY DATA: HMIS Hazard Rating No. 0 (Minimal)

Stability: Stable. Not sensitive to mechanical impact.

Incompatibility: Strong mineral acids. Hydrofluoric acid slowly dissolves silicon dioxides (Silicon Tetrafluoride, a toxic substance, is formed.).

Hazardous Decomposition Products: Nbne known.

Hazardous Polymerization: Will not occur.

6. ENVIRONMENTAL AND DISPOSAL INFORMATION:

Action to Take for Spills/Leaks: No special procedures are required for clean-up of spills or leaks of this material. Sweep up and return for reuse or discard.

Waste Disposal Method: Does not contain hazardous chemicals as defined in 40 CFR 260. Dispose in a landfill in accordance with local, state, and federal regulations.

7. HEALTH HAZARD DATA: HMIS Hazard Rating No. 2 (Moderate)

PRIMARY ROUTE OF ENTRY: Inhalation

Effects Of Overexposure	
Inhalation:	Nuisance dust can cause temporary but reversible respiratory problems.
Eves:	Abrasive action can cause damage to the outer surface of the eye. In combination with water can cause severe irritation with corneal injury.
Skin Contact:	Abrasive action can cause slight to moderate imitation. In combination with water dermal exposure can cause severe alkali bums.
Skin Absorption:	Does not absorb through skin.
In eg stion:	Not likely source of entry due to physical nature of material.

7. HEALTH HAZARD DATA: (cont'd)

Chronic:	Product does not contain carcinogenic materials as defined by OSHA Hazardous Communications Act 1910.1200 . Materials are not known mutagenic, teratogenic, or reproductive health hazards

8. FIRST AID:

Inhalation:	Remove victim from exposure. If difficulty with breathing, administer oxygen. If breathing has stopped administer artificial respiration, preferably mouth-to-mouth. Seek medical attention.
Eves:	Flush eyes with water, lifting upper and lower lids occasionally for 15 minutes. Seek medical attention.
Skin:	Remove contaminated clothing. Wash thoroughly with soap and water. If irritation persists seek medical attention. Wash contaminated clothing before reuse.
In es~:	Do NOT induce vomiting; give large quantities of water; get immediate medical attention. If vomiting occurs spontaneously, keep head below hips to prevent aspiration of liquids into lungs. Do NOT give anything by mouth to an unconscious person.

9. SPECIAL PROTECTION INFORMATION:

Ventilation: Ventilation is recommended. Air movement must be designed to insure turnover at all locations in work area to avoid build up of airborne dust concentrations.

Personal Protection Eguinment: Do NOT wear contact lenses when working with this material. Use chemical goggles/safety glasses with side shields and Rubber/Latex gloves. Selection of specific items such as boots and apron will depend on operation. Wear respirator protection whenever airborne concentrations exceed TLV ceilings or TWA, use NIOSH/OSHA approved respirators equipped with an organic vapor cartridge for listed hazard.

Confined spaces, rooms, or tanks are areas where concern for TLV's is especially important. Reference OSHA Regulation CFR 29 1910.134 for recommended respiratory protection.

10. **ADDITIONAL INFORMATION:**

Average Shelf Life:	Refer to Product Data Sheet.
Special Instructions:	Store in cool, dry place.

REGULATORY INFORMATION:

Title III Section 302:	No reportable chemicals.
Title III Section 311/312:	Health hazard: Immediate Physical hazard: None

10. ADDITIONAL INFORMATION: (cont'd)

REGULATORY INFORMATION: (cont'd)
Title III Section 313:
State: California

No reportable chemicals.

This product contains a chemical known to the state of California to cause cancer.

Silica, Crystalline Quartz (Respirable) 14808-60-7 _< 0.1

WHMIS Classification:

Class D, Div. 2, Sub A
Class D, Div. 2, Sub B
Class E

Canadian Domestic Substance List:

TRANSPORTATION

National Motor Freight Classification (NMFC): 42130 Sub: 2 Class:50

Description: CEMENT, HYDRAULIC

Emergency Response Guide Page No.: NOT REGULATED

DOT Reportable Quantity: NOT REGULATED

Marine Pollutant: NL

P = Moderate PP = Severe WS = Water Sheen

NL= Not Listed ND = Not Determined

The information herein is given in good faith. No warranty, expressed or implied, is given regarding the accuracy of these data or the results obtained from the use thereof. Consult ChemRex, Inc. for further information.